Effects of climate variability and functional changes on carbon cycling in a temperate deciduous forest

Wu, Jian

Publication date:
2013

Document Version
Publisher's PDF, also known as Version of record

Technical University of Denmark

Effects of climate variability and functional changes on carbon cycling in a temperate deciduous forest

PhD thesis

Jian WU

2013

DTU Chemical Engineering
Department of Chemical and Biochemical Engineering

 ISBN-13: 978-87-92481-92-4

PhD thesis

Supervised by: **Andreas Ibrom**, **Leon van der Linden** and **Claus Beier**

Center for Ecology and Environmental Sustainability

Department of Chemical and Biochemical Engineering

Technical Univeristy of Denmark (DTU)

2800 Kongens Lyngby, Copenhagen

Reference to this publication should be written as: Jian Wu (2013) "Effects of climate variability and functional changes on carbon cycling in a temperate deciduous forest" PhD Thesis.

ACKNOWLEDGEMENTS

This work was supported by the EU FP7 project CARBO-extreme, the DTU Climate Centre and the Danish national project ECOCLIM (Danish Council for Strategic Research).

I would like to express my sincere thanks to my main supervisor, Professor Ibrom Andreas, for his guidance and endless encouragement throughout the whole period of the PhD project. It was really a pleasant and fruitful experience during the three years. I also thank my co-supervisors, Leon van der Linden and Claus Beier, who helped me a lot with the modelling and offered me the opportunity to work on subjects that I am interested. I want to thank also Kim Pilegaard, Klaus Larsen, Per-erik Jansson from KTH, Gitta Lasslop and Nuno Carvalhais from MPI-BGC for their support and contribution to the manuscripts that are included in this thesis. I want to thank Flurin Babst and David Frank from WSL for providing the tree ring datasets. Also, Poul Sørensen is thanked for conducting the soil respiration and litterfall measurements. Without these efforts, this work will not be feasible. We thank the land-owner Sorø Akademi for giving us access to the site and for providing site specific management data.

Thanks also to all the colleagues at the ECO, especially my office mates, Sabine, Cathrine and Petra, for making here such a nice and friendly place not only for work but also with a lot of joy. I also want to thank my friends, Dr Hu Qiang and Dr Shi Keliang who lived with me together in the nice Risø House for almost two years. Thanks also to the two football teams in Risø and Copenhagen, which I really enjoyed. I would like to thank my parents, Mr Wu Shimin, Dr Shen Jingfeng for their endless support and love. Last but not least, I would like to thank my girl freind, Zhubingbing for understanding and love. It was amazing for me to meet you in Denmark.

ABBREVIATIONS AND SYMBOLS

CO_2	Carbon Dioxide
EC	Eddy-Covariance
IAV	Interannual Variability
NEE	Net Ecosystem Exchange
GPP	Gross Primary Productivity
TER	Total Ecosystem Respiration
λH	Latent Heat Flux
H	Sensible Heat Flux
MDF	Model Data Fusion
ECB	Ecosystem Carbon Budget
S_c	Storage Change
MCMC	Markov Chain Monte Carlo
VPD	Vapour Pressure Deficit

ABSTRACT

Temperate forests are globally important carbon (C) stocks and sinks. A decadal (1997-2009) trend of increasing C uptake has been observed in an intensively studied temperate deciduous forest, Sorø (Zealand, Denmark). This gave the impetus to investigate the factors controlling the C cycling and the fundamental processes at work in this type of ecosystem. The major objectives of this study were to (1) evaluate to what extent and at what temporal scales, direct climatic variability and functional changes (e.g. changes in the structure or physiological properties) regulate the interannual variability (IAV) in the ecosystem C balance; (2) provide a synthesis of the ecosystem C budget at this site and (3) investigate whether terrestrial ecosystem models can dynamically simulate the trend of increasing C uptake. Data driven analysis, semi-empirical and process-based modelling experiments were performed in a series of studies in order to provide a complete assessment of the carbon storage and allocation within the ecosystem and clarify the mechanisms responsible for the observed variability and trend in the ecosystem C fluxes.

Combining all independently estimated ecosystem carbon budget (ECB) datasets and other calculated ECB components based on mass balance equations, a synthesis of the carbon cycling was performed. The results showed that this temperature deciduous forest was moderately productive with both high rates of gross primary production and ecosystem respiration. Approximately 62% of the gross assimilated carbon was respired by the living plants, while 21% was contributed to the soil as litter production, the latter balancing the total heterotrophic respiration. The remaining 17% was either stored in the plants (mainly as aboveground biomass) or removed from the system as wood production. In general, the ECB component datasets were consistent after the cross-checking. This, together with their characterized uncertainties, can be used in model data fusion studies.

The sensitivity of the C fluxes to climatic variability was significantly higher at shorter than at longer time scales and changed seasonally. At the annual time scale, the IAV in net ecosystem exchange of CO_2 (NEE) was mostly determined by changes in the ecosystem functional properties. This indicated that the processes controlling the function change need to be incorporated into the process-based ecosystem models. The process-based model (CoupModel) applied in this study was able to simulate the phenology and observed carbon fluxes well at short (i.e. diurnal or seasonal) time scales but did not reproduce the decadal trends in NEE when global parameter estimates were used. Annual based parameter estimates were able to reproduce the trends; changes in the yearly fitted parameters (e.g. the light use efficiency) indicated the importance of functional change, as also shown in the analysis using the semi-empirical models. A role for nitrogen demand during mast years was also demonstrated in the estimated parameters. Nitrogen cycling and dynamics were identified as possible internal factors that need further investigation.

SAMMENFATNING

Klodens skovøkosystemer udgør et vigtigt lager for kulstof. Gennem de sidste 15 år har intensive studier af kulstofbalancen i en dansk bøgeskov vist en gradvis stigning i økosystemets optag af kulstof. I denne PhD afhandling beskrives studier og resultater af videnskabelige undersøgelser, som bidrager til at forstå de mekanismer og faktorer der kontrollerer kulstofcirkulationen og de grundlæggende processer som er ansvarlige for de observerede stigninger i optagelsen af kulstof.

Formålet med studierne har været at 1) evaluere i hvilket omfang og på hvilken tidsskala variationer i klimaet og forandringer i et økosystems funktionelle egenskaber kan forklare de observerede variationer i kulstofbalancen mellem forskellige år, 2) tilvejebringe en syntese over kulstofbalancen for det pågældende skovøkosystem og 3) at undersøge om procesbaserede computermodeller kan simulere den observerede stigning i økosystemets kulstofbinding.

I PhD studiet er der gennemført en serie af data analyser, semi-empirisk modellering og procesbaseret modellering med henblik på at afklare de mekanismer, der er ansvarlige for den observerede stigning. Resultaterne af undersøgelserne viser, at kulstofbalancen er mere følsom for korttidsvariationer i klimaet (variationer mellem år) sammenlignet med variationer og forandringer over lange tidsskalaer, og at denne følsomhed er sæsonafhængig. Analyserne viser desuden, at variationen i nettoudvekslingen af CO_2 (Net Ecosystem Exchange – NEE) mellem forskellige år primært er forårsaget af ændringer i økosystemet egenskaber. Dette betyder, at hvis procesbaserede computermodeller skal være i stand til at modellere kulstofudvekslingen under fremtidige klimaforhold, skal de være i stand til at repræsentere sådanne forandringer i økosystemers funktion og egenskaber dynamisk (ikke-stationaritet af økosystem egenskaber).

PhD studiet har samlet flere uafhængigt målte datasæt som beskriver NEE, trævækst, litter produktionen og jordrespirationen og usikkerhederne på disse data. Ved opstilling af massekonserveringsligninger kunne alle væsentlige parametre for skovens kulstofbalance bestemmes. Ved hjælp af sammenhængen mellem disse parametre er konsistensen af datasættet evalueret, hvilket er en vigtig forudsætning for at data kan anvendes til modelkalibrering. Analyserne har vist, at skoven var et moderat nettodræn for atmosfærisk CO_2. Størstedelen af af det assimilerede kulstof er blevet respireret i løbet af et år mens resten er blevet brugt i trævækst. Mængden af kulstof i jorden forblev derimod uforandret.

Den procesbaserede model (COUP modellen), som blev anvendt i dette studie, simulerede træernes fænologi og de observerede kulstoffluxe tilfredsstillende indenfor korte tidsskalaer (døgn og sæson) mens observationerne ikke kunne reproduceres over hele den 13 årige tidsserie når der blev anvendt et fælles parametersæt for økosystemets egenskaber for hele perioden. Hvis modellens parametre derimod blev tilpasset år for år, blev stigningen i kulstofoptag reproduceret tilfredsstillende. Dette indikerer, at udviklingen i skovens optag af kulstof er mere afhængig af funktionelle forhold i økosystemet end af klimatiske forhold. Især bidrog ændringer af de parametre der beskriver træernes evne til at udnytte lyset til fotosyntesen (light use efficiency - LUE) til de forbedrede modelresultater. Studierne viser desuden, at træernes kvælstof behov spiller en vigtig rolle i såkaldte "oldenår", hvor LUE var markant lavere

end gennemsnitligt. Kvælstoffets rolle kræver yderligere undersøgelser. Undersøgelserne understreger værdien og brugbarheden af procesbaserede computermodeller som værktøj til at forstå økosystemers dynamik og PhD-studiet understreger vigtigheden af at kombinere semi-empiriske og procesbaserede modeller med omfattende flerdimensionale feltdata som middel til at øge forståelsen af økosystemers funktion og dynamik og til at forudsige deres fremtidige kulstofdynamik.

TABLE OF CONTENTS

LIST OF PAPERS

Papers of this thesis:

I: Wu J., van der Linden L., Lasslop G., Carvalhais N., Pilegaard K., Beier C., and Ibrom A. 2012. Effects of climate variability and functional changes on the interannual variation of the carbon balance in a temperate deciduous forest. *Biogeosciences* 9:13-28.

II: Wu J., Larsen K.S., van der Linden L., Beier C., Pilgaard K., Ibrom A.. 2012. A synthesis on carbon cycling in a Danish, temperate deciduous forest. Submitted to *Agricultural and Forest Meteorology*.

III: Wu J., Jansson P-E, L. van der Linden, Pilgaard K., Beier C., and Ibrom A. 2012. Modelling the decadal trend of ecosystem carbon fluxes demonstrates the important role of biotic changes in a temperate deciduous forest. Submitted to *Ecological modelling*.

Related co-authored papers:

IV: Wang L., Ibrom A., Korhonen J. F. J., Arnoud Frumau K. F., **Wu, J.**, Pihlatie M., and Schjoerring J. K. 2012. Interactions between leaf nitrogen status and longevity in relation to N cycling in three contrasting European forest canopies. Accepted in *Biogeosciences*.

V: Campioli M., Verbeeck H., van den Bossche J., **Wu J.**, Ibrom A., Matteucci G., Samson R., Steppe, K., Granier A. 2012. Can source-sink relationships and growth rules simulate carbon allocation for growing seasons with contrasting weather conditions? A case study for temperate stands of *Fagus sylvatica L.* Submitted to *Ecological modelling*.

1. INTRODUCTION

Terrestrial ecosystems are dynamic components of the global carbon (C) cycle: they assimilate more than ten times the current annual anthropogenic carbon dioxide (CO_2) emission (from fossil fuel combustion and land use changes) through photosynthesis (Beer et al., 2010; Friedlingstein et al., 2010a). At the same time, a similar amount of CO_2 is released back to the atmosphere by respiration from soil microorganisms and plants. The difference between these two opposing fluxes determines the net C balance of the ecosystem, which was recently determined to be a sink of 1.0 to 2.6 petagram (Pg) C yr^{-1} globally (Metz, 2007). Forests are important C stocks, covering 31% of the earth's land surface (FAO, 2010) and storing approximately 861 Pg C (Pan et al., 2011), more than the total atmospheric C stock of 805 Pg (Houghton, 2007). The estimated gross C uptake by the world's forests (excluding the emission of 3 Pg C yr^{-1} due to tropical deforestation) is on average 4 Pg C yr^{-1} in 1990-2007 (Pan et al., 2011), equivalent to almost half of the anthropogenic C emissions in 2009 (Friedlingstein et al., 2010b).

Temperate forests contribute roughly 20% and 14% of the global forest area and forest C stock, respectively (Pan et al., 2011). Despite this relatively low proportion, the C sink in temperate forests has increased by 17% during the past two decades, contrary to boreal and tropical forests, which were unchanged and decreased by 23%, respectively. In Europe, temperate forests span large areas of the western and central parts (FAO, 2010). Historically, the natural composition of forests in Europe was mainly deciduous, until human management resulted in an increase in the proportion of conifers, predominantly for economic reasons (Spiecker, 2003). Today the distribution of coniferous species in the European temperate forests far exceeds their natural range. This has stimulated concerns about their ecological functioning and new management plans to reverse the compositional change of European forests to contain more deciduous tree species (Spiecker, 2003). Given the high C sink potential and increasing importance of temperate deciduous forests in the future, questions such as how they will respond to the changing climate and whether they can continue to serve as a strong sink of atmospheric CO_2 is of interest to scientists, policy makers and the public in general.

Long-term *in situ* monitoring is an important approach to investigate ecosystem C dynamics and its response to environmental changes. Technological developments, such as advances in Eddy-Covariance (EC) methods (Baldocchi, 2003) has enabled direct measurement of net atmosphere-biosphere exchange of carbon. By recording and analyzing the year to year variation in net ecosystem exchange of CO_2 (NEE) in response to different environmental conditions, the key factors and processes that determine the ecosystem C balance can be identified. The measured NEE based on the EC system is the difference between gross primary production (GPP) and total ecosystem respiration (TER) which are both much larger than the net flux. The responses of GPP and TER to climate are complex. Some processes are direct and instantaneous, for instance the light response of photosynthesis and the temperature effects on the kinetics of photosynthesis (Sage and Kubien, 2007) and respiration (Mahecha et al., 2010b). However, there are also indirect responses, especially through changes in phenology (Richardson et al., 2010), canopy structure (Barr et al., 2004; Ibrom et al., 2006) or physiological acclimation (Luo et al., 2001). Many studies have reported enhanced C uptake

as warming extended the length of growing seasons (Black et al., 2000; Chen et al., 1999; Churkina et al., 2005; Hollinger et al., 2004; Penuelas and Filella, 2009; Pilegaard et al., 2011; Richardson et al., 2009; Tanja et al., 2003). Others show that distribution and intensity of precipitation can also indirectly affect ecosystem C balance because the induced water stress may alter the leaf area index (Barr et al., 2007; Le Dantec et al., 2000), the carbohydrate reserve status (Sala et al., 2010), the plant allocation pattern (Sack and Grubb, 2002) or the soil microbial community (Sowerby et al., 2005). These indirect responses are often not instantaneous but lagged. Hu et al. (2010) observed that reduced snow cover in the winter led to water stress in the following summer and hence limited photosynthesis in a subalpine forest. Also, climate anomalies, e.g. high temperature in spring, can increase photosynthesis in the following autumn, possibly due to enhanced leaf nitrogen content and canopy photosynthetic capacity as a result of increased nitrogen mineralization (Richardson et al., 2009).

Generally, the indirect and lagged ecosystem responses are associated with biotic ecosystem internal dynamics (e.g. changes in the structure, physiological properties or species composition) and are thus regarded as ecosystem functional change (Richardson et al., 2007). Many studies have showed that to evaluate the climate change impacts on ecosystem C balance, it is necessary to jointly consider not only the direct impact of climate variability but also the ecosystem functional change (Braswell et al., 1997; Delpierre et al., 2009; Dunn et al., 2007), although the significance of functional change may differ in different types of ecosystems. Several empirical approaches have been developed to distinguish the relative impact of climate variability and functional change. For instance, Hui et al. (2003) used a homogeneity-of-slope model and a stepwise multiple regression approach to assess the effects of functional changes in a conifer forest, concluding that functional changes account for about 10% of the observed variation in the NEE. Richardson et al. (2007) used a modified light response model and found out that at annual time scale, as much as 55% of the variation in NEE could be attributed to the biotic responses in a mixed forest. In contrast, the effect of functional changes were found to be much lower in a peatland as it is probably less disturbed (Teklemariam et al., 2010). These differences implied a possible difference in the sensitivity of these ecosystems to environmental change and disturbance.

The effect of climate variability and functional changes on the ecosystem C cycling needs to be described and properly incorporated into process-based models, which are important tools to simulate the ecosystem responses and states under future climatic conditions. Within process-based models, eco-physiological processes can either be described mechanistically, e.g. the CO_2 diffusion through the stomata and leaf surface (Collatz et al., 1991) or semi-empirically, e.g. the light response of photosynthesis (Jarvis, 1976) and environmental controls on plant phenology (Hänninen, 1995; Richardson et al., 2012). Many different process-based ecosystem models have been developed and validated against measured C fluxes in different ecosystems. Generally, the models perform reasonably well at the site level to predict the seasonal or short-term interannual variability of ecosystem C fluxes (e.g. Williams et al., 2005; Wu et al., 2011). However, they have been found to be less able to reproduce the long-term dynamics (Keenan et al., 2012b). In a recent study, Keenan et al. (2012a) assessed the ability of 16 ecosystem models to simulate 11 long-term flux datasets and found that none of the models could

consistently reproduce the observed interannual variability in the C fluxes. Similarly, several cross-site model inter-comparison studies demonstrated strong divergences in model predictions (Kramer et al., 2002; Morales et al., 2005; Siqueira et al., 2006). One of the key reasons for these model uncertainties is that the ecosystem functional changes, such as the phenology were not yet well represented in the process-based models (Richardson et al. 2012).

The optimization of process models and the investigation of future ecosystem C cycling can be integrated in so-called model data fusion (MDF) studies (Wang et al., 2009). The uncertainty in the model projections can be reduced if the observed ecological datasets, especially those on the ecosystem carbon budget (ECB), i.e. carbon allocation and storage within an ecosystem, are assimilated by the model to constrain the model parameters and indentify possible model structural deficits. Such MDF studies are especially beneficial when they are conducted at specific sites which have been intensively studied for long periods, e.g. those have shown a decadal trend of increasing C uptakes (Keenan et al., 2012b; Pilegaard et al., 2011) to investigate whether model could identify the possible causes for the ecosystem responses, e.g. whether the trend is caused by climatic forcing or by internal ecosystem functional change.

The successful optimization of process-based models using MDF is strongly dependent on the information content and quality of the assimilated datasets. Therefore, a systematic quantification of the ECB datasets is important. Measuring the different components of the ECB is challenging (Metz, 2007). At plot scales, methods and protocols, e.g. eddy covariance (Baldocchi, 2003), chamber based flux measurement (Davidson et al., 2002) and biometric inventory (Clark et al., 2001) have been established. However, the degree of standardization is still low as there are different methodological alternatives that can be applied in each of these measurements or data processing procedures. When comparing the different ECB components, an important source of uncertainty is that these datasets are mostly measured at different spatial and temporal scales (Luyssaert et al., 2009). The consistency of ECB estimates is potentially affected by the inherent heterogeneity of the ecosystem and internal dynamics over time. Therefore, it is necessary that the individual components estimates are cross-checked against each other using e.g. a multiple constraints approach (Luyssaert et al., 2009) before being used in MDF studies. Prior to the consistency assessment, it is important that the uncertainties of the ECB component estimates are properly characterized. The data uncertainty is as important as the data values themselves (Raupach et al., 2005) for the optimization and development of process-based models (Friedlingstein et al., 2010b; Hänninen, 1995; Santaren et al., 2007). Therefore, a consistency and uncertainty estimates for the ECB datasets is a prerequisite for MDF study with process-based models (Hänninen, 1995; Raupach et al., 2005; Wang et al., 2009).

In this thesis, ecosystem C dynamics were systematically studied based on long-term (from 1997 to 2009) *in situ* monitoring of ecosystem C fluxes, C stock changes and other environmental variables in a temperate beech forest near Sorø, Denmark. A specific feature of this site is that there was a decadal trend of increasing C uptake of 23 g C m^{-2} yr^{-2} (Pilegaard et al., 2011) during the 13 year period. Therefore, it is particularly interesting to understand what are the fundamental drivers for such phenomenon. Empirical data analysis,

semi-empirical modelling and process-based modelling were combined to investigate the controlling factors at both short and long time scales.

1.1 Study objectives

The main objective of this thesis was to investigate the external effect of climate variability and the internal effect of functional change on the ecosystem C cycling in a temperate deciduous forest. We sought to acquire knowledge about the underlying ecosystem processes at the site, which could also be further used to optimize process-based models that can be used in projection for the future ecosystem states. The specific objectives are:

1) provide an overview about the ecosystem C dynamics and environmental changes during the long-term study period.

2) understand how climate variability affects ecosystem C fluxes at different time scales.

3) investigate the source of variability in carbon fluxes, i.e. the relative importance of climate variability and functional changes on the ecosystem C cycling.

4) provide a synthesis over all currently available ECB datasets at this site and derive complete assessment of the carbon balance and its components, including information about their uncertainty and consistency.

5) evaluate whether process-based models could dynamically simulate the changes in the ecosystem functioning and the long-term variability in the carbon uptake at this temperate deciduous forest.

1.2 Structure of the thesis

This thesis consists of three papers.

In **Paper I**, first we used a data-driven analysis to describe the interannual variability in observed C fluxes in response to environmental variables. Second, employing a semi-empirical model, we analyzed to what extent and at which temporal scales, climate variability and functional change affected the ecosystem C dynamics. The semi-empirical modelling approach developed in this paper for disentangling the effects of climate variability and functional change. This method improved upon that of Richardson et al. (2007), as it is able to capture seasonal patterns of ecosystem functional change and has the flexibility to be applied at other sites.

In **Paper II**, uncertainty and consistency assessments were performed for all the ECB components and a synthesis of the ECB datasets was derived. This enables us to (*i*) investigate the fate of the carbon in the ecosystem and (*ii*) ensure that the ECB datasets are consistent and can be used for the optimization of process-based models.

In **Paper III**, we used a process-based model to investigate the model's ability to simulate the long-term trend of increasing carbon uptake that was observed a this forest site. In this study, a process-based model was optimized and applied to simulate the ecosystem C dynamics, using a multiple constraint approach. The model performance was evaluated at diurnal, seasonal and inter-annual time scales and the drivers for the short-term variability and long-term trend of increasing carbon uptake were indentified.

The other two co-authored paper were not considered as part of this PhD thesis. However they are related to the theme of our study: 1) the results of this

thesis were used in **paper IV** ; 2) the leaf nitrogen status investigated in **paper V** is a key factor controlling the ecosystem functional change

2. MATERIAL AND METHODS

2.1 Site description

Field measurements were taken at the Euroflux network station Sorø on Zealand, Denmark (55°29´N, 11°38´E). Mean annual temperature during the measurement period was 8.5 °C and mean annual sum of precipitation was 564 mm. The dominant tree species is European beech (*Fagus sylvatica*) with approximately 20% conifers, mainly Norway spruce (*Picea abies*) and European larch (*Larix decidua*). In 2010, the stand around the flux tower was 89 years old, the average tree height was 28 m and the diameter at breast height was 41 cm. Soils were classified as Alfisols or Mollisols (depending on the base saturation) with 10-40 cm deep organic layers. Leaf area index peaked at 4-5 m^{-2} m^{-2} and no significant trend was observed in 2000-2009 (Pilegaard et al., 2011). Further information on the instrumentation can be found in Pilegaard et al. (2003). The fetch and footprint analysis are given in Dellwik and Jensen (2000, 2005), Göckede et al. (2008) and Pilegaard et al. (2011).

2.2 Field measurements and data processing methods

The datasets used in the analysis of this thesis include the Eddy Covariance (EC) based C fluxes (e.g. the NEE and partitioned GPP and TER) and inventory based ancillary datasets (e.g. soil respiration, litter production and biomass C stocks). These continuously or discontinuously measured the ecosystem C fluxes and budgets were also up-scaled to an annual basis using different methods. In the following sections the direct measurements, post-processing and up-scaling methods are presented.

2.2.1 NEE

The NEE between the biosphere and atmosphere was measured with a closed path EC system at 43 m above ground and the data processing followed the standard procedure of Aubinet et al. (2000). Spectral corrections were applied to the flux data according to Ibrom et al. (2007), using a spectral transfer function approach. The data processing procedure generally comprises (1) storage correction; (2) correction for low turbulent mixing (u_* filtering) and (3) gapfilling. In **paper II**, we also developed a new approach to investigate the source area inhomogeneity related uncertainties on the annual NEE estimates. The details are presented in the sections that follow.

In **paper I** and **III**, the flux data from this site in 1997-2009 were corrected for storage change (S_c) in the air column underneath the sensor using the concentration measurements at the EC system (43 m). In paper II, we derived a new estimate of S_c with data obtained from a profile system in 2005-2009. The S_c was calculated according to Aubinet et al. (2001) in Eq. 1 and added to the measured flux.

$$S_c = \frac{P_a}{R \cdot T_a} \int_0^h \frac{\partial c(z)}{\partial t} dz \quad (1)$$

where P_a is the atmospheric pressure (Pa), R is the universal gas constant (J K^{-1} mol^{-1}), T_a is the air temperature (K), c is the CO_2 concentration (mol fraction) at specific height (z) along the vertical profile (7 depths) and t is time.

In general, the measured carbon fluxes are systematically lower when the wind speed fell below a certain threshold (Papale et al., 2006). This is interpreted as an effect of unmeasured advective mass transport. To avoid a systematic underestimation, the turbulent flux data were filtered for low turbulent mixing at stable stratification. In **paper I**, the fluxes were filtered for low turbulent mixing at stable stratification when the friction velocity was lower than 0.1 m s^{-1}. In **paper II**, two different criteria were applied in order to evaluate the uncertainty caused by the u_* filtering. Firstly, in accordance with paper I, the nighttime fluxes were filtered when the friction velocity (u_*) was smaller than 0.1 m s^{-1} in all years. These filtered NEE datasets are denoted as $NEE_{0.1}$. Secondly, we applied the method according to Papale et al. (2006), which is currently the standard data processing procedure in the FLUXNET network. With this method, the u_* filtering was for both daytime and nighttime data, the u_* threshold varied between years and was, on average, about 0.25 m s^{-1}, these filtered NEE datasets are denoted as $NEE_{0.25}$. In **paper III**, the non-gapfilled $NEE_{0.25}$ data were used to optimize the process-based model.

Gapfilling was needed to derive annual estimates for the ecosystem C budget. In **paper I**, the gaps in the NEE datasets were filled with a moving look-up table, as described in Pilegaard et al. (2011). In **paper II**, we used two other methods for gapfilling including the marginal distribution sampling (MDS; Reichstein et al., 2005) and a hyperbolic light response regression model based on daytime data (HBLR; Lasslop et al., 2010). The uncertainty produced by the gapfilling methods was evaluated by comparing the different estimates. In **paper III**, only non-gapfilled NEE datasets were used.

Apart from the uncertainties related to S_c, u_* filtering and gapfilling, a so far unresolved problem for the EC measurements is the estimation of the uncertainty in NEE due to fetch limitation and site inhomogeneity. Micrometeorological flux measurements require large homogeneous source areas that can, however, hardly be met in many FLUXNET sites. The natural site variability and human interventions such as clear cut and thinning can lead to structural and functional variability within the footprint of the flux measurements. Depending on wind direction and atmospheric stability, the flux source area changes over time. Therefore, the annual sums of NEE might be biased to certain sectors of the site due to the frequency distribution of the wind directions. Therefore, in **paper II**, we developed a simple empirical approach to evaluate the effects of horizontal inhomogeneity on annual NEE estimates at our site. This effect was estimated by comparing the NEE datasets (complete and only the daytime or nighttime NEE) from 8 different forest sectors (classified by 8 wind directions) at similar environmental conditions (T_a, short wave radiation, R_g, and volumetric soil water content, θ) and ecosystem functional states (leafed and non-leafed periods).

The analysis consisted of 4 steps. In the first step, the complete (K), daytime (J) and nighttime (L) NEE datasets were classified into 1000, 1000 and 100 potential conditions, respectively, for the flux comparison based on a full factorial combination of 10 equal sample size T_a classes, 10 daytime R_g classes (for nighttime 1 radiation class), 5 θ and 2 functional classes (leafed and non leafed periods). The specific condition (e.g. non-leafed period when the T_a is with 2-5°C, R_g is within 34-96 W and θ is within 20-25%) for the flux comparison is denoted as Ω. The actual number of Ω (K, J or L) is lower than the potential value (1000, 1000, 100) because not all the combinations exist, and as the analyses are conducted only at Ω when NEE fluxes exist in all the 8

wind directions. In the second step, the mean NEE (for the complete, daytime or nighttime datasets) at each Ω was calculated for all the eight wind directions. The fluxes from different wind direction at the same Ω are expected to be the same if the site is homogeneous. Following this, a weighted average NEE for each wind direction, which took into account the frequency of each Ω was calculated in Eq. 2:

$$F_{wdi} = \frac{\sum_{k=1}^{K} (\overline{f}_{\Omega_k, wd_i} \varpi_{\Omega_k})}{\sum_{k=1}^{K} \varpi_{\Omega_k}} \quad (2)$$

where $f_{\Omega k,wdi}$ are the mean NEE (complete, daytime or night time respectively) from the i^{th} wind direction at each specific Ω; $\omega_{\Omega k}$ are the frequency of each Ω.

In the third step, the estimated F_{wdi} was normalized Eq. 3. The derived, $F_{wdi,\,norm}$ represent the relative deviations of the NEE from a certain forest sector from the average. These values were further compared with the forest compositions in the corresponding sectors.

$$F_{wdi,\,norm} = \frac{F_{wdi}}{\overline{F_{wdi}}} \quad (3)$$

2.2.2 GPP and TER

The observed NEE is the net flux of two opposing fluxes, GPP and TER; these can be partitioned from the directly measured NEE using empirical methods. In **paper I**, TER was estimated based on nighttime data and extrapolated to daytime conditions according to the Eq. 4:

$$\mathrm{TER} = r_b Q_{10}^{\frac{T_s - T_0}{10}} \quad (4)$$

where T_0 is the reference soil temperature at 2 cm depth (0 °C), r_b is the base respiration at T_0, T_s is the measured soil temperature at 2 cm and Q_{10} is the temperature sensitivity parameter and set to a constant value of 2. Base respiration was estimated for every night and Eq.1 was used to extrapolate the nighttime ecosystem respiration over daytime based on soil temperature measured at daytime. GPP is thus calculated as the difference between TER and NEE.

In **paper II**, we used two flux partitioning methods to assess the uncertainties of partitioning methods on estimated GPP and TER. Two methods were used including: (1) nighttime based (NB; Reichstein et al., 2005): respiration measured at night was extrapolated to daytime using the short term air temperature regression model; (2) daytime based (DB; Lasslop et al., 2010): a hyperbolic light response curve, which takes into account the temperature sensitivity of respiration and the VPD limitation of photosynthesis, was fitted to daytime NEE. The uncertainty due to flux partitioning is also characterized by comparing all the different GPP and TER estimates.

2.2.3 Soil respiration

Soil respiration (R_s) was an important ecosystem C fluxes. It was measured using a portable gas exchange system combined with a soil CO_2 flux chamber (LI-6400; LICOR Bioscience, Lincoln, NE, USA). Twelve permanent collars were inserted into the soil one year before the measurements started. R_s was measured every two weeks or monthly between the year 2002-2005 and 2008-

2009. On most days, measurements were made hourly between 9:00 and 15:00 in 12 replicated locations (i.e. 84 measurements per day). Additional, there was a one-day campaign when R_s was measured over 24 hours. Three empirical R_s models were parameterized to extrapolate the discontinuous R_s measurements to form a continuous time series and an annual R_s budget. The models fitted were as follows:

Model I (Eq. 5):

$$R_s = R_{10} Q_{10}^{(T_s - T_{10})/10} \tag{5}$$

where R_{10} is R_s at reference temperature T_{10}; Q_{10} is the temperature sensitivity; T_s is the soil temperature.

Model II after (Beven and Freer, 2001):

$$R_s = R_{283} \exp\left[-E_0\left(\frac{1}{T_s + 273.15 - T_0} - \frac{1}{T - T_0}\right)\right] \tag{6}$$

where R_{283} is the base respiration at soil temperature of 10°C ; T_0 and E_0 are the fitted parameters.

Model III, which considers the soil water content, after (Granier et al., 2000):

$$R_s = a_0 \theta \exp(b_0 T_s) \tag{7}$$

where θ is the soil water content and T_s is the soil temperature; a_0 and b_0 are the fitted parameters.

We used Bayesian calibration, which simultaneously takes into account the uncertainties in the input data and uses the model structures to estimate the probability distributions of the model parameters, thus quantifying the uncertainty in the model predictions (Linkosalo et al., 2000). For this the Markov Chain Monte Carlo (MCMC) Metropolis-Hastings random walk algorithm was used to search for the posterior distribution within the initially defined prior distribution of the parameter space. The likelihood function L is given in Eq. 8:

$$L = \prod_{i=1}^{n} \frac{1}{\sqrt{2\pi\sigma_i^2}} \exp\left[-\frac{1}{2}\left(\frac{o_i - s_i}{\sigma_i}\right)^2\right] \tag{8}$$

where o_i is the ith observation; s_i is the ith simulated value; σ_i is the data uncertainty, represented as the standard deviation of the R_s measurements. The prior distribution of each parameter was defined according to values published in peer-reviewed literature; these distributions were sampled over the 50000 MCMC iterations performed for each model.

2.2.4 Litter production

Aboveground litter (L_{AG}) was collected in 25 litter traps (80 cm diameter) located southwest of the flux tower (Pilegaard et al., 2003) since 2003. Litter was collected from the traps every 2 months, oven dried (70 °C) and weighed. The measured C concentration in the litter samples was 0.51 g C per g dry mass. Total litter fall was calculated as the product of the average net weight and C concentrations, divided by the average sampling area of the litter traps (0.5 m^{-2}). The below ground litter inputs (L_{BG}) was not directly measured during the study period and assumed to be the same as fine root productions, calculated according to a DBH dependent regression model (Le Goff and Ottorini, 2001).

2.2.5 Tree growth

Tree growth for both the aboveground ground (G_{AG}) and belowground (G_{BG}) compartments were estimated based on tree ring data, height measurements, biomass expansion functions (BEF) and carbon content of the specific plant compartments. In December 2009, 102 tree ring cores (2 cores per tree) were taken in a central plot proximal to the tower and a sub-plot covering the fetch to the prevailing wind direction (Flurin Babst and David Frank, Swiss Federal Institute of Technology, WSL, Switzerland). The summed tree ring widths were in accordance with DBH measurements in 2009, therefore the annual tree ring width was used as an approximation of DBH increments. Tree heights were measured in 2005 and 2008-2010 and a linear increment from 2005-2007 was assumed. The compartments of the standing biomass (stem, branches and coarse roots) for individual trees were calculated according to a BEF specific for beech trees in Denmark (Wu et al., 2012). The standard error of the fitted parameter of the BEF was used to propagate the uncertainty range of the biomass stock and increment using 1000 Monte Carlo iterations. The carbon content of the biomass was measured in the European project Forest carbon and nitrogen trajectories (FORCAST) and set as 0.46, 0.47, and 0.48 g C per g dry mass for the stem, branches and coarse roots, respectively (personal communication, Giorgio Matteucci, CNR-ISAFOM, Italy). The stand was thinned in the beginning of the study period with a reduction of tree density by ca. 10 %. In the year of thinning, the tree growth was estimated as the sum of biomass increment and the mass of the harvested trees. The relation between of exported wood and biomass that was left on site was estimated using the BEF functions for brushwood and total tree biomass after Wutzler et al. (2008). It was assumed that timber was completely exported from the forest, while the remainder was converted to woody debris.

2.3 A synthesis of the Ecosystem C budget (ECB)

In **paper II**, a synthesis for the ECB at this site was conducted. This provided information on the C flow into the ecosystem through photosynthesis, C flow out of the ecosystem through respiration or leaching in different compartments and storage either the plant increment, soil organic matter enrichments or biomass extractions. Because not all the ECB components were directly measured, the independently estimated ECB components from study, i.e. the EC-based estimates of NEP, GPP and Re, chamber-based estimates of Rs, inventory-based estimates of L_{AG}, L_{BG}, G_{AG}, G_{BG}, together with the estimated leaching of dissolved organic carbon (DOC_{leach}) by Kindler et al. (2010) in 2006-2008 were used to derive other unmeasured ECB components using the mass balance equations. The calculation follows 5 steps as in Eq. 9-14. Firstly the net primary production (NPP) was calculated as the sum of growth and litter production (Eq. 9).

$$\mathrm{NPP} = G_{AG} + G_{BG} + L_{AG} + L_{BG} \quad (9)$$

Secondly, autotrophic respiration, R_a was calculated as the difference between GPP and NPP:

$$R_a = \mathrm{GPP} - \mathrm{NPP} \quad (10)$$

In the third step, heterotrophic respiration R_h was calculated as the difference between R_e and R_a in Eq. 11. Subsequently, the below ground autotrophic respiration $R_{a,\,BG}$ was calculated as the difference between R_s and R_h as Eq. 12

while $R_{a,\,AG}$ was derived as Eq. 13. The change in the SOC pools ΔSOC was calculated in Eq. 28.

$$R_h = R_e - R_a \tag{11}$$

$$R_{a,\,BG} = R_s - R_h \tag{12}$$

$$R_{a,\,AG} = R_a - R_{a,\,BG} \tag{13}$$

$$\Delta SOC = L_{AG} + L_{BG} - R_h - DOC_{leach} \tag{14}$$

2.4 Data-driven analysis: direct effects of climate variability on C fluxes

To evaluate the ecosystem response to climatic variability, bivariate correlation analysis was performed in **paper I** between integrals of the annual carbon fluxes and mean annual climate variables, i.e. air temperature T_{air}, global radiation R_g, volumetric soil water content SWC in the top soil, and precipitation PPT, using data from 13 years. In the second step, the same correlation analysis was applied at sub-annual time scale with a 30 day moving window. Pearson's correlation coefficients (n=13) were calculated between periodical flux integrals (30 day sum of the GPP and TER) and mean periodical climate variables (e.g. mean T_{air} for DOY 1-30) from each of the 13 years. With the 30 day moving window, the first correlation coefficient calculated represented the period DOY 1-30 and was centred at DOY 15. The second correlation coefficient was calculated by moving the window one day forward, representing the period DOY 2-31. In this way, correlation coefficients were calculated throughout the whole year. The resulting time series of correlation coefficients related the interannual variability of the carbon flux to a potential climatic driver in a certain period of a year. This enabled the analysis of interannual variability at sub-annual time scales.

2.5 Semi-empirical modelling

In **paper I**, a semi-empirical modelling approach was developed to distinguish the relative impact of direct climate variability and functional changes on the interannual variability in NEE. The analysis consists of two steps.

In the first step, the annual NEE datasets were used to estimate a set of parameters of the a semi-empirical model, which consisted of a rectangular hyperbolic light response model (Falge et al., 2001) and a Lloyd & Taylor (1994) respiration model. The effects of air humidity on photosynthesis was modelled after Körner (1995). The model is described in Eq. 15 and 16. The interannual variation of the parameter estimates was interpreted as functional changes.

$$NEE = -\frac{\alpha\beta R_g}{\alpha R_g + \beta} + r_b \exp\left(E_0\left(\frac{1}{T_{ref} - T_0} - \frac{1}{T_{air} - T_0}\right)\right) \tag{15}$$

where T_{air} is the air temperature; T_0 (°C) is a constant (-46.02 °C); R_g (W m^{-2}) is the global radiation; a (µmol CO_2 J^{-1}) is the light use efficiency; β (µmol CO_2 m^{-2} s^{-1}) is the instantaneous maximum canopy photosynthetic capacity (Eq. 4), which represents both the structural and physiological properties (e.g. leaf area index, leaf photosynthesis capacity, C3 or C4 photosynthesis pathway species composition); r_b (µmol CO_2 m^{-2} s^{-1}) is the base respiration at reference temperature (T_{ref}=15 °C); E_0 (°C) is the temperature sensitivity.

$$\beta = \begin{cases} \beta_0, \text{VPD}<\text{VPD}_0 \\ \beta_0 \exp\left(-k\left(\text{VPD-VPD}_0\right)\right), \text{VPD}>\text{VPD}_0 \end{cases} \quad (16)$$

where k (hPa^{-1}) is a scaling parameter estimating the effects of vapour pressure deficit (VPD) on β and VPD_0 is a threshold value set as 10 hPa, above which the stomatal conductance reduces β. The parameters (E_0, r_b, a, β, k) of the model were estimated in two steps:

(1) All parameters were allowed to vary throughout the year: E_0 was derived from nighttime NEE every 2 days using a 12 day window. a, β, r_b and k were estimated based on daytime NEE every two days, with a 4 day moving window.

(2) In the first step, the parameters k and E_0 were not well constrained. Therefore, we fixed E_0 and k as the median of the previous estimates (E_0=141.4 °C, k=0.09 hPa^{-1}), after which a, β, and r_b were re-estimated based on daytime data every two days, with a 4 day moving window. Parameter estimation was conducted by minimizing the same weighted least squares cost function as in the first modelling approach (for details see Lasslop et al., 2010) and the half-hourly fluxes were computed using gap-filled parameter sets (distance weighted average between the two adjacent parameters) and climate data.

In the second step, the parameter and climate time series were applied to distinguish the effect of climate variability and functional changes on NEE using a "cross-modelling" approach. By application of the parameter time series of one year to all the other years and comparing the differences in the modelled fluxes, the effects of direct climate forcing on the carbon fluxes can be investigated, and *vice versa* for the effects of the parameters. Model simulations with fixed climate (using climate data of one year for all other years) and fixed parameters (using parameter dataset of one year for all other years) were performed, resulting in a 13 x 13 matrix of model predictions. In each cell of this matrix, the simulated results contained 17520 half-hourly data points, which were further aggregated by day, week, month, season and year for statistical analysis. Therefore, the datasets in each column represented the modelled fluxes with fixed climate using climate data of a particular year i ($F_{clifix,\ i}$) and the datasets in each row represented the modelled fluxes with fixed parameter using parameter time series of year i ($F_{parfix,\ i}$). The diagonal of the matrix represents the original modelled fluxes ($F_{original}$). The differences between $F_{original}$ and F_{clifix} represent the variability that is driven directly by the climate while the differences between $F_{original}$ and F_{parfix} represent the variability that is driven by the changing model parameters, which we interpret as functional change. We applied a sums of squares approach to distinguish between the relative effect of climate and model parameters on the IAV in NEE, GPP and TER at multiple time scales ranging from daily to yearly. The proportion of IAV in the carbon fluxes explained by climate variability (E_{cli}) and parameter change (E_{par}) was determined by Eq. 17 and Eq. 18, respectively.

$$E_{cli} = \overline{\sigma(F_{original} - F_{clifix,i})} \Big/ \left(\overline{\sigma(F_{original} - F_{clifix,i})} + \overline{\sigma(F_{original} - F_{parfix,i})}\right) \quad (17)$$

where σ is the variance of the interannual variation of the carbon fluxes.

$$E_{par} = 1 - E_{cli} \quad (18)$$

2.6 Process-based modelling

Process-based models are important tools to simulate the ecosystem responses and states under future climatic conditions. In **paper III**, we applied a dynamic ecosystem model, CoupModel, to simulate the changes in the ecosystem functioning (e.g. phenology and canopy development) and the long-term variability in the carbon uptake at this site. Based on the information obtained from the ECB synthesis in **paper II**, a multiple constrain approach was implemented to optimize the model.

CoupModel is a one-dimensional process-based ecosystem model that can be used to simulate the coupled biological and physical processes in soil-plant-atmosphere systems (Jansson, 2012; Jansson and Karlberg, 2004; Jansson et al., 2008). Hourly meteorological measurements of air temperature, global radiation, relative humidity, wind speed and precipitation were used as boundary conditions. The model represents vertical layers of the soil profile and heat and water fluxes are calculated based on the soil physical parameters and climate inputs. The simulated soil temperature and moisture, together with the climate drivers regulate the biotic ecosystem processes such as phenology, photosynthesis, plant respiration and decomposition of litter and soil organic matter. In addition, the biotic ecosystem dynamics feedback to the simulated physical environment. For instance, the simulated plant structure will affect the aerodynamic conductance at the atmosphere and leaf surface; likewise, changes in LAI alter the energy and water balance at the soil surface. A detailed description of CoupModel can be found in Jansson and Moon (2001), Jansson and Karlberg (2004) and Wu et al. (2011). The model equations and parameters relevant for this paper are given in Appendix 1 in **paper III**.

In this study, the model was initialized in August 1996 and calibrated for the period 1997-2009. The initial C pools in the vegetation and soil were given as parameters based on the measured ancillary datasets. The soil physical parameters were either measured, e.g. parameters for the water retention curve or estimated based on soil texture data, e.g. the soil thermal properties. Some biological parameters such as the specific leaf area and plant height were also measured on site. The data necessary for the model initialization are available in BADM (Biological-ancillary-disturbance-management) format at the European Fluxes Database (http://gaia.agraria.unitus.it/).

Two modelling experiments were performed. In the first, the model was calibrated against the whole 13 year (1997-2009) datasets, where 29 parameters that were expected to be sensitive to the carbon and water dynamics (Table 1 in **paper III**) were selected for calibration according to experiences of model application and a sensitivity study by Svensson et al. (2008b). The prior distributions of the model parameters were set to reasonably wide ranges with uniform distributions that were based on literature and previous model applications (e.g. Svensson et al., 2008a; Wu et al., 2011). A total of 30000 model runs were performed in the first modelling experiment sampling the parameter values from uniform distributions.

The acceptance of behavioural models (i.e. models simulation with same structure but different parameter values) was based on specific user-defined criteria (Beven and Freer, 2001; Liu et al., 2009). Two different constraints were considered: 1) only the hourly NEE datasets (denoted as Ω_{NEE}) and 2) multiple constrain approach using the hourly daytime and night-time NEE, latent (λE) and sensible heat (H) fluxes and other ancillary datasets (denoted as

$\Omega_{Multiple}$) were used to select the behavioural models to determine the posterior parameter distributions.

In order to test the hypothesis that functional changes in the ecosystem (e.g. light use efficiency, humus decomposition rates) has occurred over the period of observation and affected the annual C uptake capacity of the forest, a second modelling experiment (3000 model runs) was designed based on the optimized posterior parameter sets in the first modelling experiment. In this modelling experiment, the number of sampled parameters was reduced to seven of those that control photosynthesis and respiration and they were allowed to vary between years. In this way the inter-annual variability of ecosystem functioning is captured and represented by the parameter estimates generated for each year.

3. RESULTS

3.1 Interannual variability in the climate and carbon fluxes

The interannual variation in NEE (a negative sign corresponding to carbon uptake) and the climate variables were analyzed at both sub-annual (daily value smoothed with a 30-day moving average) and annual time scales in **paper I**. The variability is displayed as fluctuations (around the mean) relative to the standard deviations in a certain time window over the 13 years (Fig. 1). This presentation enables a standardized comparison of the anomalies in both carbon fluxes and climate variables with their interannual variability, during a particular period of a given year.

In 1998, the forest was a source of carbon where the deviation of NEE from the 13-year annual mean was about 2 standard deviations (SD) above average (more positive corresponding to less uptake). Following this, a trend of increasing carbon uptake in the forest was observed, manifested in a higher net uptake during the latest years 2008-2009 when the NEE was almost 2SD below average (Fig. 1). Except for these years, the annual NEE deviations were less than 1 SD. Generally, there was a tendency from above average towards below average except in 2003 and 2006, when the forest appeared to have a reduced rate of carbon uptake.

At sub-annual time scales, carbon uptake was less than average in almost all periods of the years from 1997 to 1999, except in autumn 1999 when the uptake was about 1SD above average. In 2000-2006 the NEE anomaly fluctuated remarkably within each year, ranging from 2 SD above average in winter 2000 to 2 SD below average in autumn 2005. Regardless of the high variability at short time scales, these NEE anomalies tended to compensate each other, resulting in annual fluxes close to the 13 year average. From 2007 to 2009, NEE was continuously below average with higher carbon uptake except in two short periods of summer 2007 and the beginning of 2008.

The mean annual air temperature of the only source year 1998 was the lowest over the 13 year period, with more than 1 SD below average. Meanwhile, overcast weather (lowest incoming radiation) and the slightly higher than average precipitation kept the soil water content at 1 SD above average. The opposite conditions prevailed in 2008 compared to 1998, when a higher radiation (almost 2 SD above average) was accompanied with higher air temperature and evaporative demand which significantly reduced the soil water content.

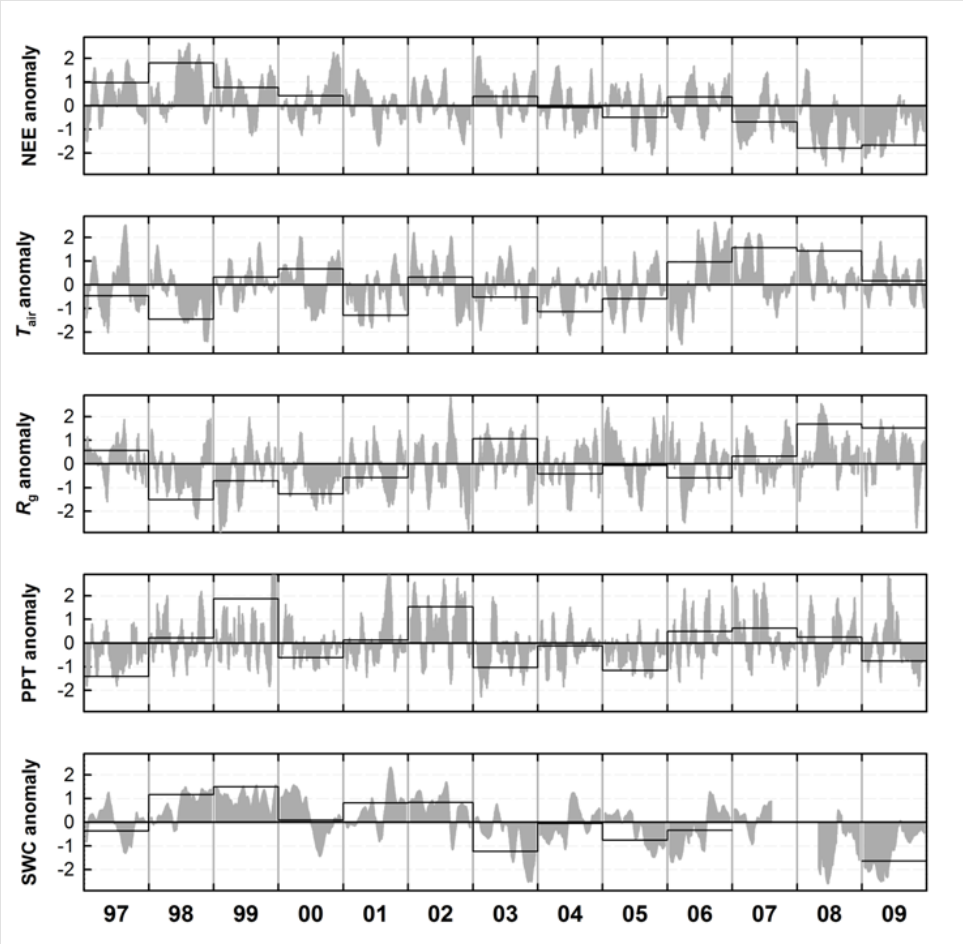

Fig. 1: Deviation of NEE, air temperature (T_{air}), global radiation (R_g), precipitation (PPT) and soil water content (SWC) from the 13-year annual average (black solid line) and daily average values (grey areas). The daily data were smoothed with a 30 day moving average. The y-axis gives the standard deviation from the mean (e.g. the annual NEE anomaly in 1998 is about 2 SD above the 13-year average with less uptake of carbon).

3.2 Direct effects of climatic variability on ecosystem C cycling

The correlation analysis in **paper I** (c.f. section 2.4) showed that at the annual time scale, none of the climate variables had a significant correlation with the component C fluxes. However, the correlations were found significant at shorter time scales (Fig. 2). Gross primary production was highly correlated with T_{air} ($r<-0.69$, $p<0.01$) throughout the entire year except during the summer (Fig. 2a). When the soil was usually dry in the summer, it apparently confounded the stimulating effects of temperature on photosynthesis. The correlation coefficient between GPP and T_{air} was lowest ($r<-0.8$, $p<0.01$) in April (leaf flush) and October (leaf fall), indicating that the phenology and leaf development were temperature sensitive. Radiation was also negatively correlated with GPP during spring and autumn. The correlation coefficients increased directly after leaf senescence but decreased during winter, representing the photosynthesis of the conifers that account for 20% of the trees within the footprint. Over a large part of the year, the correlation between GPP and SWC was not significant, possibly because the deep rooting system allowed sufficient water supply even when the water in the top soil was depleted. Nevertheless, a trend of decreasing correlation coefficients during the

summer was obvious and the value was lowest in Aug-Sep. The correlation between T_{air} and TER (Fig. 2b) was positive during the spring, autumn and winter but also turned negative during summer due to the confounding effect of SWC. TER and GPP were significantly correlated during large parts of spring and summer.

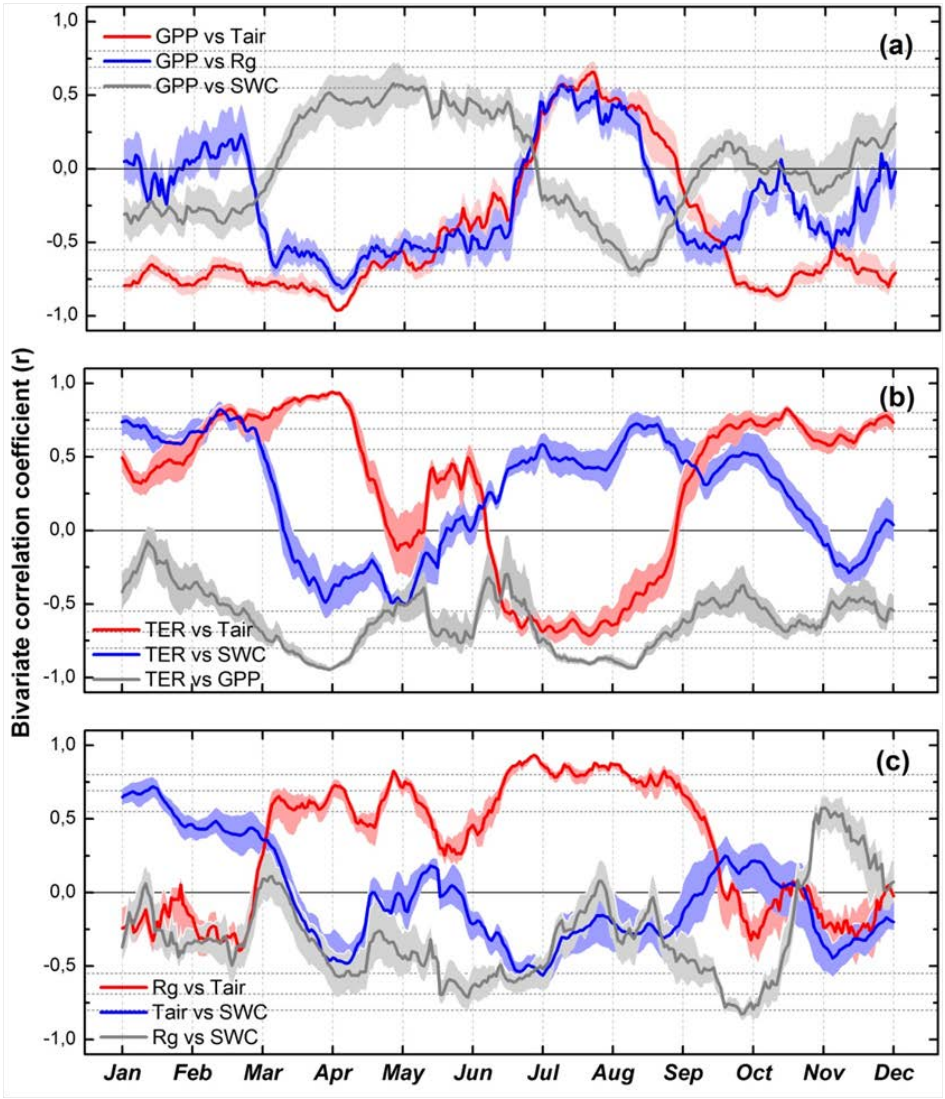

Fig. 2: Bivariate correlation between**: (a)** periodical GPP integral (30 day moving window) with periodical mean air temperature (T_{air}), soil water content (SWC) and global radiation (R_g). **(b):** periodical TER integral with periodical mean climate variables and GPP. **(c):** the climate variables. Dashed horizontal lines indicate different levels of statistical significance (p=0.05, 0.01 and 0.001). The shaded area indicates the uncertainties of the correlation coefficients, as data of each individual year was excluded from the correlation analysis.

Because the climate variables were also inter correlated (Fig. 2c), the attribution of the interannual variability in carbon flux to specific climatic variables was sometimes difficult. Therefore, a semi-empirical model were used as a tool to systematically investigate how much the ecosystem C dynamics can be attributed to the direct effect of climate variability in **paper I**. The analysis of the 13 x 13 matrix of model predictions (see section 2.5) showed that at annual time scales, only 18-22% of the variance in NEE can be explained by

interannual variation in the climate variables (Fig. 3). In general, the percentage of the total variance in the carbon flux caused by climate variability decreased with the level of temporal integration. GPP was much more sensitive to variation in climate than TER was. At the daily time scale, climate variability accounted for more than 67-71% of the variation in GPP. The effect of climate variability on TER was very low (19-22%), even at the daily time scale. This is most likely because the dominant component of TER is soil respiration, a process which is highly dependent on substrate availability and microbial activities (Davidson et al., 2006). This then results in reduced climatic effects on TER, compared to the above-ground processes, such as photosynthesis and phenology. On the other hand, because GPP and TER are only influenced by certain climate variables in the model structure (Eq. 16 and 17), the unaccounted effect of other climate variables (e.g. soil water content) on GPP and TER could be propagated into the parameters and thus result in the underestimation of the effect of climate variability.

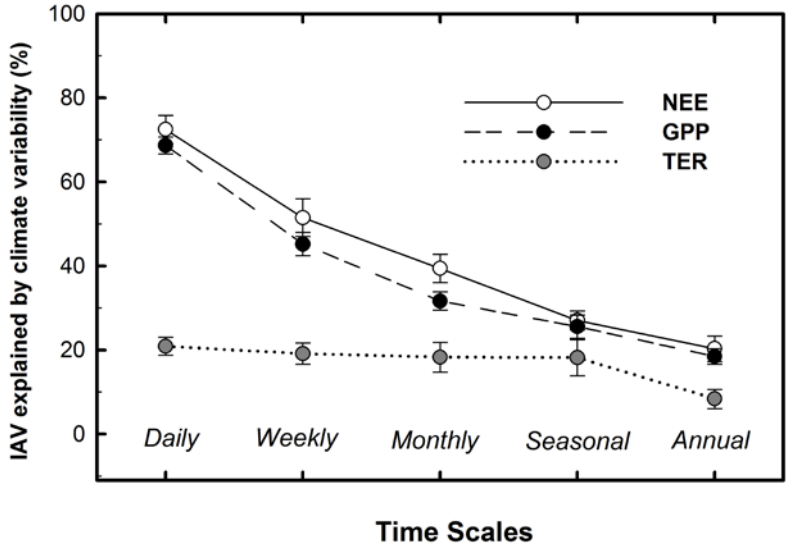

Fig. 3: Percentage of interannual variation in modelled carbon fluxes caused by climatic variability at different time scales calculated with the semi-empirical model (Eq. 15-16). The error bars show the standard deviation of the estimates.

The effect of climate variability on ecosystem C cycling was also investigated in a process-based modelling study in **paper III**. The applied CoupModel was driven by the climatic forcing and well represented the ecosystem C dynamics at diurnal and seasonal time scales. The monthly diurnal course for the model-data mismatch (Fig. 4) showed that the diurnal cycle was well simulated throughout the year. In April the simulated daytime NEE was apparently lower than the measurements, due to the unaccounted small fraction of coniferous photosynthesis in the model. After May when the canopy was fully developed, the starting and ending of photosynthesis were correctly represented by the model, although the C uptake during mid-day was slightly overestimated. The magnitude of night-time NEE was also well simulated during both the winter and the growing season.

3.3 Effects of functional changes on ecosystem C cycling

One main objective of this study was to separate the influence of functional change from direct effects of climatic variability. This was achieved by

analyzing simulations of the semi-empirical model with fixed climate or parameters (c.f. section 2.5) in **paper I**. Based on the analysis, we found that other photosynthesis and respiration related parameters were changed in different years and indirectly affected the ecosystem C balance. Interannual variation in the modelled NEE differed when either the parameters or the climate variables were fixed (Fig. 5).

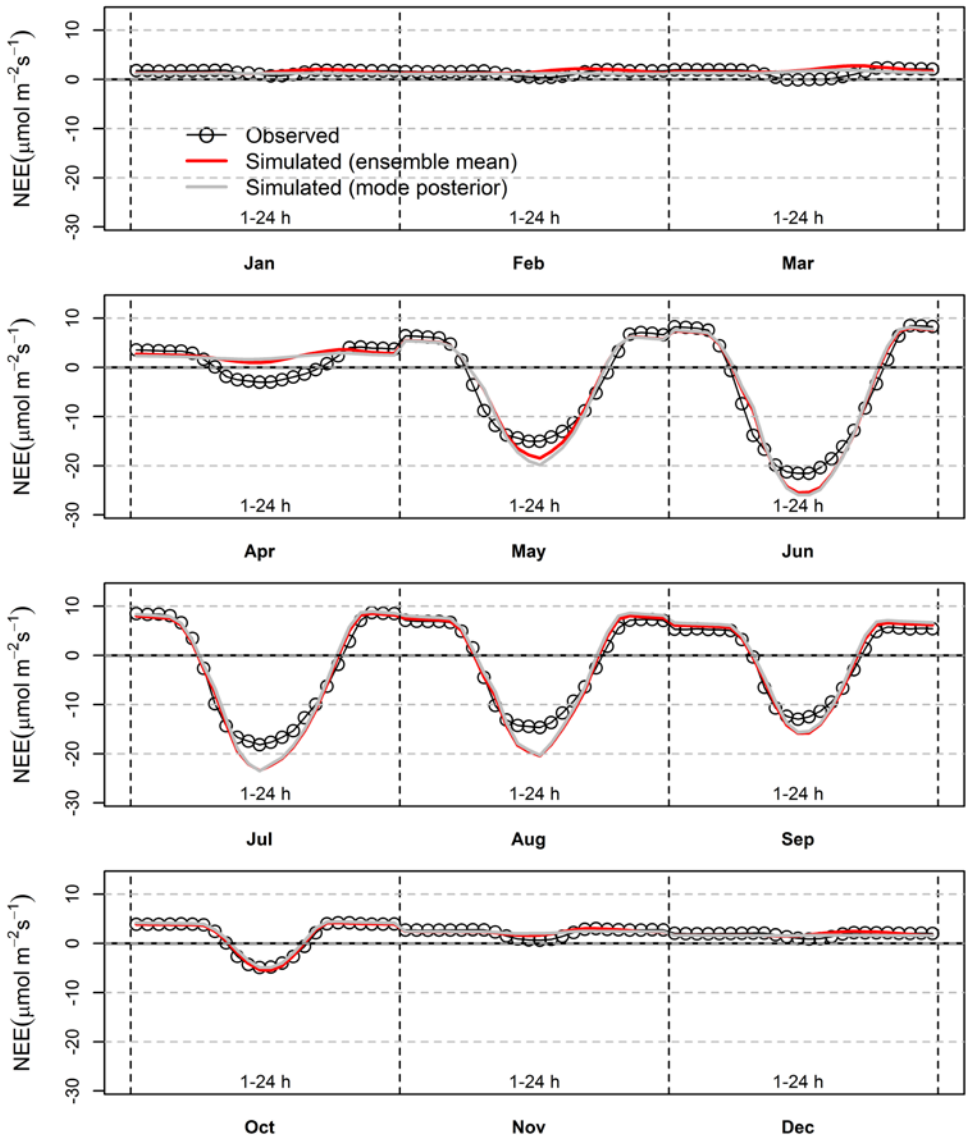

Figure 4: Observed and simulated averaged, diurnal course of NEE (ensemble mean and single run using the mode of the posterior parameter distribution) from Jan to Dec.

When the parameters were fixed, i.e. assuming the ecosystem status during the 13 years was constant (Fig. 5b), the modelled fluxes NEE_{parfix} ranged between -231 g C m^{-2} yr^{-1} in 2009 and -27 g C m^{-2} yr^{-1} in 2006. When the climate time series were fixed, NEE_{clifix} ranged between 81 g C m^{-2} yr^{-1} in 1998 and -293 g C m^{-2} yr^{-1} in 2005 (Fig. 5c). The IAV in the originally modelled fluxes $NEE_{original}$ (Fig. 6a) were better reproduced when the changes in the parameter time series were included. The correlation between the $NEE_{original}$ and NEE_{clifix} was 0.9

($p<0.01$). In contrast, correlation between the NEE_{parfix} and $NEE_{original}$ was not significant. This showed that that the 13 year trend of increasing carbon uptake was more strongly driven by the aggregated effect of the parameters than the climatic factors. As was shown in Fig. 3, about 78-82% of the variance in NEE was attributable to the functional change at annual time scales.

The functional change effect on ecosystem C cycling at longer time scales was supported by the process-based modelling results in **paper III.** With the globally fitted parameter sets in the first modelling experiment (i.e. calibrated

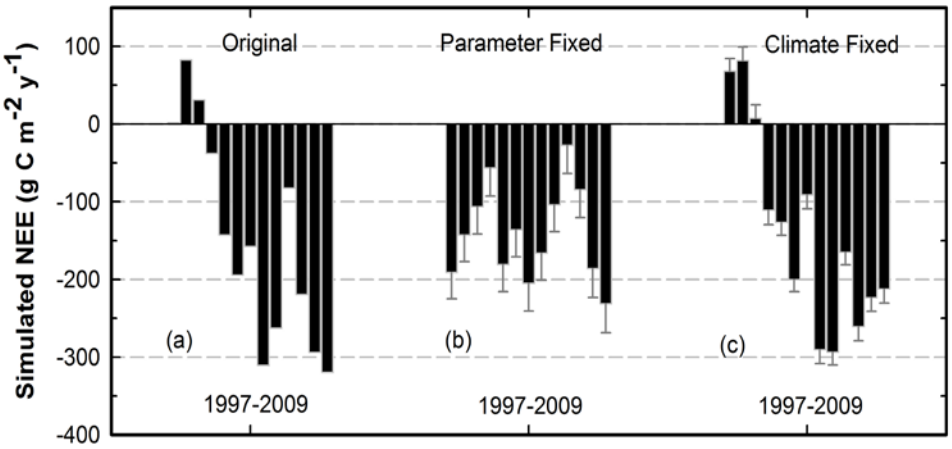

Fig. 5: Interannual variation in simulated NEE (a) $NEE_{original}$: using the original climate and parameter time series in each of the 13 years; (b) NEE_{parfix}: parameters kept constant; (c) NEE_{clifix}: climate kept constant. Each value of NEE_{parfix} and NEE_{clifix} represents an ensemble mean value of the 13 simulations where the parameter, or climate time series from 1997-2009 was applied in sequence. The error bars show the standard error.

against the whole 13-year datasets, c.f. section 2.6), the decadal trend of increasing carbon uptake of the forest was not reproduced by the model (Fig. 6b), even though the extended carbon uptake period during the 13 year was successfully captured by the model (Fig 6a). The carbon uptake was overestimated in 1997-2000 and underestimated in 2005-2009. In the second step of the model calibration, the interannual variability in the carbon uptake was successfully simulated with yearly fitted model parameters (Fig. 6b). For the 7 yearly fitted parameters, only light use efficiency showed an increasing trend in 1997-2009 (Fig. 6c). The other 6 parameters were less well constrained and the mode of the posterior parameter distributions did not show a trend during the 13 year period (Table 3 in **paper III**).

3.4 A synthesis of the carbon balance datasets

The ecosystem C budget datasets were synthesized in **paper II**. The flow diagram in Fig. 7 gives a comprehensive representation of the carbon cycling in the beech forest. It connects the carbon fluxes with either the system boundaries or the ecosystem internal pools. On the left hand side the CO_2 fluxes are given, on the right hand side the organic fluxes and stock changes. Most of the ECB components in the diagram have been measured in the field or been directly calculated from such measurements using models. A few of

the entities have been derived as residuals from the mass balance equations (eq. ΔSOC). This is the reason for perfect closure of the budget.

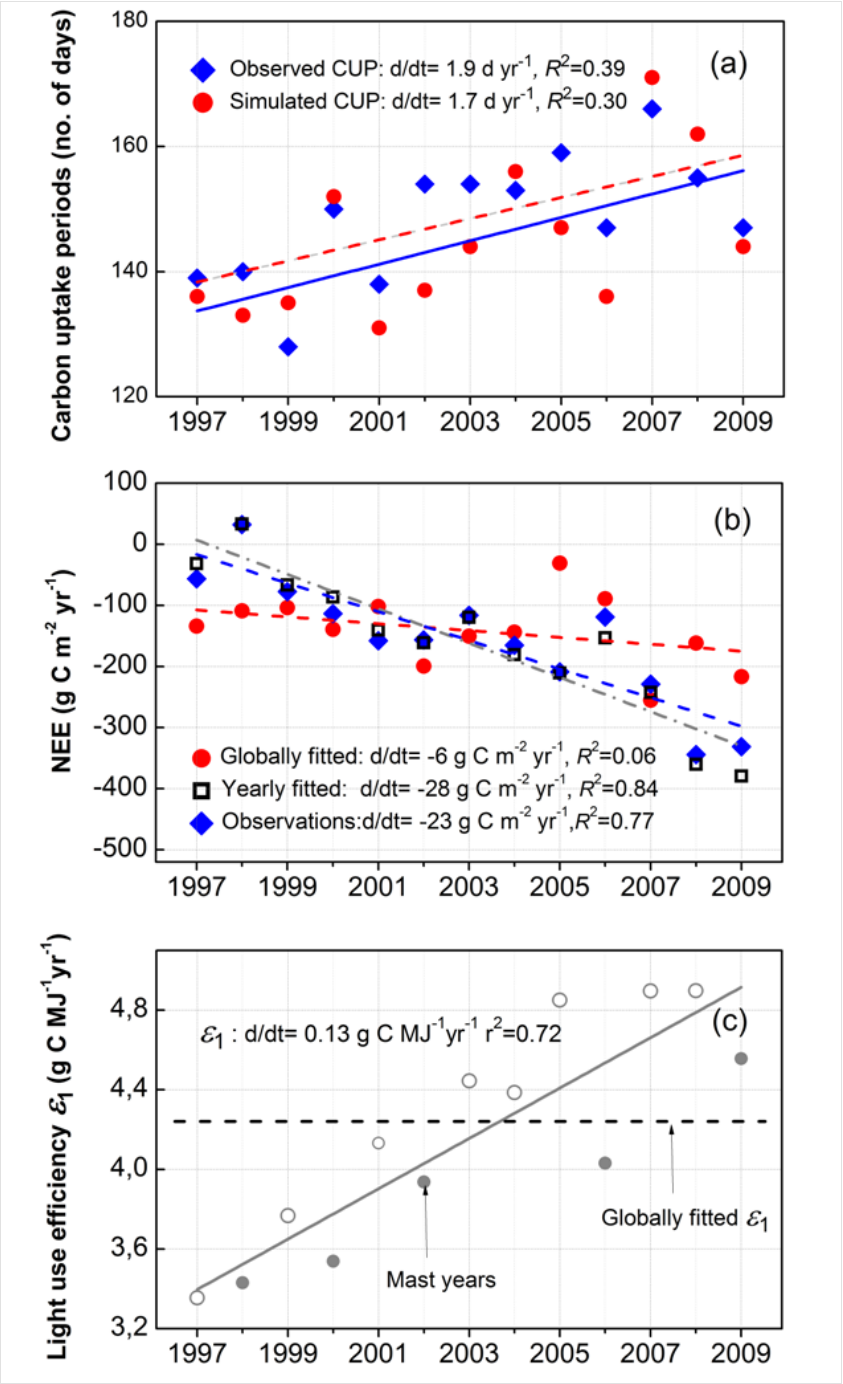

Fig. 6: (a) Observed and simulated carbon uptake period (CUP) in 1997-2009. **(b)** Observed and simulated (using globally and yearly fitted parameter sets) annual NEE in 1997-2009, the trend lines were linear regressions of the observation and model outputs with yearly fitted parameters. **(c)** Interannual variation in the yearly fitted light use efficiency, ε_1 the grey dots represent mast years and the horizontal dashed line was the globally fitted ε_1.

The GPP, the annual gross carbon influx into the ecosystem, is the largest flux of the carbon cycle. The arrows inside the tree pools (Fig. 7) show how the assimilated C was distributed in the ecosystem. More than half of the GPP, i.e.,

62% was respired by the tree stand. The rest was, by definition, NPP, i.e., the sum of tree growth (44% of NPP) and litter production (56%). While the tree growth was clearly dominated by the aboveground wood production (85% of the tree growth) the litter production was of similar magnitude, with the aboveground litter production being ca. 20% higher than the belowground litter production. According to our estimation, about 35% of the average annual tree growth was removed by wood exports over the entire period and 13.4 % of the annual tree growth was transferred to woody debris. The input of organic C into the soil amounted to 442 g C m^{-2} yr^{-1}. At the same time the CO_2 loss by heterotrophic respiration was 451 g C m^{-2} yr^{-1} .The soil budget was closed, i.e. -33 g C m^{-2} yr^{-1}, as the organic carbon input was almost balanced by the heterotrophic CO_2 output and DOC leaching (25 g C m^{-2} yr^{-1}, Kindler et al., 2011).

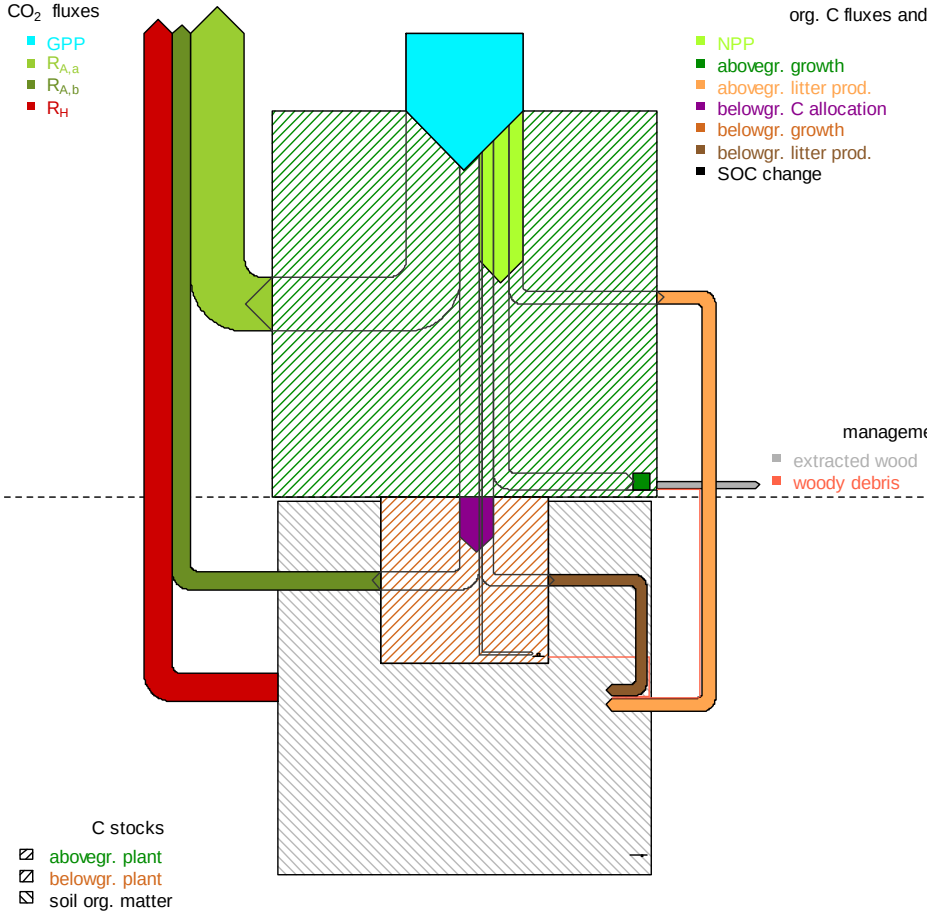

Fig. 7: Flow diagram of the carbon cycling in the beech forest at Sorø. Pools are displayed as quadratic rectangles filled with a line pattern, fluxes are represented by solid arrows and stock changes are bar charts. The widths of the flux arrows and stock change bars are scaled according to their annual average values. The width of the GPP arrow represents 1882 g C m-2 yr-1. The area of the rectangles of the pools is scaled to their sizes; the aboveground tree pool represents, e.g., 9885 g C m-2. The 5 year average values and their uncertainties can be found in Tables 3, 5 and 6 and in the text. Fluxes of organic and biologically related inorganic carbon (DOC, DIC) to the ground water, i.e. 25 and 12 g C m-2yr-1, for DOC and DIC respectively (Kindler et al., 2011), have been omitted in the graph but have been included in the stock change calculations (DOC) and ecosystem CO2 losses (DIC).

The total CO_2 losses from the ecosystem amounted to 86 % of GPP, the remainder of 14 % was transformed to organic carbon in the ecosystem. This net effect of the carbon cycle during the observed period can be summarized with a statement that the Sorø beech forest mainly produced wood, 1/3 of it exported by thinning and 2/3 staying at the site. About 2/3 of the total ecosystem carbon content was in the tree stand (9886 ± 231 g C m^{-2} aboveground and 1846 ± 160 g C m^{-2} below), 1/3 was stored in the soil (9254 ± 2809 g C m^{-2}, 0-60 cm, sampling in 2004, Schrumpf et al. 2011). The very high variability in the soil is due to some areas of slightly lower relief that were subsequently wetter, where the SOC content was often observed to be twice that as recorded in the drier more elevated areas.

3.5 Model optimization using the multiple constrain approach

The ecosystem C budget synthesis in **paper II** (section 3.4) provided important information (e.g. data uncertainty and consistency) for the model data fusion exercise in **paper III**. When the different datasets were used to calibrate the model (c.f. section 2.6), the posterior distribution of most parameters was different from their prior uniform distributions (Fig. 8). With the first constraint, Ω_{NEE}, only a few parameters (e.g. ε_1, l_{Lc1} and ψ_c, parameter definitions were given in Table 1 of **paper III**) were constrained; the posterior ranges of most other parameters were still similar to their prior. This low degree of parameter identification was improved when the multiple constraint approach was imposed ($\Omega_{Multiple}$). The posterior distributions of parameters controlling photosynthesis (e.g. ε_1, p_{ol}), respiration (e.g. k_l and k_h), phenology (e.g. t_{el}), allocation (e.g. f_l and f_r) and transpiration (e.g. T_{trig} and g_{vpd}) were all constrained as the day-time NEE, night-time NEE, LAI, biomass stocks, and λE were jointly used to constrain the model.

With both of the two different constraints, Ω_{NEE} and $\Omega_{Multiple}$, the ensemble mean of the modelled outputs represented the measurements well, with almost equally good R^2 and ME (see Table 2 in **paper III**). The variability of the hourly NEE during the 13-year period was captured by the model (R^2: 0.72 and 0.75), partly as a product of the well simulated the LAI dynamics (R^2: 0.86 and 0.88). The soil heat processes were better simulated than the soil water transport and storage. The model explained approximately 92% and 60% of the variability in the measured soil temperature and soil water content respectively. In contrast, the uncertainty (i.e. the range of the R^2 and ME for the accepted runs) of all the model outputs was significantly lower with $\Omega_{Multiple}$ compared to Ω_{NEE}. The model simulation using the mode of the posterior parameters of $\Omega_{Multiple}$ (Fig. 4) performed equally well as the ensemble mean of the accepted runs (see Table 2 in **paper III**). However, the simulation using the mode of the posterior parameters of Ω_{NEE} performed worse than the corresponding ensemble mean (see Table 2 in **paper III**).

4. DISCUSSION

4.1 Drivers for the long-term trend of increasing carbon uptake

The most important finding of **paper I** is that the decadal trend of increasing C uptake at this temperate deciduous forest was more strongly driven by the changes in the ecosystem functional properties than the direct effect of climatic variability. The variation in the mean annual climate could not entirely explain the interannual variation in the annual ecosystem C fluxes. Instead, the response of C fluxes to climate variability was much stronger at shorter time

scales (Fig. 2). For more than 80% of the year, the C flux was significantly correlated with at least one of the investigated climate variable, which differed across seasons (Fig. 2). This significant seasonality of the ecosystem responses to climatic variability demonstrated the importance of the seasonal distribution of the climate anomalies on the ecosystem C balances. Our results showed that this temperate deciduous forest will be sensitive to increases in summer drought. Altered precipitation patterns, i.e. increased rainfall variability rather than changes in annual precipitation are likely to affect ecosystem carbon balances in the future (Knapp et al., 2002). The average climate change is expected to be accompanied by increased variability and weather extremes (Easterling et al., 2000a; Easterling et al., 2000b). Climate change projections for Denmark that suggest that a small increase in precipitation will occur, but mainly during winter, while the likelihood of summer droughts will increase (Christensen and Christensen, 2007). Our results suggest that in addition to the changes in average climate, increased climatic variability could alter the ecosystem carbon balance more strongly, as the climate anomalies are projected to take place predominantly during biologically active periods.

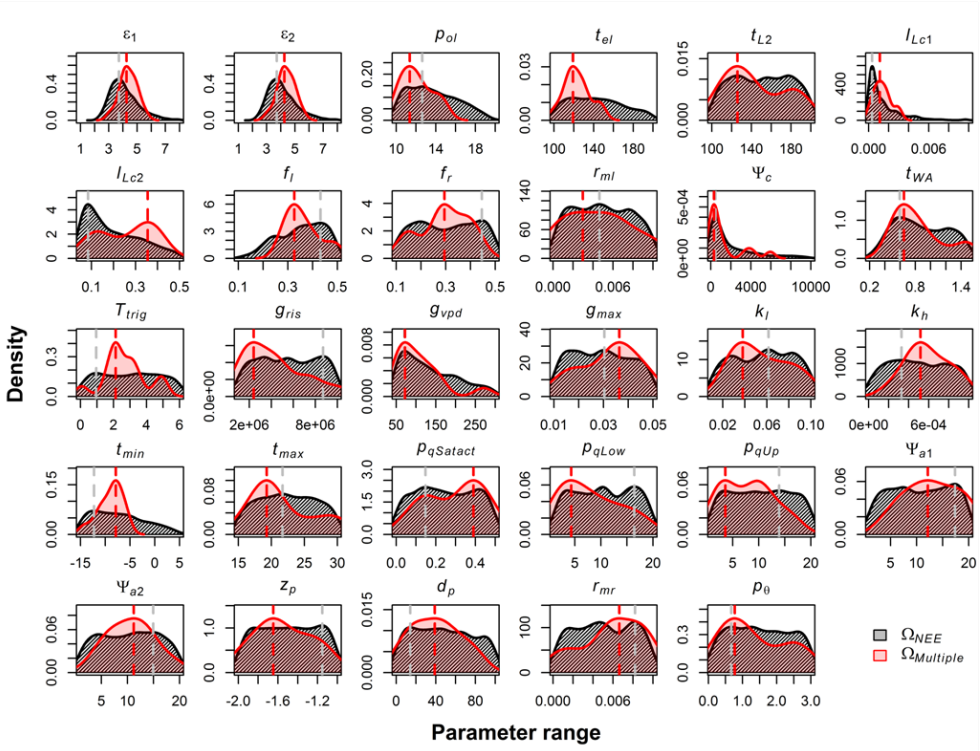

Figure 8: Posterior parameter distributions (density plot) after the model was globally fitted to the 13-year datasets using two different constraints, Ω_{NEE} and $\Omega_{\mathrm{Multiple}}$ (see text for details). The prior parameter distributions are set as uniform and the parameter descriptions are given in Table 1. The dashed vertical lines are the mode of the posterior parameter distribution. Acceptance criteria of the behavioural models are given in Table 2.

The results of **paper I** showed that at an annual time scale, as much as 80% of the interannual variability in the C fluxes can be attributed to the ecosystem functional changes. This high magnitude could be because the structure and function of the temperate deciduous ecosystems are more sensitivity to environmental change and disturbance than other type of ecosystems. As

shown in a number of published studies, the impact of functional change decreases in the order: deciduous forest (this study), mixed forest (Richardson et al., 2007), conifer forest (Hui et al., 2003) and peatland (Teklemariam et al., 2010). Cross-site studies on the ecosystem carbon balance also found that deciduous forests tend to be more sensitive than evergreen conifer forests to climate variability (Yuan et al., 2009) and phenological transitions (Richardson et al., 2010). These differences in the adaptive capacity to changing climate between deciduous and evergreen forests may drive shifts in the composition within mixed forests (Richardson et al., 2010).

The estimated impact of functional change in **paper I** is not without uncertainties, mainly due to the core assumption that functional change is solely represented by the changes in parameters of the semi-empirical model (Eq. 15 and 16). This assumption is challenged by the simplicity of the model structure, e.g., the temperature regulation of GPP and the SWC regulation of TER were not explicitly specified in the model structure. Testing the residual climatic effects on the model predictions showed that the TER-related parameters were not completely independent from SWC, which has led to a small overestimation of functional change (c.f. section 4.2 in **paper I**).

In order to overcome this limitation, we used a dynamic process-based model in **paper III** to simulate the ecosystem response to the climate variability (which are the drivers of the model). In this way, the climatic effects on ecosystem processes are more comprehensively taken into account in comparison to the simple semi-empirical model. For instance, SWC was simulated for different soil layers and its effect on respiration and photosynthesis were accounted for in the model. After the optimization, the process-based model performed reasonably well at diurnal and seasonal time scales (Fig. 4) but failed to accurately reproduce the interannual variability in the ecosystem C uptakes, even though the phenology and increasing trend of C uptake periods were successfully captured by the model (Fig. 6). The small magnitude but high frequency model errors accumulated and resulted in a large bias in the simulated annual C balance at the interannual time scale; similar results have been found in many other modelling studies (e.g., Siqueira et al., 2006; Keenan et al., 2012). These results confirmed our hypothesis that the long-term C dynamics cannot be solely explained by climate variables, as was also demonstrated in **paper I** with the semi-empirical model.

The failure to predict the long-term C dynamics with the process-based model in **paper III** can be caused by the inaccurate representation of the biotic ecosystem responses (Richardson et al., 2007; Wu et al., 2012). One possible reason for this model-data mismatch is that the applied model structures (within CoupModel) did not dynamically simulate the effects of, e.g., changing canopy nitrogen contents. In the second model experiment (c.f. section 2.6), the seven parameters, controlling photosynthesis, phenology and respiration, and allowed to vary inter-annually, are considered proximate for ecosystem functional change. The estimated light use efficiency varied between years and showed a systematic trend during the 13-year period, corresponding to the hypothesis presented by Pilegaard et al. (2011). On the other hand, this model-data mismatch can also be caused by missing divers. For instance, a potential CO_2 fertilization effect over the 13 year period is not accounted for in the model, as a light use efficiency dependent photosynthesis model was applied within CoupModel. However, on a global scale the atmospheric CO_2 concentration has increased by 25ppm during study period (Friedlingstein et al.,

2010). This could have only partly contributed to the increased light use efficiency in 1997-2009. Therefore, it is most likely the ecosystem internal nitrogen cycling has affected the C cycling. An interesting finding was that the between year reductions in the light use efficiency were strongly associated with the mast years, e.g. fruiting events, thus it is likely that the production of fruits was nitrogen dependent and reduced the leaf nitrogen content, thus, photosynthetic capacity. These results, together with the results in paper I indicated a comprehensive investigation of ecosystem N dynamics is essential for understanding the long-term trend of increasing C uptake.

4.2 The strength and limitation of the empirical modelling approach

The combination of modelling and data analysis provides insight into the complex interactions between the direct climatic effects and the biotic ecosystem responses, by partitioning their roles in determining the interannual variation of the ecosystem carbon fluxes. In **paper I**, empirical models were used to this end. A major strength of the statistical modelling approach is that it does not require an explicit parameterization of the complex ecosystem process in detail. It has been proposed that in order to realistically distinguish between the effect of climate variability and functional change using a parameter extraction method, a mechanistic model must be used (Leuning, 2011). However, many processes, such as phenology, are considered indirectly by the parameter estimation method. These responses to current and previous climate can be considered to be structural change and are captured by this method. Also, the information contained in the flux data alone is likely insufficient to distinguish between detailed ecosystem processes (Wang et al., 2009). The risk of over-parameterization is a strong justification to keep the model structure simple. For example, detailed processes such as direct and diffuse radiation and the separation of autotrophic and heterotrophic respiration were not implemented. The effects of many of those processes are aggregated into the parameters of the empirical model used. To address the concerns of the simplicity of our model structure, instead of adding a mechanistic sub-module, we tested the effect of removing the VPD sub-module (c.f. section 2.4 in **paper I**). The results suggested that the partitioning between the climate and parameter effects was not changed. We therefore conclude that the available information within the CO2 flux data was captured by the flexible modelling approach.

On the other hand, statistical models have limited potential to elucidate the causes behind the identified functional change, despite being able to successfully distinguish between the direct climatic effects and the changes of ecosystem functioning. The model and fitted parameters cannot be used for predictive purposes or extrapolation. As indicated by Groenendijk et al. (2011), although specific site-year derived parameters give the best prediction of observed fluxes, they are generally too specific to be used over large spatial scales. However, the modelling approach can be applied to flux data from other sites to obtain site specific parameters and quantify the importance of functional change for the IAV of carbon fluxes in different ecosystems.

4.3 Process-based modelling and multiple constraints approach

Process-based models can be used to simulate the ecosystem states in response to future climate change but are currently challenged by both missing-processes (i.e. relative simple model structure compared to the natural processes) and over-parameterization (i.e. extremely difficult to evaluate the

numerous processes individually due to equifinality of model predictions). Therefore, long-term observed datasets together with their uncertainty and consistency evaluation (**paper II**) are important information that can be used to optimize the model and indentify model structural deficits.

In **paper III**, by constraining the CoupModel with long-term measurements of NEE datasets, the ensemble mean of the model outputs produced reasonably good estimates for both the NEE and other validation datasets. However, the accepted ensemble of behavioural models showed a high degree of equifinality, i.e. a number of different models could produce equally good results when compared to calibrated variable (Beven and Freer, 2001), resulting in high uncertainties in the estimates of other validated variables. This indicated that some behavioural models with certain parameterizations were accepted for the wrong reasons. For instance, the model could well represent the NEE (R^2: 0.71-0.73) when the LAI dynamics was incorrectly represented (lowest R^2=0.46). The problem of equifinality was also shown in the unconstrained posterior parameters (Fig. 8) which was similar to many other MDF studies, where it was shown that the information content of the high frequency NEE datasets was not sufficient to constrain the parameters related to the different ecosystem component C fluxes, e.g. the autotrophic and heterotrophic respiration from different C pools (Keenan et al., 2012b; Richardson et al., 2012; Sacks et al., 2007; Wang et al., 2009).

On the other hand, the success of MDF studies also depends on how efficiently the information in the assimilated datasets is used. For example, the uncertainty in the model outputs was reduced when the NEE datasets were averaged in time (e.g. monthly and annually) and added to the model calibration (Keenan et al., 2012b). Sacks et al. (2007) showed that optimizing the model on a twice-daily (instead of hourly or daily) time step significantly improved the model's ability to accurately predict the component C fluxes. Mahecha et al. (2010a) proposed a method to quantify the model-data disagreements at various time-frequency domains; the decomposed high or low frequency signals could also potentially be used to optimize the model parameters. In this study, when NEE was separated into daytime and night-time values before use in the model calibration (in Ω_{Multiple}), the parameters controlling the litter and humus decomposition rate were better constrained. In general, the parameter uncertainties were reduced when additional constraints were incorporated. Including the LAI, biomass stock and λE in the calibration strongly constrained 9 key model parameters and successfully reduced posterior uncertainty in all of the remaining 20 parameters. These results suggested that for future MDF exercises, the flux studies should be accompanied by biological process studies and ecosystem structural assessments to ensure the data availability that can overcome the model over-parameterization.

With the multiple constraints approach, the diurnal and seasonal dynamics of the ecosystem C fluxes can be well represented by the model (Fig. 4). However, the long-term C dynamics was not well captured with the globally fitted parameter sets (Fig. 6). This can be caused by the inaccurate representation of the biotic ecosystem responses (Richardson et al., 2007; Wu et al., 2012). One hypothesis for this model-data mismatch is that the applied model structures (within CoupModel) used a fixed nitrogen response to photosynthesis, and thus did not dynamically simulate the effects of, e.g., changing canopy nitrogen contents. In the second model experiment, the 7 parameters controlling

photosynthesis, phenology and respiration, were allowed to vary inter-annually and considered proximate for the ecosystem functional change. The estimated light use efficiency varied between years and showed a systematic trend during the 13-year period, corresponding to the hypothesis presented by Pilegaard et al. (2011). On the other hand, this model-data mismatch can also be caused by the missing model divers. For instance the CO_2 fertilization effects during the 13 year period were not accounted in the model as the present version of CoupModel used a light use efficiency dependent photosynthesis module. On a global scale the atmospheric CO_2 concentration has increased by 25ppm during study period (Friedlingstein et al., 2010). This could only partly have contributed to the increased light use efficiency in 1997-2009. Therefore, it is most likely the ecosystem internal nitrogen cycling has affected light use efficiency. An interesting finding was that the strong negative light use efficiency fluctuations were strongly associated with the occurrence of mast years. This indicates that the reallocation of nitrogen to the nuts might deplete stored nutrients and lowered the N content of the leaves To prove this hypothesis, direct measurements on the nut production and its role in the N-turnover of the ecosystem are needed. Direct evidence of resource depletion in the masting trees is rare. Sala et al. (2012) examined the timing and magnitude of stored nutrient depletion after a heavy mast events in a conifer forest and confirmed that mast events deplete stored tree internal nutrients (including nitrogen and phosphorus) and reduced the leaf photosynthetic rates. Therefore, a proper incorporation of the between year variability of nuts should be considered in future modelling of the forest ecosystems.

5. CONCLUSIONS

The long term ecosystem carbon cycling in a temperate deciduous forest was systematically studied in a series of data synthesis, semi-empirical and process-based modelling studies. The investigated forest was a moderate sink of atmospheric CO_2 during the study period with both high rates of photosynthesis and respiration. These C fluxes were strongly controlled by climate variability short time scales but this impact weakened as the time integral increased. At longer temporal scales, the effect of ecosystem functional change became progressively larger and appeared to dominate the interannual variability in ecosystem carbon balance. With the semi-empirical modelling approach, the observed trend of increasing carbon uptake was found to be driven by ecosystem functional changes rather than direct effects of decadal climatic variability. This was supported by a subsequent process-based modelling study where we used the same dataset to test whether the dynamic process-based model could simulate the short-term and long-term ecosystem C dynamics. After the model calibration, the diurnal and seasonal patterns of carbon were successfully simulated, while the degree of equifinality was significantly reduced using the multiple constraints approach. The interannual variability in the ecosystem C uptake could not be correctly simulated unless the biological parameters were allowed to vary temporally. These results confirmed that the long-term trend of increasing C uptake at Sorø were strongly driven by the biotic changes in the ecosystem status. Processes such as the nitrogen cycling in the ecosystem needs to be further investigated and incorporated into the process-based models.

6. FUTURE WORK

Biophysical parameters such as the canopy photosynthetic capacity, leaf chlorophyll content and canopy nitrogen distribution need to be monitored using both field observations or remote sensing (Houborg and Boegh, 2008). The processes governing nitrogen dynamics and their interaction with photosynthesis needs to be incorporated into process-based models.

The methods developed in the present thesis e.g. 1) the semi-empirical modelling approach to distinguish the effect of climate variability and functional change; 2) consistency assessment method for the ecosystem carbon balance datasets; 3) evaluation of the source area variation related uncertainty for NEE should be applied in other sites to demonstrate or refute their general applicability.

7. REFERENCES

Baldocchi, D., 2003. Assessing the eddy covariance technique for evaluating carbon dioxide exchange rates of ecosystems: past, present and future. Global Change Biology, 9(4): 479-492.

Barr, A. et al., 2007. Climatic controls on the carbon and water balances of a boreal aspen forest, 1994–2003. Global Change Biology, 13(3): 561-576.

Barr, A. et al., 2004. Inter-annual variability in the leaf area index of a boreal aspen-hazelnut forest in relation to net ecosystem production. Agricultural and Forest Meteorology, 126(3-4): 237-255.

Beer, C. et al., 2010. Terrestrial Gross Carbon Dioxide Uptake: Global Distribution and Covariation with Climate. Science, 329(5993): 834-838.

Beven, K. and Freer, J., 2001. Equifinality, data assimilation, and uncertainty estimation in mechanistic modelling of complex environmental systems using the GLUE methodology. Journal of Hydrology, 249(1): 11-29.

Black, T. et al., 2000. Increased carbon sequestration by a boreal deciduous forest in years with a warm spring. Geophysical Research Letters, 27(9): 1271-1274.

Braswell, B.H., Schimel, D.S., Linder, E. and Moore, B., 1997. The Response of Global Terrestrial Ecosystems to Interannual Temperature Variability. Science, 278(5339): 870-873.

Chen, W. et al., 1999. Effects of climatic variability on the annual carbon sequestration by a boreal aspen forest. Global Change Biology, 5(1): 41-53.

Christensen, J.H. and Christensen, O.B., 2007. A summary of the PRUDENCE model projections of changes in European climate by the end of this century. Climatic Change, 81: 7-30.

Churkina, G., Schimel, D., Braswell, B. and Xiao, X., 2005. Spatial analysis of growing season length control over net ecosystem exchange. Global Change Biology, 11(10): 1777-1787.

Clark, D. et al., 2001. Measuring net primary production in forests: concepts and field methods. Ecological Applications, 11(2): 356-370.

Collatz, G., Ball, J., Grivet, C. and Berry, J., 1991. Physiological and environmental regulation of stomatal conductance, photosynthesis and transpiration: a model that includes a laminar boundary layer. Agricultural and Forest Meteorology, 54(2-4): 107-136.

Davidson, E., Janssens, I. and Luo, Y., 2006. On the variability of respiration in terrestrial ecosystems: moving beyond Q10. Global Change Biology, 12(2): 154-164.

Davidson, E., Savage, K., Verchot, L. and Navarro, R., 2002. Minimizing artifacts and biases in chamber-based measurements of soil respiration. Agricultural and Forest Meteorology, 113(1-4): 21-37.

Delpierre, N. et al., 2009. Exceptional carbon uptake in European forests during the warm spring of 2007: a data–model analysis. Global Change Biology, 15(6): 1455-1474.

Dunn, A.L., Barford, C.C., Wofsy, S.C., Goulden, M.L. and Daube, B.C., 2007. A long-term record of carbon exchange in a boreal black spruce forest: means, responses to interannual variability, and decadal trends. Global Change Biology, 13(3): 577-590.

Falge, E. et al., 2001. Gap filling strategies for defensible annual sums of net ecosystem exchange. Agricultural and Forest Meteorology, 107(1): 43-69.

FAO, 2010. Global forest resources assessment forestry paper. Food and Agriculture Organization of the United Nations, Rome.

Friedlingstein, P. et al., 2010a. Update on CO2 emissions. Nature Geoscience, 3(12): 811-812.

Friedlingstein, P. et al., 2010b. Update on CO2 emissions. Nature Geoscience, 3(12): 811-812.

Granier, A. et al., 2000. The carbon balance of a young beech forest. Functional Ecology, 14(3): 312-325.

Groenendijk, M. et al., 2011. Assessing parameter variability in a photosynthesis model within and between plant functional types using global Fluxnet eddy covariance data. Agricultural and Forest Meteorology, 151(1): 22-38.

Hänninen, H., 1995. Effects of climatic change on trees from cool and temperate regions: an ecophysiological approach to modelling of bud burst phenology. Canadian Journal of Botany/Revue Canadienne de Botanique, 73(2): 183-201.

Hollinger, D. et al., 2004. Spatial and temporal variability in forest–atmosphere CO2 exchange. Global Change Biology, 10(10): 1689-1706.

Houborg, R. and Boegh, E., 2008. Mapping leaf chlorophyll and leaf area index using inverse and forward canopy reflectance modeling and SPOT reflectance data. Remote sensing of environment, 112(1): 186-202.

Houghton, R., 2007. Balancing the global carbon budget. Annu. Rev. Earth Planet. Sci., 35: 313-347.

Hu, J., Moore, D., Burns, S. and Monson, R., 2010. Longer growing seasons lead to less carbon sequestration by a subalpine forest. Global Change Biology, 16(2): 771-783.

Hui, D., Luo, Y. and Katul, G., 2003. Partitioning interannual variability in net ecosystem exchange between climatic variability and functional change. Tree Physiology, 23(7): 433.

Ibrom, A. et al., 2006. A comparative analysis of simulated and observed photosynthetic CO2 uptake in two coniferous forest canopies. Tree Physiology, 26(7): 845-864.

Jansson, P., 2012. CoupModel: Model Use, Calibration, and Validation. Transactions of the ASABE, 55(4): 1337-1346.

Jansson, P. and Karlberg, L., 2004. COUP manual–Coupled heat and mass transfer model for soil-plantatmosphere systems. Technical manual for the CoupModel: 1–453.

Jansson, P., Svensson, M., Kleja, D. and Gustafsson, D., 2008. Simulated climate change impacts on fluxes of carbon in Norway spruce ecosystems along a climatic transect in Sweden. Biogeochemistry, 89(1): 81-94.

Jansson, P.E. and Moon, D.S., 2001. A coupled model of water, heat and mass transfer using object orientation to improve flexibility and functionality. Environmental Modelling & Software, 16(1): 37-46.

Jarvis, P., 1976. The interpretation of the variations in leaf water potential and stomatal conductance found in canopies in the field. Philosophical Transactions of the Royal Society of London. Series B, Biological Sciences, 273(927): 593-610.

Keenan, T.F. et al., 2012a. Terrestrial biosphere model performance for inter-annual variability of land-atmosphere CO2 exchange. Global Change Biology, 18(6): 1971-1987.

Keenan, T.F., Davidson, E., Moffat, A.M., Munger, W. and Richardson, A.D., 2012b. Using model-data fusion to interpret past trends, and quantify uncertainties in future projections, of terrestrial ecosystem carbon cycling. Global Change Biology, 18(8): 2555-2569.

Körner, C., 1995. Leaf diffusive conductances in the major vegetation types of the globe. In: E.-D. Schulze (Editor), Ecophysiology of photosynthesis. Springer Verlag, Berlin, pp. 463–490.

Kramer, K. et al., 2002. Evaluation of six process based forest growth models using eddy covariance measurements of CO2 and H2O fluxes at six forest sites in Europe. Global Change Biology, 8(3): 213-230.

Lasslop, G. et al., 2010. Separation of net ecosystem exchange into assimilation and respiration using a light response curve approach: critical issues and global evaluation. Global Change Biology, 16(1): 187-208.

Le Dantec, V., Dufrêne, E. and Saugier, B., 2000. Interannual and spatial variation in maximum leaf area index of temperate deciduous stands. Forest Ecology and Management, 134(1-3): 71-81.

Le Goff, N. and Ottorini, J.M., 2001. Root biomass and biomass increment in a beech (Fagus sylvatica L.) stand in North-East France. Annals of Forest Science, 58(1): 1-13.

Leuning, R., 2011. Interactive comment on "Effects of climate variability and functional changes on the interannual variation of the carbon balance in a temperate deciduous forest" by J. Wu et al. Biogeosciences Discuss, 8: C4065–C4065.

Linkosalo, T., Carter, T.R., Häkkinen, R. and Hari, P., 2000. Predicting spring phenology and frost damage risk of Betula spp. under climatic warming: a comparison of two models. Tree Physiology, 20(17): 1175-1182.

Liu, Y., Freer, J., Beven, K. and Matgen, P., 2009. Towards a limits of acceptability approach to the calibration of hydrological models: Extending observation error. Journal of Hydrology, 367(1-2): 93-103.

Lloyd, J. and Taylor, J., 1994. On the temperature dependence of soil respiration. Functional Ecology, 8(3): 315-323.

Luo, Y., Wan, S., Hui, D. and Wallace, L., 2001. Acclimatization of soil respiration to warming in a tall grass prairie. Nature, 413(6856): 622-625.

Luyssaert, S. et al., 2009. Toward a consistency cross-check of eddy covariance flux–based and biometric estimates of ecosystem carbon balance. Global Biogeochemical Cycles, 23(3).

Mahecha, M. et al., 2010a. Comparing observations and process-based simulations of biosphere-atmosphere exchanges on multiple timescales. Journal of Geophysical Research, 115(G2): G02003.

Mahecha, M.D. et al., 2010b. Global Convergence in the Temperature Sensitivity of Respiration at Ecosystem Level. Science, 329(5993): 838-840.

Metz, B., 2007. Climate change 2007: mitigation of climate change: contribution of Working Group III to the Fourth Assessment Report of the IIntergovernmental Panel on Climate Change. Cambridge University Press.

Morales, P. et al., 2005. Comparing and evaluating process ‐ based ecosystem model predictions of carbon and water fluxes in major European forest biomes. Global Change Biology, 11(12): 2211-2233.

Pan, Y. et al., 2011. A large and persistent carbon sink in the world's forests. Science, 333(6045): 988-993.

Papale, D. et al., 2006. Towards a standardized processing of Net Ecosystem Exchange measured with eddy covariance technique: algorithms and uncertainty estimation. Biogeosciences, 3(4): 571-583.

Penuelas, J. and Filella, I., 2009. Phenology feedbacks on climate change. Science, 324(5929): 887-888.

Pilegaard, K., Ibrom, A., Courtney, M.S., Hummelsh j, P. and Jensen, N.O., 2011. Increasing net CO2 uptake by a Danish beech forest during the period from 1996 to 2009. Agricultural and Forest Meteorology, 151(7): 934-946.

Pilegaard, K. et al., 2003. Field measurements of atmosphere-biosphere interactions in a Danish beech forest. Boreal Environment Research, 8(4): 315-333.

Raupach, M. et al., 2005. Model–data synthesis in terrestrial carbon observation: methods, data requirements and data uncertainty specifications. Global Change Biology, 11(3): 378-397.

Reichstein, M. et al., 2005. On the separation of net ecosystem exchange into assimilation and ecosystem respiration: review and improved algorithm. Global Change Biology, 11(9): 1424-1439.

Richardson, A. et al., 2010. Influence of spring and autumn phenological transitions on forest ecosystem productivity. Philosophical Transactions of the Royal Society B: Biological Sciences, 365(1555): 3227-3246.

Richardson, A., Hollinger, D., Aber, J., Ollinger, S. and Braswell, B., 2007. Environmental variation is directly responsible for short but not long term variation in forest atmosphere carbon exchange. Global Change Biology, 13(4): 788-803.

Richardson, A. et al., 2009. Influence of spring phenology on seasonal and annual carbon balance in two contrasting New England forests. Tree Physiology, 29(3): 321-331.

Richardson, A.D. et al., 2012. Terrestrial biosphere models need better representation of vegetation phenology: results from the North American Carbon Program Site Synthesis. Global Change Biology.

Sack, L. and Grubb, P.J., 2002. The combined impacts of deep shade and drought on the growth and biomass allocation of shade-tolerant woody seedlings. Oecologia, 131(2): 175-185.

Sacks, W.J., Schimel, D.S. and Monson, R.K., 2007. Coupling between carbon cycling and climate in a high-elevation, subalpine forest: a model-data fusion analysis. Oecologia, 151(1): 54-68.

Sage, R.F. and Kubien, D.S., 2007. The temperature response of C3 and C4 photosynthesis. Plant Cell and Environment, 30(9): 1086–1106.

Sala, A., Hopping, K., McIntire, E.J.B., Delzon, S. and Crone, E.E., 2012. Masting in whitebark pine (Pinus albicaulis) depletes stored nutrients. New Phytologist, 196(1): 189-199.

Sala, A., Piper, F. and Hoch, G., 2010. Physiological mechanisms of drought ‐ induced tree mortality are far from being resolved. New Phytologist, 186(2): 274-281.

Santaren, D., Peylin, P., Viovy, N. and Ciais, P., 2007. Optimizing a process-based ecosystem model with eddy-covariance flux measurements: A pine forest in southern France. Global Biogeochemical Cycles, 21(2).

Siqueira, M. et al., 2006. Multiscale model intercomparisons of CO2 and H2O exchange rates in a maturing southeastern US pine forest. Global Change Biology, 12(7): 1189-1207.

Sowerby, A. et al., 2005. Microbial community changes in heathland soil communities along a geographical gradient: interaction with climate change manipulations. Soil Biology and Biochemistry, 37(10): 1805-1813.

Spiecker, H., 2003. Silvicultural management in maintaining biodiversity and resistance of forests in Europe--temperate zone. Journal of Environmental Management, 67(1): 55-65.

Svensson, M., Jansson, P. and Berggren Kleja, D., 2008a. Modelling soil C sequestration in spruce forest ecosystems along a Swedish transect based on current conditions. Biogeochemistry, 89(1): 95-119.

Svensson, M. et al., 2008b. Bayesian calibration of a model describing carbon, water and heat fluxes for a Swedish boreal forest stand. Ecological Modelling, 213(3-4): 331-344.

Tanja, S. et al., 2003. Air temperature triggers the recovery of evergreen boreal forest photosynthesis in spring. Global Change Biology, 9(10): 1410-1426.

Teklemariam, T., Lafleur, P., Moore, T., Roulet, N. and Humphreys, E., 2010. The direct and indirect effects of inter-annual meteorological variability on ecosystem carbon dioxide exchange at a temperate ombrotrophic bog. Agricultural and Forest Meteorology, 150: 1402-1411.

Wang, Y.P., Trudinger, C.M. and Enting, I.G., 2009. A review of applications of model–data fusion to studies of terrestrial carbon fluxes at different scales. Agricultural and Forest Meteorology, 149(11): 1829-1842.

Williams, M., Schwarz, P., Law, B., Irvine, J. and Kurpius, M., 2005. An improved analysis of forest carbon dynamics using data assimilation. Global Change Biology, 11(1): 89-105.

Wu, S.H., Jansson, P.E. and Kolari, P., 2011. Modeling seasonal course of carbon fluxes and evapotranspiration in response to low temperature and moisture in a boreal Scots pine ecosystem. Ecological Modelling.

Wu, S.H., Jansson, P.E. and Kolari, P., 2012. The role of air and soil temperature in the seasonality of photosynthesis and transpiration in a boreal Scots pine ecosystem. Agricultural and Forest Meteorology, 156: 85-103.

Wutzler, T., Wirth, C. and Schumacher, J., 2008. Generic biomass functions for Common beech (Fagus sylvatica) in Central Europe: predictions and components of uncertainty. Canadian Journal of Forest Research, 38(6): 1661-1675.

Yuan, W. et al., 2009. Latitudinal patterns of magnitude and interannual variability in net ecosystem exchange regulated by biological and environmental variables. Global Change Biology, 15(12): 2905-2920.

Paper I

Biogeosciences, 9, 13–28, 2012
www.biogeosciences.net/9/13/2012/
doi:10.5194/bg-9-13-2012

Biogeosciences

Effects of climate variability and functional changes on the interannual variation of the carbon balance in a temperate deciduous forest

J. Wu[1], L. van der Linden[1], G. Lasslop[2,3], N. Carvalhais[2,4], K. Pilegaard[1], C. Beier[1], and A. Ibrom[1]

[1]Biosystems Division, Risø National Laboratory for Sustainable Energy, Technical University of Denmark, 4000 Roskilde, Denmark
[2]Max-Planck Institute for Biogeochemistry, 07701 Jena, Germany
[3]Max-Planck Institute for Meteorology, 20146 Hamburg, Germany
[4]CENSE, Departamento de Ciências e Engenharia do Ambiente, Faculdade de Ciências e Tecnologia (FCT), Universidade Nova de Lisboa, 2825–516 Caparica, Portugal

Correspondence to: J. Wu (jiwu@risoe.dtu.dk)

Received: 11 August 2011 – Published in Biogeosciences Discuss.: 9 September 2011
Revised: 14 December 2011 – Accepted: 14 December 2011 – Published: 3 January 2012

Abstract. The net ecosystem exchange of CO_2 (NEE) between the atmosphere and a temperate beech forest showed a significant interannual variation (IAV) and a decadal trend of increasing carbon uptake (Pilegaard et al., 2011). The objectives of this study were to evaluate to what extent and at which temporal scale, direct climatic variability and changes in ecosystem functional properties regulated the IAV of the carbon balance at this site. Correlation analysis showed that the sensitivity of carbon fluxes to climatic variability was significantly higher at shorter than at longer time scales and changed seasonally. Ecosystem response anomalies implied that changes in the distribution of climate anomalies during the vegetation period will have stronger impacts on future ecosystem carbon balances than changes in average climate.

We improved a published modelling approach which distinguishes the direct climatic effects from changes in ecosystem functioning (Richardson et al., 2007) by employing the semi empirical model published by Lasslop et al. (2010b). Fitting the model in short moving windows enabled large flexibility to adjust the parameters to the seasonal course of the ecosystem functional state. At the annual time scale as much as 80 % of the IAV in NEE was attributed to the variation in photosynthesis and respiration related model parameters. Our results suggest that the observed decadal NEE trend at the investigated site was dominated by changes in ecosystem functioning. In general this study showed the importance of understanding the mechanisms of ecosystem functional change. Incorporating ecosystem functional change into process based models will reduce the uncertainties in long-term predictions of ecosystem carbon balances in global climate change projections.

1 Introduction

Terrestrial ecosystems assimilate more than ten times the current annual anthropogenic carbon dioxide (CO_2) emission through photosynthesis (Beer et al., 2010; Friedlingstein et al., 2010). At the same time, a similar amount of CO_2 is released back to the atmosphere by respiration from soil microorganisms and plants. The difference between these two opposing fluxes determines the net carbon balance of the ecosystem, which varies across time and space (Luyssaert et al., 2007; Stoy et al., 2009; Yuan et al., 2009). Small perturbations in the climate or ecosystem status may alter the equilibrium between photosynthesis and respiration. Whether the terrestrial ecosystems will act as a sink or a source of CO_2 is important, because approximately 25 % of anthropogenic CO_2 emissions are being re-fixed by the terrestrial ecosystems (Friedlingstein et al., 2010; Houghton, 2007). Therefore, understanding the spatiotemporal variability of the ecosystem carbon balance

and the mechanisms that control it is crucial for assessing the vulnerability of the terrestrial carbon pools under future changing climate conditions (Reichstein et al., 2007; Heimann and Reichstein, 2008).

One important approach to understand the ecosystem carbon dynamics is to investigate the interannual variation (IAV) of net ecosystem exchange of CO_2 (NEE) with long-term eddy covariance measurements (Baldocchi, 2003). By analyzing the year to year variation in NEE under different climatic conditions, the key factors and processes that determine the ecosystem carbon balance may be identified. The measured NEE is the difference between gross primary production (GPP) and total ecosystem respiration (TER) which are both much larger than the net flux. The responses of GPP and TER to climate are complex. Some processes are direct and instantaneous, for instance the light response of photosynthesis and the temperature effects on the kinetics of photosynthesis (Sage and Kubien, 2007) and respiration (Mahecha et al., 2010). However, there are also indirect responses, especially through changes in phenology (Richardson et al., 2010), canopy structure (Barr et al., 2004; Ibrom et al., 2006) or physiological acclimation (Luo et al., 2001). Many studies have reported enhanced carbon uptake as warming extended the length of growing seasons (Chen et al., 1999; Black et al., 2000; Suni et al., 2003; Hollinger et al., 2004; Churkina et al., 2005; Penuelas and Filella, 2009; Richardson et al., 2009; Pilegaard et al., 2011). Others show that distribution and intensity of precipitation can also indirectly affect ecosystem carbon balance because the induced water stress could alter the leaf area index (LAI) (Le Dantec et al., 2000; Barr et al., 2007), the carbohydrate reserve status (Sala et al., 2010), the plant allocation pattern (Sack and Grubb, 2002) or the soil microbial community (Sowerby et al., 2005). These indirect responses are often not instantaneous but lagged. Hu et al. (2010) observed that reduced snow cover in the winter led to water stress in the following summer and hence limited photosynthesis in a subalpine forest. Also, climate anomalies, e.g. high temperature in spring, can increase photosynthesis in the following autumn, possibly due to enhanced leaf nitrogen content and canopy photosynthetic capacity as a result of increased nitrogen mineralisation (Richardson et al., 2009).

Several studies have suggested that to evaluate the climate change impacts on the ecosystem carbon balance, it is important to jointly consider the direct, indirect and lagged responses (Braswell et al., 1997; Delpierre et al., 2009; Dunn et al., 2007). However, to explicitly distinguish between these responses is difficult. Richardson et al. (2010) illustrated with four conceptual models that phenological transitions, which are defined here as an indirect response, can have direct, indirect and lagged impacts on ecosystem productivities. In a simpler approach, the ecosystem responses were classified into direct and biotic responses to environmental forcing (Richardson et al., 2007). The biotic responses were described by the parameters of an ecosystem model (e.g. maximum canopy photosynthetic capacity and base respiration). Interannual variability in biotic responses was regarded as functional change.

Functional change can be changes in the structure, physiological properties or species composition of an ecosystem and can occur at either short or long time scales. It is a challenge to assess functional change over the whole succession of an ecosystem because most observations and experiments are conducted over relatively short periods (Symstad et al., 2003; Misson et al., 2010). Therefore, any functional change inferred can only represent the change within an ecosystem over the period of observation. Nevertheless, distinguishing the effects of climate variability and functional change on IAV of the carbon balance at a specific stage of an ecosystem is of interest. It allows the evaluation of the necessity of incorporating functional change modules into mechanistic models, which are used to project future ecosystem carbon balances. Hui et al. (2003) used a homogeneity-of-slope model and a stepwise multiple regression approach to assess the IAV of the biotic responses of the Duke Forest, concluding that functional changes accounted for about 10 % of the observed variation in the NEE. Richardson et al. (2007) concluded that it is important to consider the time scale when trying to partition the source of variance in NEE. With the parameters of a modified light response model fitted to NEE in each year, as much as 55 % of the variation could be attributed to the biotic responses at an annual time scale. In contrast, the effect of functional changes were found to be much lower in a peatland (Teklemariam et al., 2010).

Both the abiotic (i.e. direct) and biotic responses to climate variability have seasonal patterns. For instance, the limiting factor for photosynthesis may change at different periods of the year. Also, key parameters (e.g. canopy maximum photosynthetic capacity) can vary seasonally (Hollinger et al., 2004; Wang et al., 2007; Thum et al., 2008). Recently, more studies have concentrated on the analysis of the carbon dynamics in individual seasons (Piao et al., 2008; Wang et al., 2011). Piao et al. (2008) showed that the warming effect in autumn accounts for the annual carbon loss (with a sensitivity of $0.2\,\mathrm{Pg\,C\,^{\circ}C^{-1}}$) in northern terrestrial ecosystems. This was supported by a site level study where the autumn temperature dominated the annual carbon balance (Vesala et al., 2010). From these findings we conclude that the IAV of ecosystem carbon balances should not only be analyzed at annual but also at sub-annual time scales (e.g. weekly, monthly or seasonally).

At a temperate beech forest near Sorø, Zealand Denmark, NEE was quasi-continuously measured over the past 13 yr (1997–2009). The annual NEE (a negative sign corresponding to a net sink) ranged from a source of $32\,\mathrm{g\,C\,m^{-2}\,yr^{-1}}$ in 1998 to a sink of $-344\,\mathrm{g\,C\,m^{-2}\,yr^{-1}}$ in 2008. A decadal trend of NEE at this site has been reported by Pilegaard et al. (2011), with an average increase in net uptake of $23\,\mathrm{g\,C\,m^{-2}\,yr^{-2}}$. The study indicated that an extended carbon uptake period explained 33 % of the trend and

hypothesised that an increased maximum photosynthetic capacity during the growing season could be another important factor explaining the trend.

The aim of this study was to investigate the IAV of carbon fluxes at Sorø with respect to (1) the seasonal pattern of the ecosystem responses and (2) the source of variability in carbon fluxes. We investigated to what extent and at which temporal scales, climatic variability and changes in ecosystem functional properties determined the IAV of the carbon balance. Empirical models were used as tools to estimate the seasonal and interannual variation of the ecosystem functional properties and to distinguish their impact on the carbon fluxes from the direct climatic effects. An additional methodological focus was to improve published methods with a new approach. We tested the hypothesis that the observed long-term trend of increasing carbon uptake is mostly driven by changes in ecosystem functional properties, despite the significant role of weather variability at short time scales.

2 Material and methods

2.1 Site description

Field measurements were taken at the Euroflux network station Sorø on Zealand, Denmark (55°29′ N, 11°38′ E). Mean annual temperature during the measurement period was 8.5 °C and mean annual sum of precipitation was 564 mm. The dominant tree species is European beech (*Fagus sylvatica*) with approximately 20 % conifers, mainly Norway spruce (*Picea abies*) and European larch (*Larix decidua*). In 2010, the stand around the flux tower was 89 yr old, the average tree height was 28 m and the average diameter at breast height was 41 cm. Soils were classified as Alfisols or Mollisols (depending on the base saturation) with 10–40 cm deep organic layers. Leaf area index peaked at 4–5 m^{-2} m^{-2} and no significant trend was observed in 2000–2009 (Pilegaard et al., 2011). Further information on the instrumentation can be found in Pilegaard et al. (2003). The soil and vegetation are described in Ladekarl (2001) and Pilegaard et al. (2001). The fetch and footprint analysis are given in Dellwik and Jensen (2000, 2005), Göckede et al. (2008) and Pilegaard et al. (2011).

2.2 Flux measurements and partitioning

Thirteen years (1997–2009) of half-hourly measurements of NEE and climate data were used in the present analysis. The flux measurements were conducted at 43 m above ground and the data processing followed the standard procedure of Aubinet et al. (2000) with modifications described in Pilegaard et al. (2011). Spectral corrections were applied to the flux data according to Ibrom et al. (2007), using a spectral transfer function approach. The fluxes were filtered for low turbulent mixing at stable stratification when the friction velocity (u_*) was lower than 0.1 m s^{-1}. The net ecosystem CO_2 exchange was calculated as the sum of CO_2 storage change below the sensor and the measured turbulent CO_2 flux. The gap-filling method was described in Pilegaard et al. (2011). Total ecosystem respiration (a positive sign corresponding to a release of CO_2 to the atmosphere) was estimated based on nighttime data and extrapolated to daytime conditions according to the following equation:

$$\mathrm{TER} = r_\mathrm{b} Q_{10}^{\frac{T_\mathrm{S}-T_0}{10}} \quad (1)$$

where T_0 is the reference soil temperature at 2 cm depth (0 °C), r_b is the base respiration at T_0, T_s is the measured soil temperature at 2 cm and Q_{10} is the temperature sensitivity parameter and set to a constant value of 2. Base respiration was estimated for every night and Eq. (1) was used to extrapolate the nighttime ecosystem respiration over daytime based on soil temperature measured at daytime. GPP (a negative sign corresponding to a net sink) was subsequently calculated as:

$$\mathrm{GPP} = \mathrm{NEE} - \mathrm{TER} \quad (2)$$

2.3 Correlation analysis

To evaluate the ecosystem response to climatic variability, bivariate correlation analysis was first performed between the annual carbon flux integrals (annual sums of NEE, GPP and TER) and the mean annual climate variables, i.e. air temperature T_air, global radiation R_g, volumetric soil water content SWC in the top soil, and precipitation PPT, using data from 13 yr. In the second step, the same correlation analysis was applied at sub-annual time scale with a 30-day moving window. Pearson's correlation coefficients ($n = 13$) were calculated between periodical flux integrals (30-day sum of the GPP and TER) and mean periodical climate variables (e.g. mean T_air for DOY 1–30) from each of the 13 yr. With the 30-day moving window, the first correlation coefficient calculated represented the period DOY 1–30 and was centred at DOY 15. The second correlation coefficient was calculated by moving the window one day forward, representing the period DOY 2–31. In this way, correlation coefficients were calculated throughout the whole year. The resulting time series of correlation coefficients related the interannual variability of the carbon flux to a potential climatic driver in a certain period of a year. This enabled the analysis of interannual variability at sub-annual time scales.

2.4 Model description and parameter estimation

Two statistical modelling approaches were applied in this study to distinguish the impact of climatic variability and ecosystem functional change on carbon fluxes. Firstly, we applied the model (referred to as Model I) and parameter estimation schemes of Richardson et al. (2007). The model consists of a simple Michaelis-Menten light response model (e.g. Hollinger et al., 2004), a Lloyd and Taylor respiration

model (1994) and a set of sigmoid scalar functions which are used to calculate potential carbon flux (under optimum environmental conditions) from the actual flux. Parameter estimation was conducted by minimizing the weighted least squares cost function (Richardson and Hollinger, 2005) in two steps. In the first step, 15 parameters were fitted to the entire 13 yr datasets. Then in the second step, 11 of the 15 parameters (10 for five environmental scalar functions and the temperature sensitivity parameter) were fixed and the remaining four parameters were allowed to vary in each year (for details see Richardson et al. 2007). The interannual variation of these four parameters was interpreted as change in the functional properties of the ecosystem.

Because the parameters of Model I were estimated at annual or longer time steps, the seasonal variation of the ecosystem functional properties cannot be reproduced. This questions its application to ecosystems with strong seasonality, such as the temperate deciduous forest in this study. Therefore, we implemented a second approach based on a similar model (referred to as Model II) but with a different parameter estimation scheme using short moving time windows (Lasslop et al., 2010b). The model consisted of a rectangular hyperbolic light response model (Falge et al., 2001) and a Lloyd and Taylor (1994) respiration model. The effects of air humidity on photosynthesis was modelled after Körner (1995). The model is described in Eqs. (3) and (4).

$$\mathrm{NEE} = -\frac{\alpha\beta R_\mathrm{g}}{\alpha R_\mathrm{g}+\beta} + r_\mathrm{b}\exp\left(E_0\left(\frac{1}{T_\mathrm{ref}-T_0}-\frac{1}{T_\mathrm{air}-T_0}\right)\right) \quad (3)$$

where T_air is the air temperature, T_0 (°C) is a constant (−46.02 °C), R_g (W m^{-2}) is the global radiation; α (µmol CO$_2$ J^{-1}) is the light use efficiency, and β (µmol CO$_2$ m^{-2} s^{-1}) is the instantaneous maximum canopy photosynthetic capacity (Eq. 4), which represents both the structural and physiological properties (e.g. leaf area index, leaf photosynthesis capacity, C3 or C4 photosynthesis pathway species composition); r_b (µmol CO$_2$ m^{-2} s^{-1}) is the base respiration at reference temperature (T_ref=15 °C); E_0 (°C) is the temperature sensitivity.

$$\beta = \left\{ \begin{array}{l} \beta_0, \mathrm{VPD} < \mathrm{VPD}_0 \\ \beta_0 \exp\left(-k\left(\mathrm{VPD}-\mathrm{VPD}_0\right)\right), \mathrm{VPD} > \mathrm{VPD}_0 \end{array} \right\} \quad (4)$$

where k (hPa^{-1}) is a scaling parameter estimating the effects of VPD on β and VPD$_0$ is a threshold value set as 10 hPa, above which the stomatal conductances reduce β. The parameters of the model (E_0, r_b, α, β, k) were estimated in two steps:

All parameters were allowed to vary throughout the year: E_0 was derived from nighttime NEE every 2 days using a 12 day window. α, β, r_b and k were estimated based on daytime NEE every two days, with a 4 day moving window.

In the first step, the parameters k and E_0 were not well constrained. Therefore, we fixed E_0 and k as the median of the previous estimates (E_0=141.4 °C, $k = 0.09$ hPa^{-1}), after which α, β, and r_b were re-estimated based on daytime data every two days, with a 4 day moving window. The temperature sensitivity can be fixed in different ways. Richardson et al. (2007) fixed it by fitting a single set of parameters globally to the data of all years. However, as demonstrated in Reichstein et al. (2005), the estimated temperature sensitivity clearly differs when it was fitted globally or with small time windows. Therefore we decided to use the median of the estimated values from short time windows. Parameter estimation was conducted by minimizing the same weighted least squares cost function as in the first modelling approach (for details see Lasslop et al., 2010b) and the half-hourly fluxes were computed using gap-filled parameter sets (distance weighted average between the two adjacent parameters) and climate data.

Changing model complexity and structure may affect the parameter estimation and thus the subsequent partitioning of variance between the climate and parameter effects (Leuning, 2011). Therefore we performed two additional runs by removing the VPD effect function (Eq. 4) and also imposing a stronger effect (with a lower threshold value VPD$_0$) to test this hypothesis.

In order to compare the seasonal course of the parameters with the structural development of the canopy, the photosynthetically active radiation (PAR) transmittance records (ratio of the PAR measured below and above canopy, details see Pilegaard et al., 2011) were used as a reference, representing the temporal course in the leaf area index.

2.5 Distinguishing the direct response from biotic changes

By application of the parameter time series of one year to all the other years and comparing the differences in the modelled fluxes, the effects of direct climate forcing on the carbon fluxes can be investigated, vice versa for the effects of the parameters. After Richardson et al. (2007), model simulations with fixed climate (using climate data of one year for all other years) and fixed parameters (using parameter dataset of one year for all other years) were performed, resulting in a 13×13 matrix of model predictions. In each cell of this matrix, the simulated results contained 17 520 half-hourly data points, which were further aggregated by day, week, month, season and year for statistical analysis. Therefore, the datasets in each column represented the modelled fluxes with fixed climate using climate data of a particular year i ($F_{\mathrm{clifix},i}$) and the datasets in each row represented the modelled fluxes with fixed parameters using parameter time series of year i ($F_{\mathrm{parfix},i}$). The diagonal of the matrix represents the original modelled fluxes (F_original). The differences between F_original and F_clifix represent the variability that is driven directly by the climate while the differences between F_original and F_parfix represent the variability that is driven by the changing model parameters, which we interpret as functional change. We applied a sums of squares

approach to distinguish between the relative effect of climate and model parameters on the IAV in NEE, GPP and TER at multiple time scales ranging from daily to yearly. The proportion of IAV in the carbon fluxes explained by climate variability (E_{cli}) and parameter change (E_{par}) was determined by Eq. (5) and (6), respectively.

$$E_{\mathrm{cli}} = \overline{\sigma\left(F_{\mathrm{original}} - F_{\mathrm{clifix},i}\right)} / \left(\overline{\sigma\left(F_{\mathrm{original}} - F_{\mathrm{clifix},i}\right)} + \overline{\sigma\left(F_{\mathrm{original}} - F_{\mathrm{parfix},i}\right)}\right) \quad (5)$$

where σ is the variance of the interannual variation of the carbon fluxes and

$$E_{\mathrm{par}} = 1 - E_{\mathrm{cli}}. \quad (6)$$

3 Results

3.1 Interannual variability in carbon fluxes and climate variables

Variation in NEE and the climate variables were analyzed at both sub-annual (daily values smoothed with a 30-day moving average) and annual time scales (Fig. 1). The variability is displayed as fluctuations (around the mean) relative to the standard deviations in a certain time window over the 13 yr. This presentation enables a standardized comparison of the anomalies in both carbon fluxes and climate variables with their interannual variability, during a particular period of a given year. In 1998, the forest was a source of carbon dioxide (Table 1) where the deviation of NEE from the 13 yr annual mean was about 2 standard deviations (SD) above average (more positive corresponding to less uptake). Following this, a trend of increasing carbon uptake in the forest was observed, manifested in a higher net uptake during the latest years 2008–2009 when the NEE was almost 2 SD below average (Fig. 1). Except for these years, the annual NEE deviations were less than 1 SD. Generally, there was a tendency from above average towards below average except in 2003 and 2006, when the forest appeared to have a reduced rate of carbon uptake.

Carbon uptake was less than average in almost all periods of the years from 1997 to 1999, except in autumn 1999 when the uptake was about 1 SD above average. In 2000–2006 the NEE anomaly fluctuated remarkably within each year, ranging from 2 SD above average in winter 2000 to 2 SD below average in autumn 2005. Regardless of the high variability at short time scales, these NEE anomalies tended to compensate each other, resulting in annual fluxes close to the 13 yr average. From 2007 to 2009, NEE was continuously below average with higher carbon uptake except in two short periods of summer 2007 and the beginning of 2008.

The mean annual air temperature of the only source year 1998 was the lowest over the 13 yr period, with more than 1 SD below average. Meanwhile, overcast weather (lowest incoming radiation) and the slightly higher than average precipitation kept the soil water content at 1 SD above average. The opposite conditions prevailed in 2008 compared to 1998, when a higher radiation (almost 2 SD above average) was accompanied with higher air temperature and evaporative demand which significantly reduced the soil water content. Note that the measurement of soil water content in 2008–2009 was slightly different from the previous years because the original TDR sensor (TRIME-EZ, Imko, Ettlingen, Germany) was replaced by a ThetaProbe ML-2x (Delta-T Devices, Cambridge, UK).The new installation was at the same location but in a shallower soil horizon (5 cm instead of 10 cm).

3.2 Relationship between the interannual variability in the carbon fluxes and climate variables

The correlation analysis related the interannual variability of the component carbon fluxes to certain climate variables. At the annual time scale, NEE was highly correlated with GPP ($r = 0.7,\ p < 0.01$) but not with TER (Table 2). TER was correlated with GPP ($r = -0.65,\ p < 0.05$). Apart from soil water content, which was positively correlated with precipitation (0.76, $p < 0.01$) and negatively correlated with radiation ($-0.77,\ p < 0.01$), there were no significant correlations among the other climate variables. Global radiation and soil water content were negatively ($-0.73,\ p < 0.01$) and positively (0.62, $p < 0.05$) correlated with NEE, respectively. Soil water content was low at high R_{g} and correlated with NEE. Surprisingly, none of the climate variables showed a significant correlation with the component fluxes, GPP and TER.

Contrary to the analysis at the annual time scale, carbon fluxes were clearly correlated with climatic variables at shorter time scales (Fig. 2). Gross primary production was highly correlated with T_{air} ($r < -0.69,\ p < 0.01$) throughout the entire year except during the summer (Fig. 2a). When the soil was usually dry in the summer, it apparently confounded the stimulating effects of temperature on photosynthesis. The correlation coefficient between GPP and T_{air} was lowest ($r < -0.8,\ p < 0.01$) in April (leaf flush) and October (leaf fall), indicating that the phenology and leaf development were temperature sensitive. Radiation was also negatively correlated with GPP during spring and autumn. The correlation coefficients increased directly after leaf senescence but decreased during winter, representing the photosynthesis of the 20 % coniferous trees within the footprint. Over a large part of the year, the correlation between GPP and SWC was not significant, possibly because the deep rooting system allowed sufficient water supply even when the water in the top soil was depleted. Nevertheless, a trend of decreasing correlation coefficients during the summer was obvious and the value was lowest in August–September. The

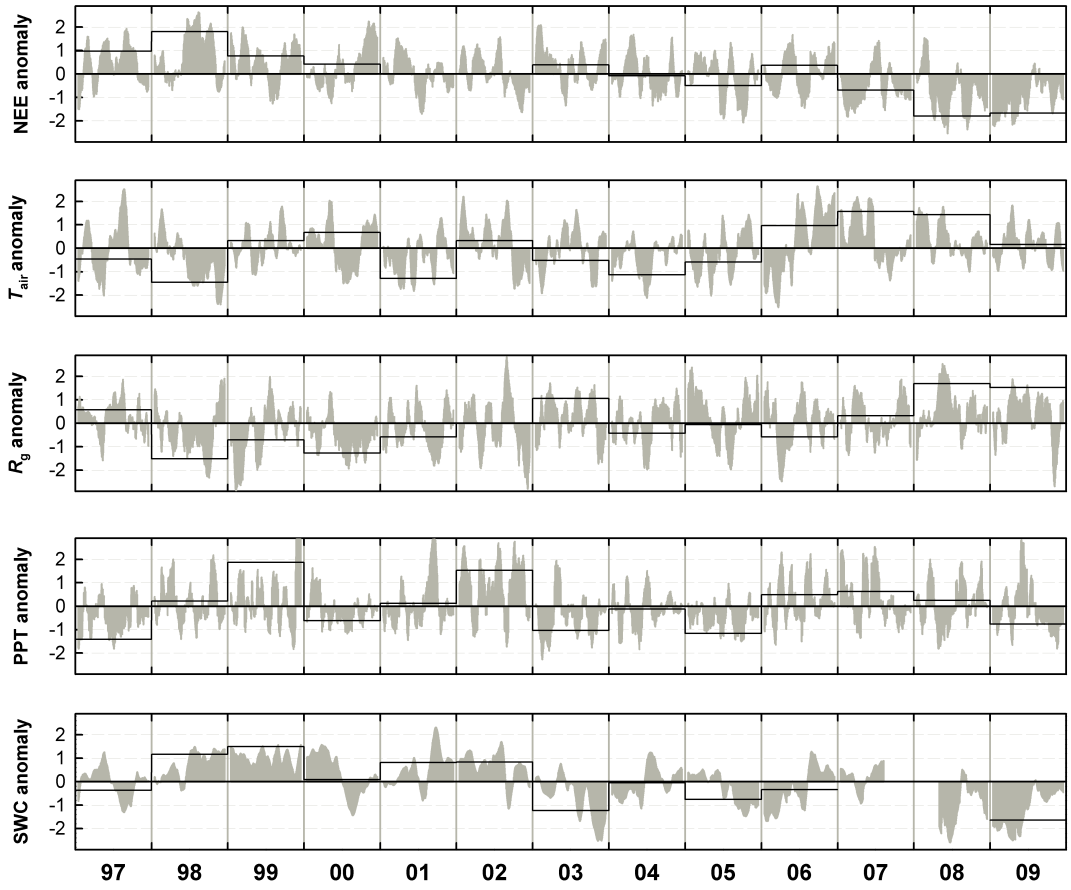

Fig. 1. Deviation of NEE, air temperature (T_{air}), global radiation (R_g), precipitation (PPT) and soil water content (SWC) from the 13 yr annual average (black solid line) and daily average values (grey areas). The daily data were smoothed with a 30-day moving average. The y-axis gives the standard deviation from the mean (e.g. the annual NEE anomaly in 1998 is about 2 SD above the 13 yr average with less uptake of carbon).

correlation between T_{air} and TER (Fig. 2b) was positive during the spring, autumn and winter but also turned negative during summer due to the confounding effect of SWC. Similar to the analysis at the annual time scale, TER and GPP were significantly correlated during large parts of spring and summer. Because the climate variables were also inter correlated (Fig. 2c), the attribution of the interannual variability in carbon flux to specific climatic variables was sometimes difficult, especially for T_{air} and R_g, which were significantly correlated during spring and summer. Global radiation and SWC were in general negatively correlated and most significantly in June and October. The comparison of the temporal variability of climate variables and carbon fluxes (Fig. 3) during the average and particular years (1998 and 2008, minimum and maximum in annual NEE) illustrates the seasonal pattern of the climate relationship together with the IAV of the carbon fluxes (Fig. 2). Relative to the average, low T_{air} and R_g were related with low GPP (Fig. 3a, b and e) in 1998, and high SWC co-occurred with high TER (Fig. 3c and f). In 2008, T_{air} and R_g were related with high GPP (Fig. 3a, b and e), and low SWC was only weakly connected to TER (Fig. 3c and f).

3.3 Model predictions and estimated parameter time series

Based on the approach of Richardson et al. (2007), Model I explained on average 77 % of the variance in the annual half-hourly measured (non gap-filled) NEE (Table 1). The root mean squared error (RMSE) was on average 3.92 µmol CO_2 m^{-2} s^{-1} and mean absolute error (MAE) was 0.24 µmol CO_2 m^{-2} s^{-1}. With the new approach (Model II), the r^2 increased to 85 % and RMSE and MAE was both lower, at 3.13 and 0.08 µmol CO_2 m^{-2} s^{-1}, respectively. The model residuals (Fig. 4) showed that Model I tended to be strongly biased across different seasons. The carbon uptake was overestimated during spring and autumn, and underestimated in summer. The predictions based on Model II matched the seasonality of carbon fluxes well; this improvement is particularly important for using this semi-empirical

Table 1. Mean annual climate variables, gap-filled and modelled NEE and model error statistics for the two semi-empirical models of forest-atmosphere CO_2 exchange. Model I is the model from Richardson et al. (2007) and Model II is the model from Lasslop et al. (2010b). The statistics of the model errors were based on non-gap filled NEE.

Year	Climate			Gap-filled and modelled NEE			Statistics of the model errors							
							Model I				Model II			
	T_{air}	R_g	SWC	NEE_{obs}	Model I	Model II	N	r^2	RMSE	MAE	N	r^2	RMSE	MAE
1997	8.3	118	23	−56	−35	1	13824	0.72	3.39	0.09	13824	0.82	2.75	0.13
1998	7.8	103	27	32	26	82	15367	0.80	3.45	0.1	15367	0.88	2.69	0.01
1999	8.7	108	27	−78	−41	31	14955	0.71	4.12	0.2	14955	0.80	3.55	0.13
2000	8.8	104	24	−113	33	−38	15401	0.77	3.99	0.43	15401	0.86	3.07	0.06
2001	7.9	109	26	−158	−135	−143	16110	0.78	3.75	0.09	16110	0.87	2.99	0.05
2002	8.7	114	26	−157	−212	−195	15764	0.80	3.17	0.15	15764	0.88	2.53	0.13
2003	8.3	121	21	−116	−45	−158	12848	0.78	3.99	0.23	12848	0.85	3.35	0.15
2004	8.0	110	24	−165	−135	−311	12656	0.75	4.57	0.33	12656	0.82	3.91	0.19
2005	8.2	113	22	−209	−150	−263	13075	0.80	3.61	0.21	13075	0.87	2.97	0.23
2006	9.0	109	23	−119	−206	−83	15675	0.73	4.11	0.19	15675	0.83	3.29	0.02
2007	9.3	116	na	−229	na	−220	8096	0.78	4.67	0.68	14910	0.86	3.24	0.02
2008	9.2	126	na	−344	na	−293	10197	0.81	4.26	0.37	16200	0.85	3.20	0.01
2009	8.6	125	21	−331	−369	−320	16523	0.78	3.91	0.06	16523	0.86	3.12	0.05
Mean	8.5	114	na	−157	na	−147	13884	0.77	3.92	0.24	14870	0.85	3.13	0.08

Air temperature, T_{air} (°C) and global radiation, R_g (Wm^{-2}) were measured above the canopy. Soil water content, SWC (%) was measured at 0–10 cm, the system broke down temporarily in 2007–2008. Methods for the gap-filling of the observed NEE, NEE_{obs} ($g\,C\,m^{-2}\,yr^{-1}$) and modelled NEE ($g\,C\,m^{-2}\,yr^{-1}$) are described in the text. Model error statistics include, the number of valid observations (N) used for parameter estimation in each year, coefficient of determination (r^2), root mean squared error, RMSE ($\mu mol\,CO_2\,m^{-2}\,s^{-1}$) and mean absolute error, MAE ($\mu mol\,CO_2\,m^{-2}\,s^{-1}$).

model as a tool to distinguish the effect of direct climate variability from the effect of functional change on NEE at sub-annual time scales.

At an annual time scale, both models reproduced the IAV in the measured NEE. The correlation coefficients between gap-filled NEE and modelled NEE of Model I and Model II were 0.85 and 0.87, respectively. Except for 2004, the modelled NEE (based on Model II) was lowest in 2008–2009 (−294 and $-348\,g\,C\,m^{-2}\,yr^{-1}$) and highest in 1998 ($82\,g\,C\,m^{-2}\,yr^{-1}$) which agreed with the gap-filled fluxes (Table 1). The discrepancy between gap-filled and modelled NEE was large in 2004, as up to 25 % of the data were missing in the growing season. While the measured NEE time series was gap-filled (Pilegaard et al., 2011), the corresponding gaps in the simulated NEE were filled using model predictions from distance weighted averages of the two gap-adjacent parameter values and climatic data. These uncertainties contributed to this discrepancy. Interannual variation in the modelled NEE ($1SD = 136\,g\,C\,m^{-2}\,yr^{-1}$) was about 30 % higher than the measured NEE ($1SD = 104\,g\,C\,m^{-2}\,yr^{-1}$).

The estimated parameter time series based on Model II varied between years. During the leafed period, mean light use efficiency (α) was highest in 2000 ($0.12\,\mu mol\,CO_2\,J^{-1}$) and lowest in 2003 and 1997 ($0.1\,\mu mol\,CO_2\,J^{-1}$). The averaged canopy maximum photosynthetic capacity (β) ranged between 35.6 (1997) to 45.5 (2006) $\mu mol\,CO_2\,m^{-2}\,s^{-1}$. The annual mean base respiration (r_b) ranged from 5.1 (2005) to 6.2 (1998) $\mu mol\,CO_2\,m^{-2}\,s^{-1}$. The seasonal variation in the parameters was stronger than the variation in the annual means. In general, α, β and r_b were all significantly higher during the growing season than in winter (Fig. 5) which is consistent with expected effects of phenology, substrate availability and plant respiratory dynamics. Both the parameter α and β were highest in early summer and decreased over the vegetation period. The base respiration ranged from 2.9 to 8.9 $\mu mol\,CO_2\,m^{-2}\,s^{-1}$ on average, it reached its peak value in July and then reduced until winter, while the SWC reached its lowest value in September and then increased again.

When the VPD effect (Eq. 4) on β was excluded from the model structure, the estimates of β were reduced considerably during the growing season (Fig. 5). This decrease was stronger in July when the relative humidity was generally lower than annual average. Because of parameter correlation, α and r_b changed during this period and the canopy photosynthesis at light saturation (P_{max}) also decreased. When a stronger VPD effect was imposed by reducing the VPD threshold value, the estimates of α, β and r_b changed in the opposite direction. The mean absolute error of the model predictions increased from 0.08 to 0.21 and $0.26\,\mu mol\,CO_2\,m^{-2}\,s^{-1}$ respectively, when the VPD effect

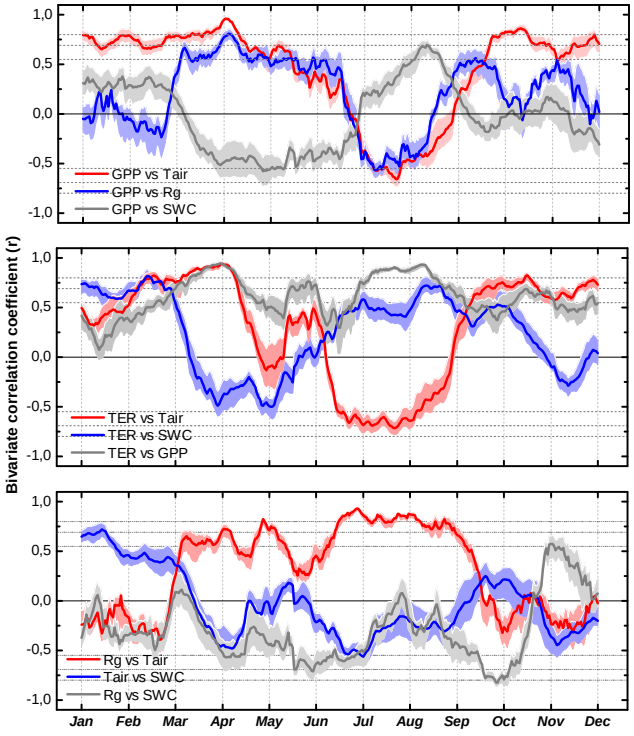

Fig. 2. Bivariate correlations between: **(a)** periodical GPP integral (30-day moving window) with periodical mean air temperature (T_{air}), soil water content (SWC) and global radiation (R_g). **(b)**: periodical TER integral with periodical mean climate variables and GPP. **(c)**: the climate variables. Dashed horizontal lines indicate different levels of statistical significance ($p = 0.05$, 0.01 and 0.001). The shaded area indicates the uncertainties (75 percentile) of the correlation coefficients, as data of each individual year was excluded from the correlation analysis.

was excluded (underestimation of carbon uptake during summer) or enhanced (overestimated carbon uptake during summer).

The comparison between the measured PAR transmission (as a proxy for the seasonal LAI development) and photosynthesis at light saturation (P_{max}) indicates that the structural change of the forest took place mainly in April and October (Fig. 5d). The sharp decrease in P_{max} marked the start of leaf senescence (mid-September) already one month before the average start time of leaf fall (November). This demonstrated that the aggregated effects of structural and physiological changes on the seasonality of NEE were well represented by our modelling approach.

3.4 Sources of interannual variability in the carbon fluxes

One main objective of this work was to separate the influence of functional change from direct effects of climatic variability. This was achieved by analyzing model simulations with

Table 2. Bivariate correlation coefficients between annual anomalies in NEE, GPP and TER and mean annual climate variables including air temperature (T_{air}), global radiation (R_g), soil water content (SWC) and precipitation (PPT). Statistically significant correlations are marked with **($p < 0.01$) and *($p < 0.05$).

	GPP	TER	T_{air}	R_g	SWC	PPT
NEE	0.7**	0.09	−0.49	−0.73**	0.62*	0.08
GPP		−0.65*	−0.34	−0.24	−0.34	−0.07
TER			−0.06	−0.44	0.14	0.19
T_{air}				0.35	−0.15	0.33
R_g					−0.77 **	−0.3
SWC						0.76 **

fixed climate or parameters (c.f. Sect. 2.5). The performance of Model II was clearly higher in terms of residuals and therefore the remaining analysis will focus on Model II. Model I will continue to be used for comparison along with the results where the VPD effect in the model structure was changed.

Interannual variation in the modelled NEE (Model II) differed when either the parameters or the climate variables were fixed (Fig. 6). When the parameters were fixed, i.e. assuming the ecosystem status during the 13 yr was constant (Fig. 6b), the modelled fluxes NEE_{parfix} ranged between $-231\,g\,C\,m^{-2}\,yr^{-1}$ in 2009 and $-27\,g\,C\,m^{-2}\,yr^{-1}$ in 2006. When the climate time series were fixed, NEE_{clifix} ranged between $81\,g\,C\,m^{-2}\,yr^{-1}$ in 1998 and $-293\,g\,C\,m^{-2}\,yr^{-1}$ in 2005 (Fig. 6c). The IAV in the originally modelled fluxes $NEE_{original}$ (Fig. 6a) were better reproduced when the changes in the parameter time series were included. The correlation between the $NEE_{original}$ and NEE_{clifix} was 0.9 ($p < 0.01$). In contrast, the correlation between the NEE_{parfix} and $NEE_{original}$ was not significant. The differences in these modelled fluxes represent the climate and parameter effects; these effects can be interpreted as the influence of changes in climatic and ecosystem functional properties, respectively.

The analysis of the 13×13 matrix of model predictions (Model II), where the parameter and climate time series of each year were applied factorially, attributed 78–82 % of the variance in NEE to the interannual variation in the parameter time series (Fig. 7). Using Model I, we obtained similar results as parameter variability accounted for 80–83 % the IAV in annual NEE. In general, the percentage of the total variance in the carbon flux caused by climatic variability decreased with the level of temporal integration. The estimated impact of climatic variability at shorter time scales using different models did not converge as much as in the annual time scale. The estimated impact of climatic variability, for the IAV in NEE based on Model II at sub-annual scales was clearly lower than those estimated based on Model I (Fig. 7). Because Model I cannot represent the seasonal pattern of parameter change with the same accuracy as Model II, it was expected that the impact of functional change will

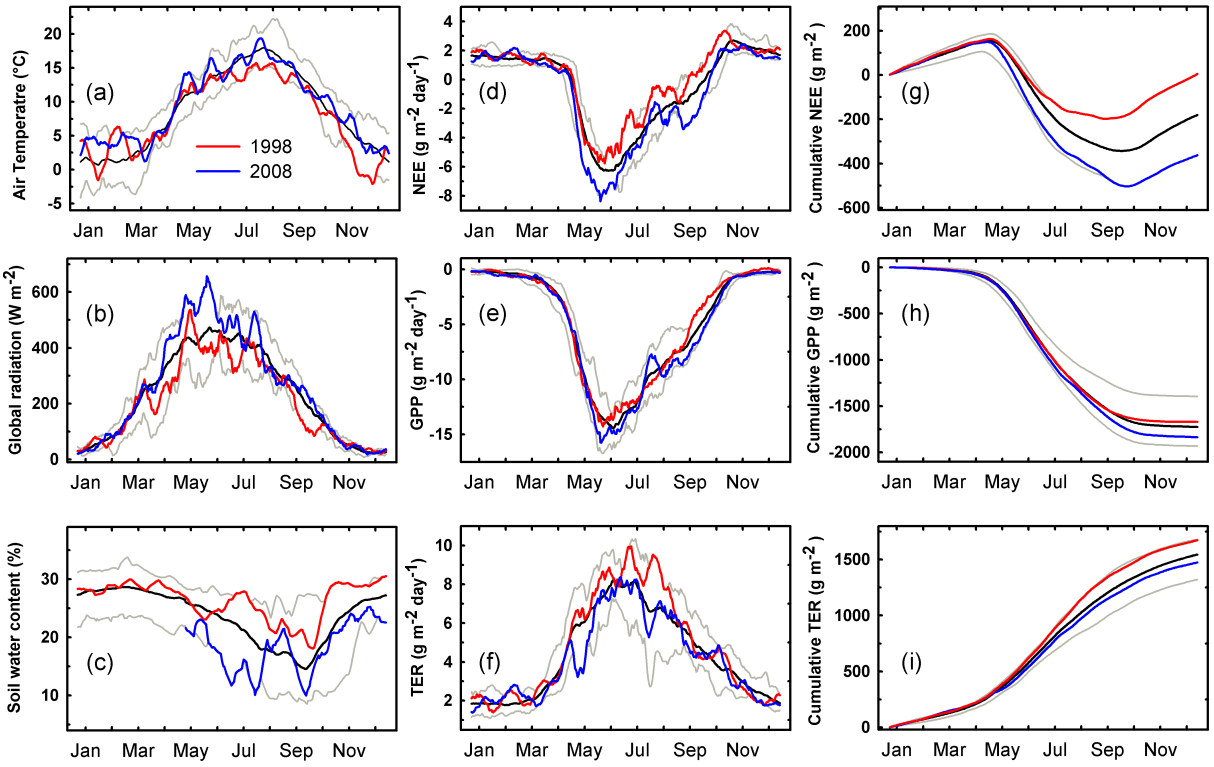

Fig. 3. The average (black line) and two example years (1998, 2008) in terms of climate **(a, b, c)**, carbon flux **(d, e, f)** and cumulative carbon flux **(g, h, i)**. All data were smoothed with a 14-day moving average. Grey lines indicate the maximum and minimum of the value on the same DOY across the 13 yr.

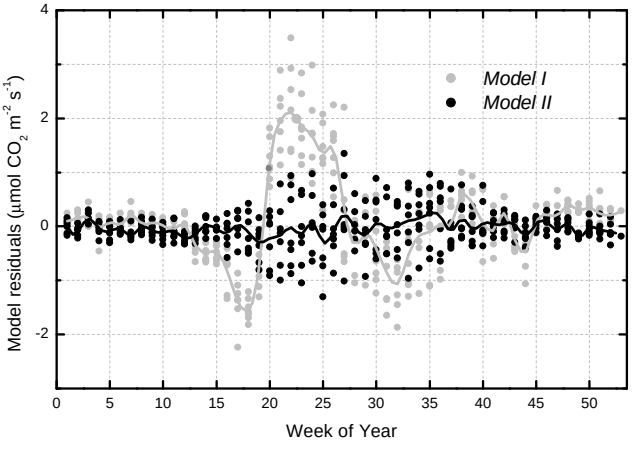

Fig. 4. Seasonal pattern of model residuals (mean errors) for the two empirical models (described in the method sections). Mean daily residuals (symbols) were grouped by weeks; the smoothed lines were calculated with a 14-day median filter.

be underestimated. We showed in the previous section that the prediction of Model I was strongly biased throughout the year (Fig. 4) and that the resulting errors were propagated in to the analysis and biased the results. The estimated parameter effect on NEE at annual time scale did not change significantly when the VPD effect in the model was removed (81–85 %) or changed (with a lower VPD_0, 79–83 %). At other time scales, the difference in the estimated impact of ecosystem functional change caused by changing the VPD function was less than 2 %.

GPP was much more sensitive to variation in climate than TER was. At the daily time scale, climate variability accounted for more than 67–71 % of the variation in GPP. The effect of climate variability on TER was very low (19–22 %), even at the daily time scale. This is most likely because the dominant component of TER is soil respiration, a process which is highly dependent on substrate availability and microbial activities (Davidson et al., 2006). This then results in reduced climatic effects on TER, compared to the aboveground processes, such as photosynthesis and phenology. On the other hand, because GPP and TER are only influenced by certain climate variables in the model structure (Eq. 3 and 4), the unaccounted effect of other climate variables on GPP and TER could be propagated into the parameters and thus result in the underestimation of the effect of climate variability. We assessed the influence of temperature on GPP which is not explicitly included in the model by plotting the simulated daily GPP at light saturation ($R_g = 1000\,Wm^{-2}$) with T_{air} (Fig. 8a). A clear relationship between T_{air} and

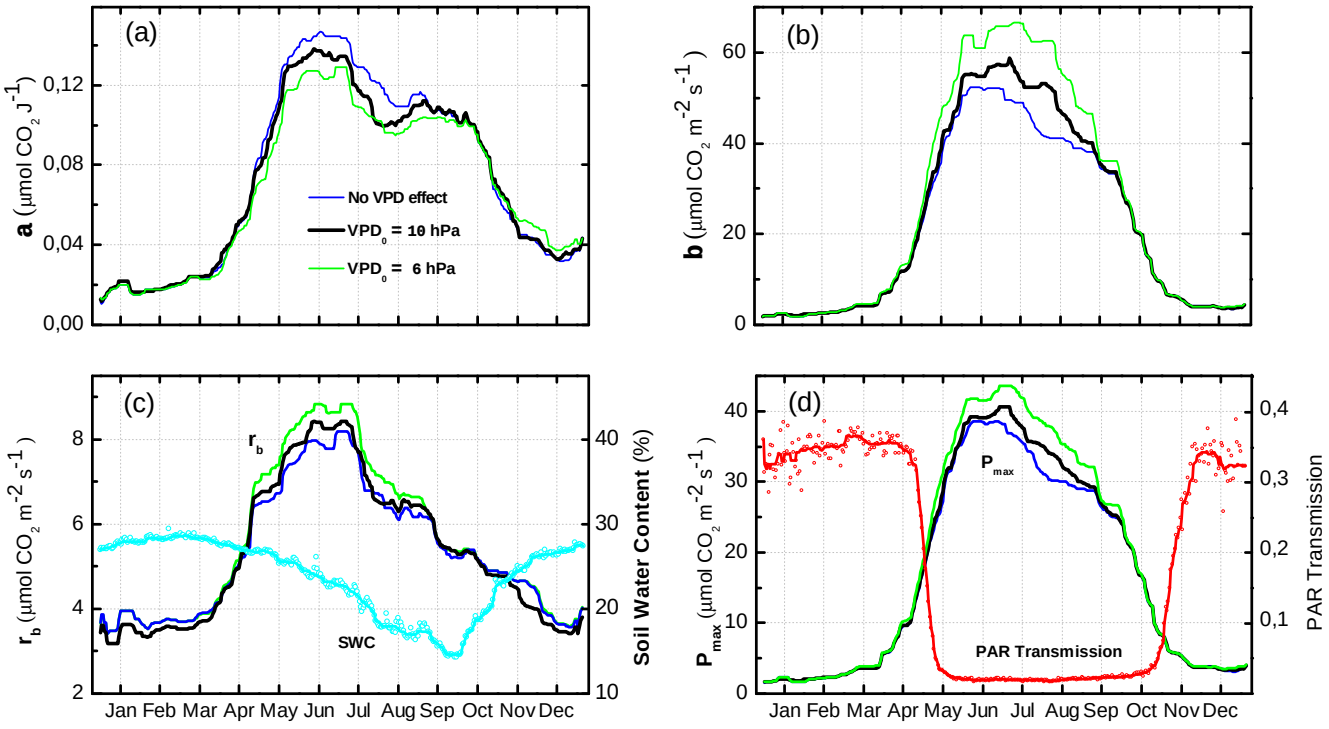

Fig. 5. Seasonal variation in **(a)**: light use efficiency (α), **(b)**: canopy maximum photosynthetic capacity (β), **(c)**: base respiration (r_b and soil water content, **(d)** canopy photosynthesis at light saturation ($R_g = 1000\,\mathrm{Wm}^{-2}$), P_{max} and PAR transmission records from Pilegaard et al. (2011). The blue line **(a, b, d)** represents the estimated parameter values when the VPD effect (Eq. 4) on β was removed; the green line represents the result when VPD_0 was set to 6 hPa. The parameter time series and P_{max} were presented as an ensemble (mean value) of all the 13 yr. PAR transmission data are the ensemble mean from 2001–2009 (measurements began in 2001). The symbols represent mean values and were smoothed with a 14-day median filter (solid line).

the GPP-related parameters was found when the whole year data was used, however, during the period when the canopy was fully developed and LAI was relatively constant (May–September), no significant relationship between T_{air} and the simulated potential GPP was found. The TER-related parameters were not completely independent from SWC. During the growing season, the predicted TER at 25 °C was still weakly correlated with SWC (Fig. 8b).

4 Discussion

4.1 Strengths and limitations of the statistical modelling approach

The combination of modelling and data analysis provides insight into the complex interactions between the direct climatic effects and the biotic ecosystem responses, by partitioning their roles in determining the interannual variation of the ecosystem carbon fluxes. In this study, two empirical models were used to this end. The comparison of an existing approach (Model I), and our approach (Model II) showed similar estimates of the impact of functional change at the annual time scale (ca. 80 %). However, our approach, which allowed the parameters to vary seasonally within year, resulted in less seasonal bias (Fig. 4), increased the degree of determination, and thus, increased the confidence in the estimate of the impact of functional change at both the annual and sub-annual time scales.

A major strength of the statistical modelling approach is that it does not require an explicit parameterization of the complex ecosystem process in detail. It has been proposed that in order to realistically distinguish between the effect of climate variability and functional change using a parameter extraction method, a mechanistic model must be used (Leuning, 2011). However, many processes, such as phenology, are considered indirectly by the parameter estimation method. These responses to current and previous climate can be considered to be ecosystem structural change and are captured by this method (Fig. 5). Also, the information contained in the flux data alone is likely insufficient to distinguish the between detailed ecosystem processes (Wang et al., 2009). The risk of over-parameterization is a strong justification to keep the model structure simple. For example, detailed processes such as direct and diffuse radiation

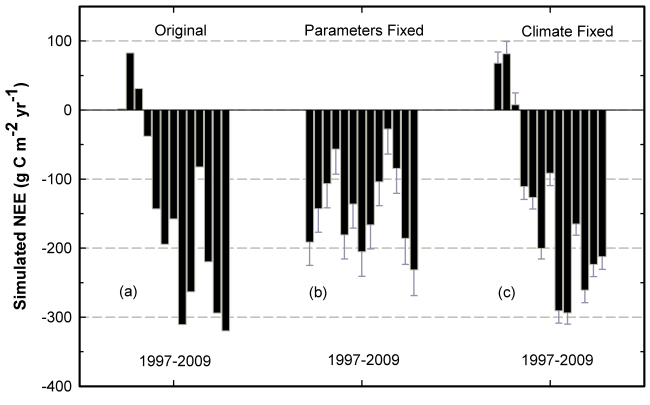

Fig. 6. Interannual variation in simulated NEE **(a)** $NEE_{original}$: using the original climate and parameter time series in each of the 13 yr; **(b)** NEE_{parfix}: parameters kept constant; **(c)** NEE_{clifix}: climate kept constant. Each value of NEE_{parfix} and NEE_{clifix} represents an ensemble mean value of the 13 simulations where the parameter, or climate time series from 1997–2009 was applied in sequence. The error bars show the standard error.

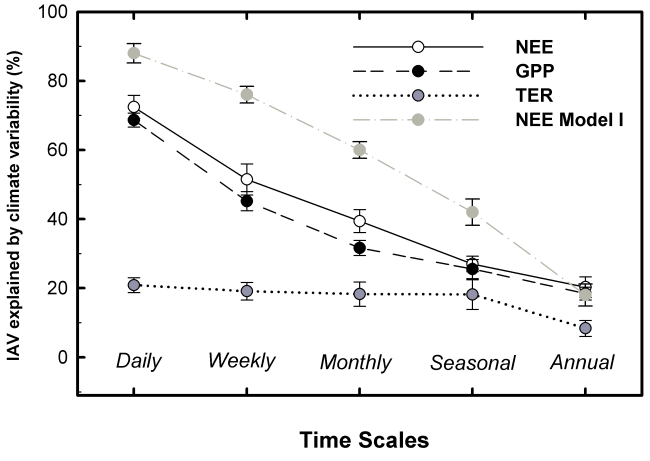

Fig. 7. Percentage of interannual variation in modelled carbon fluxes caused by climate variability at different time scales calculated with Model II and, for comparison, results from Model I for NEE. The error bars show the standard deviation of the estimates (c.f. Eq. 6).

and the separation of autotrophic and heterotrophic respiration were not implemented. The effects of many of those processes are aggregated into the parameters of the empirical model used. A mechanistic model, although desirable for other reasons, might not be an efficient way to achieve the objectives of this study, as it would need much more information to reach the same goal: the realistic representation of the seasonal ecosystem functional state. To address the concerns of the simplicity of our model structure, instead of adding a mechanistic sub-module, we tested the effect of removing the VPD sub-module. The results showed that the partitioning between the climate and parameter effects was not changed. We therefore conclude that the available information on ecosystem functional change within the CO_2 flux data was captured by the flexible modelling approach.

Statistical models have limited potential to elucidate the causes behind the identified functional change. However, this was not the primary aim of this study, as the focus was to distinguish between the direct climatic effects and the changes of ecosystem functioning. The model and fitted parameters cannot be used for predictive purposes or extrapolation. As indicated by Groenendijk et al. (2011), although specific site-year derived parameters give the best prediction of observed fluxes, they are generally too specific to be used in global studies. However, this modelling approach can be applied to flux data from other sites to obtain site specific parameters and quantify the importance of functional change for the IAV of carbon fluxes in different ecosystems. We advocate using our approach as it offers a high flexibility without requirements for additional information.

4.2 Magnitude and uncertainty of the estimated impact of functional change

The most important finding of this study is that the 13 yr trend of increasing carbon uptake was found to be more strongly driven by the aggregated effect of the parameters than the climatic factors. In addition to the changes in the maximum photosynthetic capacity and the carbon uptake period (Pilegaard et al., 2011), we found that other photosynthesis and respiration related parameters also changed in different years and indirectly affected the ecosystem carbon balance. The estimated impact of functional change on the IAV of the carbon balance at Sorø was higher than at other sites (Teklemariam et al., 2010; Richardson et al., 2007; Hui et al., 2003), although the methods applied were different. However, using the same model of Richardson et al. (2007), we found also a much higher impact of functional change at Sorø (deciduous) than at Howland Forest (mixed). The results at annual time scale at Sorø did not differ much between Model I and Model II. This is probably due to the fact that the dominance of the functional change over direct climatic effect is so strong at this site that the choice of model is not particularly important. But as our model has not been applied at other sites, this cannot be stated with sufficient certainty.

A possible reason for such tendencies could be the type and structure of the ecosystem. Based on a number of published studies, the impact of functional change decreases in the order: deciduous forest (this study), mixed forest (Richardson et al., 2007), conifer forest (Hui et al., 2003) and peatland (Teklemariam et al., 2010), implying a possible difference in the sensitivity of these ecosystems to environmental change and disturbance. Cross-site studies of IAV in the ecosystem carbon balance also found that deciduous forests tend to be more sensitive than evergreen conifer forests to climate variability (Yuan et al., 2009) and

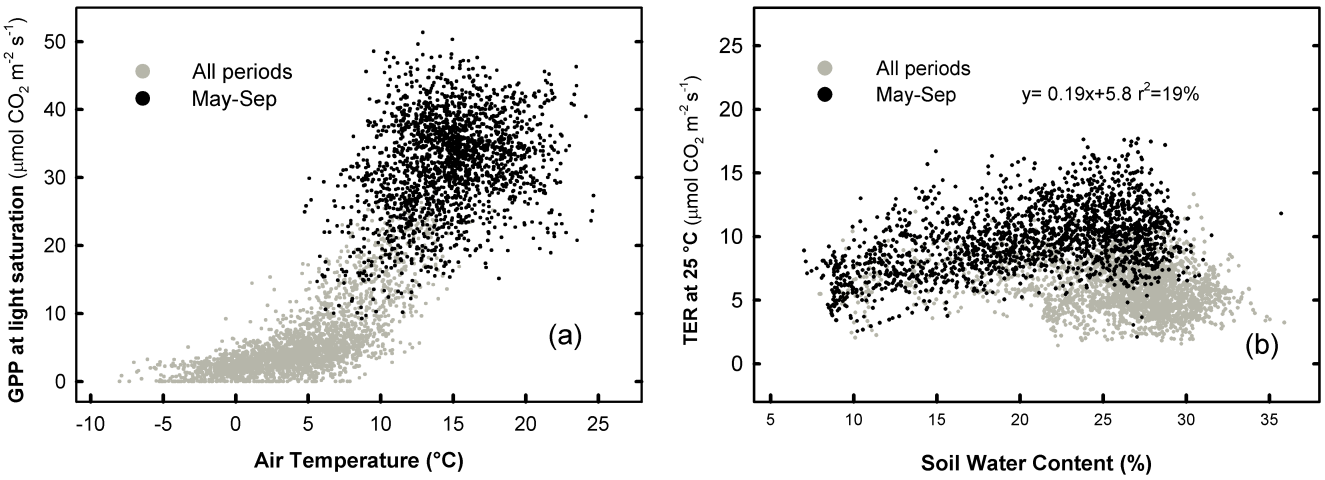

Fig. 8. Comparison of climate variables and the estimated parameters. **(a)** GPP at light saturation plotted against air temperature. **(b)** TER at 25 °C plotted against soil water content.

phenological transitions (Richardson et al., 2010). These differences in the adaptive capacity to changing climate between deciduous and evergreen forests may drive shifts in the composition within mixed forests (Richardson et al., 2010).

The estimated impact of functional change is not without uncertainties, mainly due to the core assumption that functional change is solely represented by the changes in model parameters. This assumption is challenged by the simplicity of the model structure, e.g. the temperature regulation of GPP and the SWC regulation of TER were not explicitly specified in the model structure. Testing the residual climatic effects on the model predictions showed that, although we did not explicitly account for the temperature effect on GPP in the model, it was at least partly represented by the model, possibly due to the cross correlation between temperature and VPD or temperature and radiation. Therefore the largest part of the correlation between temperature and parameters, when using the whole data set, are derived from functional changes, e.g. canopy development that were either influenced by or coincided with temperature. In contrast, the TER-related parameters were not completely independent from SWC. Approximately 19 % of the parameter effect on TER could be attributed to variation in SWC, which has led to a small overestimation of functional change.

4.3 Climate variability and average climate change

The correlation analysis between carbon fluxes and climatic variables revealed that the variation in the mean annual climate could not directly explain the IAV in the annual ecosystem carbon balance. Global radiation and soil water content were significantly correlated with NEE (Table 2). However, contrary to our expectations, neither R_g nor SWC were significantly correlated with gross photosynthesis or total ecosystem respiration, i.e. the processes that drive NEE. Ecosystem respiration was low in years with higher radiation ($r = -0.44$, $p > 0.05$), which might have strengthened the correlation between R_g and NEE. SWC was low in years with high radiation and was also correlated with NEE. Therefore, despite comparably high correlation coefficients, these correlations do not represent direct cause-effect relationships between mean annual climate variables and NEE. Rather, they are the result of the combination of the various controlling mechanisms in different seasons, as illustrated by the correlation analysis at short time scales.

At shorter time scales, the sensitivity of carbon fluxes to climate variability significantly increased. For more than 80 % of the year, the carbon flux was strongly correlated with at least one of the investigated climate variable. The climate variables, to which the carbon fluxes were most sensitive, differed across seasons (Fig. 2). These variations affected the net ecosystem carbon balance via the different climate sensitivities of GPP and TER. Depending on the sign of the response and the different sensitivity, the climatic impact on NEE is either amplified or attenuated. Analyzing the climate sensitivity of the component fluxes (GPP, TER) contributes more to the understanding of the climate sensitivity of NEE than directly analyzing the climate sensitivity of NEE itself.

This significant seasonality of the ecosystem responses to climatic variability demonstrated the importance of the seasonal distribution of the climate anomalies on future ecosystem carbon balances. Our results showed that this beech forest will be sensitive to increases in summer drought. Altered precipitation patterns, i.e. increased rainfall variability rather than changes in annual precipitation are likely to affect ecosystem carbon balances in the future (Knapp et al., 2002). The average climate change is expected to be accompanied by increased variability and weather extremes (Easterling et al., 2000a, b). Climate change projections for Denmark

that suggest that a small increase in precipitation will occur, but mainly during winter, while the likelihood of summer droughts will increase (Christensen and Christensen, 2007). Our results suggest that in addition to the changes in average climate, increased climatic variability could alter the ecosystem carbon balance more strongly, as the climate anomalies are projected to take place predominantly during biologically active periods.

4.4 Gross primary productivity as a driver of the interannual variability in net ecosystem exchange

Interannual variation in NEE in this beech forest was mostly driven by GPP whereas TER had relatively less influence. This was similar to two deciduous forests in both boreal and temperate zones (Barr et al., 2002). However, the results of these two studies differed from the conclusion of a cross-site synthesis of 15 European forests (Valentini et al., 2000) where respiration was found to determine the spatial variability in ecosystem carbon balance. According to this synthesis, net carbon uptake decreased significantly with increasing latitude, whereas total ecosystem respiration increased and gross photosynthesis tended to be rather independent of latitude. These different findings based on site specific studies and cross-site synthesis indicate that although TER tends to vary significantly and dominate the ecosystem carbon balance over large spatial scales, its influence on the temporal variability in NEE may be much weaker at site level. For deciduous forests at middle and high latitudes, the variability in GPP was much stronger and largely controlled the interannual variation of the ecosystem carbon balance.

Total ecosystem respiration was highly correlated with GPP, both at annual and sub-annual time scales. It is still under debate whether this correlation could be artificial because GPP was calculated from TER and NEE (Vickers et al., 2009). Lasslop et al. (2010a), however, showed that only the error in TER that directly propagates into GPP can cause spurious correlation. A large part of the variability of TER was however shown to be independent from GPP, and thus the correlation between GPP and TER was real, rather than spurious. This suggestion is supported by using a TER estimate derived from a fit of a respiration model to nighttime data in combination with a GPP estimate derived using a light response curve fit to daytime data. In this case the errors in one flux component cannot directly propagate to the other and the correlation remains high (Lasslop et al., 2010b). A more likely explanation for the high correlation is the covariance of the main drivers of photosynthesis and respiration, e.g. temperature and radiation. From the physiological perspective the correlation could be an effect of substrate availability on autotrophic (plant activity, i.e. growth respiration and reserve metabolism) and heterotrophic respiration (root exudates and litter production). This interpretation is supported by an increasing number of experimental studies, such as tree girdling studies (Högberg et al., 2001) or direct and quasi parallel measurement of GPP and TER during daytime with ecosystem chambers in shrublands (Larsen et al., 2007).

4.5 Implication for mechanistic models

The results of this study suggest that projection of future carbon balance of terrestrial ecosystems could be improved if the biotic responses to climate variability and thus functional change are properly incorporated into mechanistic models. Migliavacca et al. (2011) demonstrated that the spatiotemporal variability in ecosystem respiration can be better modelled when the dynamics in the biotic factors are taken into account. Modelling the IAV of the carbon balance has proven difficult (Siqueira et al., 2006). One important reason is that most parameters are usually kept constant. For example, in global models, parameters are usually static for plant functional types (Krinner, 2005; Sitch et al., 2003). Increasing model complexity by adding processes that enable change in ecosystem state (e.g. nitrogen cycling or dynamics in the microbial community) could possibly improve the situation. However, this could lead to model over-parameterization and increase the demand for validation data, thus limiting model application at large spatial scales. Flux studies should therefore be accompanied by biological process studies and ecosystem structural assessments to overcome the data limitations that result in model over-parameterization. Site level studies clearly show the necessity for further development of these functional change modules. Thus, using an alternative approach by establishing empirical functional relationships between parameters and independent variables and subsequently embedding them in the model could be an intermediate solution. Therefore, combining experimental studies, empirical and mechanistic modelling could elucidate the importance of functional changes when simulating future terrestrial carbon budgets and potentially improve the prognostic capacity of ecosystem models.

5 Conclusions

An approach to separate the direct climatic effects on the interannual variability of carbon fluxes from ecosystem functional changes (Richardson et al., 2007) was improved by employing the semi-empirical model of Lasslop et al. (2010b). By fitting the model parameters in small moving windows, the seasonality of the model parameters was accounted for more realistically. This made the representation of the seasonality of ecosystem functioning more flexible, rather than constraining them to prescribed relationships that are constant throughout the year.

Climate variability exerted a strong control on the carbon fluxes at short time scales but this impact weakened as the time integral increased. At longer temporal scales, the effect of ecosystem functional change became progressively larger and appeared to dominate the interannual variability in the

ecosystem carbon balance. From the high climate sensitivity at short time scales we conclude that the ecosystem will be sensitive to the seasonal distribution of climate anomalies that are expected to increase in the future. The observed trend of increasing carbon uptake (Pilegaard et al., 2011) was found to be driven by ecosystem functional changes rather than direct effects of decadal climatic variability. Such strong effects demonstrate the need to integrate ecosystem functional change into mechanistic models, if they are to realistically predict future ecosystem carbon balances and thus feedbacks to climate change.

Acknowledgements. This work was supported by the EU FP7 project CARBO-extreme, the DTU Climate Centre and the Danish national project ECOCLIM (Danish Council for Strategic Research). We thank Ray Leuning, Werner Eugster, an anonymous reviewer and the editor, Georg Wohlfahrt, for many critical and valuable comments on the manuscript.

Edited by: G. Wohlfahrt

References

Aubinet, M., Grelle, A., Ibrom, A., Rannik, S., Moncrieff, J., Foken, T., Kowalski, A., Martin, P., Berbigier, P., and Bernhofer, C.: Estimates of the annual net carbon and water exchange of forests: the EUROFLUX methodology, Adv. Ecol. Res., 30, 113–175, 2000.

Baldocchi, D.: Assessing the eddy covariance technique for evaluating carbon dioxide exchange rates of ecosystems: past, present and future, Global Change Biol., 9, 479–492, 2003.

Barr, A., Griffis, T., Black, T., Lee, X., Staebler, R., Fuentes, J., Chen, Z., and Morgenstern, K.: Comparing the carbon budgets of boreal and temperate deciduous forest stands, Can. J. Forest Res., 32, 813–822, 2002.

Barr, A., Black, T., Hogg, E., Kljun, N., Morgenstern, K., and Nesic, Z.: Inter-annual variability in the leaf area index of a boreal aspen-hazelnut forest in relation to net ecosystem production, Agr. Forest Meteorol., 126, 237–255, 2004.

Barr, A., Black, T., Hogg, E., Griffis, T., Morgenstern, K., Kljun, N., Theede, A., and Nesic, Z.: Climatic controls on the carbon and water balances of a boreal aspen forest, 1994–2003, Global Change Biol., 13, 561–576, 2007.

Beer, C., Reichstein, M., Tomelleri, E., Ciais, P., Jung, M., Carvalhais, N., Rodenbeck, C., Arain, M. A., Baldocchi, D., Bonan, G. B., Bondeau, A., Cescatti, A., Lasslop, G., Lindroth, A., Lomas, M., Luyssaert, S., Margolis, H., Oleson, K. W., Roupsard, O., Veenendaal, E., Viovy, N., Williams, C., Woodward, F. I., and Papale, D.: Terrestrial Gross Carbon Dioxide Uptake: Global Distribution and Covariation with Climate, Science, 329, 834–838, doi:10.1126/science.1184984, 2010.

Black, T., Chen, W., Barr, A., Arain, M., Chen, Z., Nesic, Z., Hogg, E., Neumann, H., and Yang, P.: Increased carbon sequestration by a boreal deciduous forest in years with a warm spring, Geophys. Res. Lett., 27, 1271–1274, 2000.

Braswell, B. H., Schimel, D. S., Linder, E., and Moore, B.: The Response of Global Terrestrial Ecosystems to Interannual Temperature Variability, Science, 278, 870–873, doi:10.1126/science.278.5339.870, 1997.

Chen, W., Black, T., Yang, P., Barr, A., Neumann, H., Nesic, Z., Blanken, P., Novak, M., Eley, J., and Ketler, R.: Effects of climatic variability on the annual carbon sequestration by a boreal aspen forest, Global Change Biol., 5, 41–53, 1999.

Christensen, J. H. and Christensen, O. B.: A summary of the PRUDENCE model projections of changes in European climate by the end of this century, Climatic Change, 81, 7–30, 2007.

Churkina, G., Schimel, D., Braswell, B., and Xiao, X.: Spatial analysis of growing season length control over net ecosystem exchange, Global Change Biol., 11, 1777–1787, 2005.

Davidson, E., Janssens, I., and Luo, Y.: On the variability of respiration in terrestrial ecosystems: moving beyond Q_{10}, Global Change Biol., 12, 154–164, 2006.

Dellwik, E. and Jensen, N. O.: Internal equilibrium layer growth over forest, Theor. Appl. Climatol., 66, 173–184, 2000.

Dellwik, E. and Jensen, N. O.: Flux-profile relationships over a fetch limited beech forest, Bound.-Lay. Meteorol., 115, 179–204, 2005.

Delpierre, N., Soudani, K., Francois, C., Köstner, B., Pontailler, J. Y., Nikinmaa, E., Misson, L., Aubinet, M., Bernhofer, C., and Granier, A.: Exceptional carbon uptake in European forests during the warm spring of 2007: a data–model analysis, Global Change Biol., 15, 1455–1474, 2009.

Dunn, A. L., Barford, C. C., Wofsy, S. C., Goulden, M. L., and Daube, B. C.: A long-term record of carbon exchange in a boreal black spruce forest: means, responses to interannual variability, and decadal trends, Global Change Biol., 13, 577–590, doi:10.1111/j.1365-2486.2006.01221.x, 2007.

Falge, E., Baldocchi, D., Olson, R., Anthoni, P., Aubinet, M., Bernhofer, C., Burba, G., Ceulemans, R., Clement, R., Dolman, H., Granier, A., Gross, P., Grünwald, T., Hollinger, D., Jensen, N.-O., Katul, G., Keronen, P., Kowalski, A., Lai, C. T., Law, B. E., Meyers, T., Moncrieff, J., Moors, E., Munger, J. W., Pilegaard, K., Rannik, Ü., Rebmann, C., Suyker, A., Tenhunen, J., Tu, K., Verma, S., Vesala, T., Wilson, K., and Wofsy, S.: Gap filling strategies for defensible annual sums of net ecosystem exchange, Agr. Forest Meteorol., 107, 43–69, doi:10.1016/s0168-1923(00)00225-2, 2001.

Friedlingstein, P., Houghton, R., Marland, G., Hackler, J., Boden, T., Conway, T., Canadell, J., Raupach, M., Ciais, P., and Le Quéré, C.: Update on CO_2 emissions, Nat. Geosci., 3, 811–812, 2010.

Göckede, M., Foken, T., Aubinet, M., Aurela, M., Banza, J., Bernhofer, C., Bonnefond, J. M., Brunet, Y., Carrara, A., Clement, R., Dellwik, E., Elbers, J., Eugster, W., Fuhrer, J., Granier, A., Grünwald, T., Heinesch, B., Janssens, I. A., Knohl, A., Koeble, R., Laurila, T., Longdoz, B., Manca, G., Marek, M., Markkanen, T., Mateus, J., Matteucci, G., Mauder, M., Migliavacca, M., Minerbi, S., Moncrieff, J., Montagnani, L., Moors, E., Ourcival, J.-M., Papale, D., Pereira, J., Pilegaard, K., Pita, G., Rambal, S., Rebmann, C., Rodrigues, A., Rotenberg, E., Sanz, M. J., Sedlak, P., Seufert, G., Siebicke, L., Soussana, J. F., Valentini, R., Vesala, T., Verbeeck, H., and Yakir, D.: Quality control of CarboEurope flux data - Part 1: Coupling footprint analyses with flux data quality assessment to evaluate sites in forest ecosystems, Biogeosciences, 5, 433–450, doi:10.5194/bg-5-433-2008, 2008.

Groenendijk, M., Dolman, A. J., Molen, M. K. v. d., Leuning, R., Arneth, A., Delpierre, N., Gash, J. H. C., Lindroth, A., Richardson, A. D., Verbeeck, H., and Wohlfahrt, G.: Assessing parameter variability in a photosynthesis model within and between plant functional types using global Fluxnet eddy covariance data, Agr. Forest Meteorol., 151, 22–38, 2011.

Heimann, M. and Reichstein, M.: Terrestrial ecosystem carbon dynamics and climate feedbacks, Nature, 451, 289–292, 2008.

Högberg, P., Nordgren, A., Buchmann, N., Taylor, A. F. S., Ekblad, A., Högberg, M. N., Nyberg, G., Ottosson-Löfvenius, M., and Read, D. J.: Large-scale forest girdling shows that current photosynthesis drives soil respiration, Nature, 411, 789–792, 2001.

Hollinger, D., Aber, J., Dail, B., Davidson, E., Goltz, S., Hughes, H., Leclerc, M., Lee, J., Richardson, A., and Rodrigues, C.: Spatial and temporal variability in forest-atmosphere CO_2 exchange, Global Change Biol., 10, 1689–1706, 2004.

Houghton, R.: Balancing the global carbon budget, Annu. Rev. Earth Planet. Sci., 35, 313–347, 2007.

Hu, J., Moore, D., Burns, S., and Monson, R.: Longer growing seasons lead to less carbon sequestration by a subalpine forest, Global Change Biol., 16, 771–783, 2010.

Hui, D., Luo, Y., and Katul, G.: Partitioning interannual variability in net ecosystem exchange between climatic variability and functional change, Tree Physiol., 23, 433–442, 2003.

Ibrom, A., Jarvis, P. G., Clement, R., Morgenstern, K., Oltchev, A., Medlyn, B. E., Wang, Y. P., Wingate, L., Moncrieff, J. B., and Gravenhorst, G.: A comparative analysis of simulated and observed photosynthetic CO_2 uptake in two coniferous forest canopies, Tree Physiol., 26, 845–864, 2006.

Ibrom, A., Dellwik, E., Flyvbjerg, H., Jensen, N. O., and Pilegaard, K.: Strong low-pass filtering effects on water vapour flux measurements with closed-path eddy correlation systems, Agr. Forest Meteorol., 147, 140–156, 2007.

Krinner, G., Viovy, N., de Noblet-Ducoudré, N., Ogée, J., Polcher, J., Friedlingstein, P., Ciais, P., Sitch, S., and Prentice, I. C.: A dynamic global vegetation model for studies of the coupled atmosphere-biosphere system, Global Biogeochem. Cy., 19, GB1015, doi:10.1029/2003gb002199, 2005.

Körner, C.: Leaf diffusive conductances in the major vegetation types of the globe, in: Ecophysiology of photosynthesis, edited by: Schulze, E.-D., Springer Verlag, Berlin, 463–490, 1995.

Ladekarl, U.: Soil moisture, evapotranspiration and groundwater recharge in forest and heathland, Ph.D. Thesis, Department of Earth Sciences, University of Aarhus, Denmark, 2001.

Larsen, K. S., Ibrom, A., Jonasson, S., Michelsen, A., and Beier, C.: Significance of cold season respiration and photosynthesis in a subarctic heath ecosystem in Northern Sweden, Global Change Biol., 13, 1498–1508, 2007.

Lasslop, G., Reichstein, M., Detto, M., Richardson, A. D., and Baldocchi, D. D.: Comment on Vickers et al.: Self-correlation between assimilation and respiration resulting from flux partitioning of eddy-covariance CO_2 fluxes, Agr. Forest Meteorol., 150, 312–314, 2010a.

Lasslop, G., Reichstein, M., Papale, D., Richardson, A., Arneth, A., Barr, A., Stoy, P., and Wohlfahrt, G.: Separation of net ecosystem exchange into assimilation and respiration using a light response curve approach: critical issues and global evaluation, Global Change Biol., 16, 187–208, 2010b.

Le Dantec, V., Dufrêne, E., and Saugier, B.: Interannual and spatial variation in maximum leaf area index of temperate deciduous stands, Forest Ecol. Manag., 134, 71–81, 2000.

Leuning, R.: Wu, J., van der Linden, L., Lasslop, G., Carvalhais, N., Pilegaard, K., Beier, C., and Ibrom, A.: Effects of climate variability and functional changes on the interannual variation of the carbon balance in a temperate deciduous forest, Biogeosciences Discuss., 8, 9125–9163, doi:10.5194/bgd-8-9125-2011, 2011.

Lloyd, J. and Taylor, J.: On the temperature dependence of soil respiration, Funct. Ecol., 8, 315–323, 1994.

Luo, Y., Wan, S., Hui, D., and Wallace, L.: Acclimatization of soil respiration to warming in a tall grass prairie, Nature, 413, 622–625, 2001.

Luyssaert, S., Inglima, I., Jung, M., Richardson, A., Reichstein, M., Papale, D., Piao, S., Schulze, E., Wingate, L., and Matteucci, G.: CO_2 balance of boreal, temperate, and tropical forests derived from a global database, Global Change Biol., 13, 2509–2537, 2007.

Mahecha, M. D., Reichstein, M., Carvalhais, N., Lasslop, G., Lange, H., Seneviratne, S. I., Vargas, R., Ammann, C., Arain, M. A., Cescatti, A., Janssens, I. A., Migliavacca, M., Montagnani, L., and Richardson, A. D.: Global Convergence in the Temperature Sensitivity of Respiration at Ecosystem Level, Science, 329, 838–840, doi:10.1126/science.1189587, 2010.

Migliavacca, M., Reichstein, M., Richardson, A. D., Colombo, R., Sutton, M. A., Lasslop, G., Tomelleri, E., Wohlfahrt, G., Carvalhais, N., and Cescatti, A.: Semiempirical modeling of abiotic and biotic factors controlling ecosystem respiration across eddy covariance sites, Global Change Biol., 17, 390–409, 2011.

Misson, L., Rocheteau, A., Rambal, S., Ourcival, J.-M., Limousin, J.-M., and Rodriguez, R.: Functional changes in the control of carbon fluxes after 3 years of increased drought in a Mediterranean evergreen forest?, Global Change Biol., 16, 2461–2475, doi:10.1111/j.1365-2486.2009.02121.x, 2010.

Penuelas, J. and Filella, I.: Phenology feedbacks on climate change, Science, 324, 887–888, 2009.

Piao, S., Ciais, P., Friedlingstein, P., Peylin, P., Reichstein, M., Luyssaert, S., Margolis, H., Fang, J., Barr, A., Chen, A., Grelle, A., Hollinger, D. Y., Laurila, T., Lindroth, A., Richardson, A. D., and Vesala, T.: Net carbon dioxide losses of northern ecosystems in response to autumn warming, Nature, 451, 49–52, doi:10.1038/nature06444, 2008.

Pilegaard, K., Hummelsh, J, P., Jensen, N., and Chen, Z.: Two years of continuous CO_2 eddy-flux measurements over a Danish beech forest, Agr. Forest Meteorol., 107, 29–41, 2001.

Pilegaard, K., Mikkelsen, T. N., Beier, C., Jensen, N. O., Ambus, P., and Ro-Poulsen, H.: Field measurements of atmosphere-biosphere interactions in a Danish beech forest, Boreal Environ. Res., 8, 315–333, 2003.

Pilegaard, K., Ibrom, A., Courtney, M. S., Hummelsh, J, P., and Jensen, N. O.: Increasing net CO_2 uptake by a Danish beech forest during the period from 1996 to 2009, Agr. Forest Meteorol., 151, 934–946, 2011.

Reichstein, M., Falge, E., Baldocchi, D., Papale, D., Aubinet, M., Berbigier, P., Bernhofer, C., Buchmann, N., Gilmanov, T., and Granier, A.: On the separation of net ecosystem exchange into assimilation and ecosystem respiration: review and improved algorithm, Global Change Biol., 11, 1424–1439, 2005.

Reichstein, M., Papale, D., Valentini, R., Aubinet, M., Bernhofer, C., Knohl, A., Laurila, T., Lindroth, A., Moors, E., and Pilegaard,

K.: Determinants of terrestrial ecosystem carbon balance inferred from European eddy covariance flux sites, Geophys. Res. Lett., 34, L01402, doi:10.1029/2006gl027880, 2007.

Richardson, A. and Hollinger, D.: Statistical modeling of ecosystem respiration using eddy covariance data: maximum likelihood parameter estimation, and Monte Carlo simulation of model and parameter uncertainty, applied to three simple models, Agr. Forest Meteorol., 131, 191–208, 2005.

Richardson, A., Hollinger, D., Aber, J., Ollinger, S., and Braswell, B.: Environmental variation is directly responsible for short but not long term variation in forest atmosphere carbon exchange, Global Change Biol., 13, 788–803, 2007.

Richardson, A., Hollinger, D., Dail, D., Lee, J., Munger, J., and O'keefe, J.: Influence of spring phenology on seasonal and annual carbon balance in two contrasting New England forests, Tree Physiol., 29, 321–331, 2009.

Richardson, A., Andy Black, T., Ciais, P., Delbart, N., Friedl, M., Gobron, N., Hollinger, D., Kutsch, W., Longdoz, B., and Luyssaert, S.: Influence of spring and autumn phenological transitions on forest ecosystem productivity, Phil. Trans. R. Soc. B, 365, 3227–3246, 2010.

Sack, L. and Grubb, P. J.: The combined impacts of deep shade and drought on the growth and biomass allocation of shade-tolerant woody seedlings, Oecologia, 131, 175–185, 2002.

Sage, R. F. and Kubien, D. S.: The temperature response of C3 and C4 photosynthesis, Plant Cell Environ., 30, 1086–1106, 2007.

Sala, A., Piper, F., and Hoch, G.: Physiological mechanisms of drought-induced tree mortality are far from being resolved, New Phytol., 186, 274–281, 2010.

Siqueira, M., Katul, G., Sampson, D., Stoy, P., Juang, J. Y., McCarthy, H., and Oren, R.: Multiscale model intercomparisons of CO_2 and H_2O exchange rates in a maturing southeastern US pine forest, Global Change Biol., 12, 1189–1207, 2006.

Sitch, S., Smith, B., Prentice, I. C., Arneth, A., Bondeau, A., Cramer, W., Kaplan, J. O., Levis, S., Lucht, W., and Sykes, M.: Evaluation of ecosystem dynamics, plant geography and terrestrial carbon cycling in the LPJ dynamic global vegetation model, Global Change Biol., 9, 161–185, 2003.

Sowerby, A., Emmett, B., Beier, C., Tietema, A., Peòuelas, J., Estiarte, M., Van Meeteren, M. J. M., Hughes, S., and Freeman, C.: Microbial community changes in heathland soil communities along a geographical gradient: interaction with climate change manipulations, Soil Biol. Biochem., 37, 1805–1813, 2005.

Stoy, P. C., Richardson, A. D., Baldocchi, D. D., Katul, G. G., Stanovick, J., Mahecha, M. D., Reichstein, M., Detto, M., Law, B. E., Wohlfahrt, G., Arriga, N., Campos, J., McCaughey, J. H., Montagnani, L., Paw U, K. T., Sevanto, S., and Williams, M.: Biosphere-atmosphere exchange of CO_2 in relation to climate: a cross-biome analysis across multiple time scales, Biogeosciences, 6, 2297–2312, doi:10.5194/bg-6-2297-2009, 2009.

Suni, T., Berninger, F., Vesala, T., Markkanen, T., Hari, P., Mäkelä, A., Ilvesniemi, H., Hänninen, H., Nikinmaa, E., and Huttula, T.: Air temperature triggers the recovery of evergreen boreal forest photosynthesis in spring, Global Change Biol., 9, 1410–1426, 2003.

Symstad, A. J., Chapin III, F. S., Wall, D. H., Gross, K. L., Huenneke, L. F., Mittelbach, G. G., Peters, D. P. C., and Tilman, D.: Long-term and large-scale perspectives on the relationship between biodiversity and ecosystem functioning, Bioscience, 53, 89–98, 2003.

Teklemariam, T., Lafleur, P., Moore, T., Roulet, N., and Humphreys, E.: The direct and indirect effects of inter-annual meteorological variability on ecosystem carbon dioxide exchange at a temperate ombrotrophic bog, Agr. Forest Meteorol., 150, 1402–1411, 2010.

Thum, T., Aalto, T., Laurila, T., Aurela, M., Lindroth, A., and Vesala, T.: Assessing seasonality of biochemical CO_2 exchange model parameters from micrometeorological flux observations at boreal coniferous forest, Biogeosciences, 5, 1625–1639, doi:10.5194/bg-5-1625-2008, 2008.

Valentini, R., Matteucci, G., Dolman, A., Schulze, E. D., Rebmann, C., Moors, E., Granier, A., Gross, P., Jensen, N., and Pilegaard, K.: Respiration as the main determinant of carbon balance in European forests, Nature, 404, 861–865, 2000.

Vesala, T., Launiainen, S., Kolari, P., Pumpanen, J., Sevanto, S., Hari, P., Nikinmaa, E., Kaski, P., Mannila, H., Ukkonen, E., Piao, S. L., and Ciais, P.: Autumn temperature and carbon balance of a boreal Scots pine forest in Southern Finland, Biogeosciences, 7, 163–176, doi:10.5194/bg-7-163-2010, 2010.

Vickers, D., Thomas, C. K., Martin, J. G., and Law, B.: Self-correlation between assimilation and respiration resulting from flux partitioning of eddy-covariance CO_2 fluxes, Agr. Forest Meteorol., 149, 1552–1555, 2009.

Wang, T., Ciais, P., Piao, S. L., Ottlé, C., Brender, P., Maignan, F., Arain, A., Cescatti, A., Gianelle, D., Gough, C., Gu, L., Lafleur, P., Laurila, T., Marcolla, B., Margolis, H., Montagnani, L., Moors, E., Saigusa, N., Vesala, T., Wohlfahrt, G., Koven, C., Black, A., Dellwik, E., Don, A., Hollinger, D., Knohl, A., Monson, R., Munger, J., Suyker, A., Varlagin, A., and Verma, S.: Controls on winter ecosystem respiration in temperate and boreal ecosystems, Biogeosciences, 8, 2009–2025, doi:10.5194/bg-8-2009-2011, 2011.

Wang, Y. P., Baldocchi, D., Leuning, R. A. Y., Falge, E. V. A., and Vesala, T.: Estimating parameters in a land-surface model by applying nonlinear inversion to eddy covariance flux measurements from eight FLUXNET sites, Global Change Biol., 13, 652–670, doi:10.1111/j.1365-2486.2006.01225.x, 2007.

Wang, Y. P., Trudinger, C. M., and Enting, I. G.: A review of applications of model–data fusion to studies of terrestrial carbon fluxes at different scales, Agr. Forest Meteorol., 149, 1829–1842, doi:10.1016/j.agrformet.2009.07.009, 2009.

Yuan, W., Luo, Y., Richardson, A., Oren, R., Luyssaert, S., Janssens, I., Ceulemans, R., Zhou, X., Grünwald, T., and Aubinet, M.: Latitudinal patterns of magnitude and interannual variability in net ecosystem exchange regulated by biological and environmental variables, Global Change Biol., 15, 2905–2920, 2009.

Paper II

Synthesis on the carbon budget and cycling in a Danish, temperate deciduous forest

J. Wu[1], K.S. Larsen[1], L. van der Linden[1,2], C. Beier[1], Kim Pilegaard[1], A. Ibrom[1]

1. Technical University of Denmark, Department of Chemical and Biochemical Engineering, 2800 Kongens Lyngby, Denmark
2. Australian Water Quality Centre, 5000, Adelaide, Australia

Abstract

A synthesis of five years (2006-2010) of data on carbon cycling in a temperate deciduous forest, Sorø (Zealand, Denmark) was performed by combining all available data from eddy covariance, chamber, suction cups and biometric measurements. The net ecosystem exchange of CO_2 (NEE), soil respiration, tree growth, litter production and the leaching of dissolved organic carbon were independently estimated and used to calculate other unmeasured ecosystem carbon budget (ECB) components, based on mass balance equations. This provided a complete assessment of the carbon storage and allocation within the ecosystem. The results showed that this temperature deciduous forest was a moderate carbon sink (258 ± 41 g C m^{-2} yr^{-1}) with both high rates of gross primary production (GPP, 1881 ± 95 g C m^{-2} yr^{-1}) and ecosystem respiration (R_e, 1624 ± 197 g C m^{-2} yr^{-1}). Approximately 62% of the gross assimilated carbon was respired by the living plants, while 21% was contributed to the soil as litter production, the latter balancing the total heterotrophic respiration. The remaining 17% was either stored in the plants (mainly as aboveground biomass) or removed from the system as wood yield. By

aggregating different ECB component data, the ecosystem carbon balance was assessed, with particular focus on the changes in the soil organic carbon (SOC) stock. The SOC was considered to be unchanged over the period of observation, given the high degree of uncertainty associated with the small loss detected (33 ± 85 g C m^{-2} yr^{-1}). The ECB component data were generally consistent, except for one of the derived fluxes, the aboveground autotrophic respiration, which appeared to be higher than expected. The potential causes for this, i.e. the underestimation of soil respiration and/or the overestimation of R_e are discussed. The plausibility analyses reported here, using multiple ECB data sets together with simple mass conservation equations and to evaluate data consistency on the basis of the estimated residual terms is widely applicable in other experimental sites, even when some of the carbon fluxes and stock changes are not measured independently.

Key words: Ecosystem carbon budget, net ecosystem CO_2 exchange, net primary productivity (NPP), soil respiration, tree growth, soil carbon, mass balance equations, consistency, uncertainty

1 Introduction

The net carbon budget in forest ecosystems is the difference between uptake by photosynthesis and release predominantly by respiration but also through processes such as leaching of dissolved organic carbon (DOC), soil erosion and volatilisation of organic carbon substances. Quantification of the ecosystem carbon budget (ECB), i.e., carbon allocation and storage within an ecosystem, is important for understanding both the ecosystem functioning and its interactions with changing climatic conditions and anthropogenic intervention (Heimann and Reichstein, 2008; Schimel, 1995). In order to assess the role of the terrestrial biosphere for the mitigation of global climate change, it is necessary to investigate the fate of carbon that is assimilated through photosynthesis. This is still a major challenge at global scale (Houghton, 2003) and has only been achieved in a few site level studies (Gough et al., 2008; Granier et al., 2008; Luyssaert et al., 2007). At plot scale, methods and protocols have been developed for the measurement of CO_2 fluxes, e.g. the eddy covariance technique (Aubinet et al., 2000; Baldocchi, 2003) and chamber methods (Davidson et al., 2002), and the assessment of carbon storage in biomass (Clark et al., 2001) and soils (Schrumpf et al., 2011). Despite the attempts of larger research networks, such as EUROFLUX (Valentini et al., 2000), AMERIFLUX (Ocheltree and Loescher, 2007) to harmonise the methods, there are still different, equally valid methodological alternatives being applied depending on the experience of the different scientific communities.

When comparing different ECB components, an important source of uncertainty is that individual components are measured at different spatial and temporal scales (Luyssaert et al., 2009). The consistency of the ECB component estimates is potentially affected by the inherent heterogeneity of the ecosystem. Therefore, it is necessary to cross-check the individual component estimates against each

other using e.g. a multiple constraints approach (Luyssaert et al., 2009) before using the data, e.g., in model-data fusion studies (Raupach et al., 2005).

The consistency of the ECB datasets can in the best case be evaluated by comparing a quantity (e.g. the net ecosystem productivity) that is measured with different independent methods (Black et al., 2007; Field and Kaduk, 2004; Harmon et al., 2004; Keith et al., 2009; Miller et al., 2004) at the same temporal and spatial scale. This can be (1) micrometeorological methods to assess the atmospheric fluxes, (2) inventories of stock changes in the biomass and soil or (3) the bottom up modelling of ecophysiological processes from chamber measurements (leaves, stems, roots and soil). However, such consistency assessment requires that all ECB components are estimated for the same time interval, which is not realised in the majority of flux observation or forest inventory sites. The evaluation of data consistency, when only part of the ECB datasets is available, is therefore important.

Prior to a consistency assessment, it is important that the uncertainties of the ECB component estimates are properly characterized. Ecological datasets with properly characterized uncertainties are needed for the development and testing of process models (Carvalhais et al., 2010; Santaren et al., 2007; Williams et al., 2009), which are simultaneously challenged by over-simplification (model structure too simple to represent the natural processes) and over-parameterization (data availability too limited to constrain the model parameters) (Ibrom et al., 2006; Paw et al., 2000). Progress in data assimilation techniques makes it possible to incorporate the data uncertainties into the objective function of the model-data optimization scheme (Luo et al., 2009; Raupach et al., 2005; Van Oijen et al., 2005; Wang et al., 2009). A prerequisite of such model data fusion exercises is a consistent ECB dataset including information about the uncertainties of the components (Raupach et al., 2005; Wang et al., 2009; Williams et al., 2009).

Data uncertainty is an unknown error that can be expressed as the probability distribution of the true value around the measured estimate (Richardson et al., 2012). These uncertainties can be random (Ibrom et al., 2006; Richardson and Hollinger, 2005a) or systematic (e.g. biased sampling and calibration errors). Whereas the probability distribution of random errors can be characterized empirically from multiple measurements (Lasslop et al., 2008; Richardson and Hollinger, 2005a), systematic errors can often not be identified by statistical measures and are difficult to quantify. Systematic errors follow rather from theoretical analysis, e.g. through comparison of the real situation with theoretical assumptions made in deriving the theory for flux estimation (ideal situation). However the consequence of deviation from the ideal situation cannot always be quantified. For instance, the uncertainty in atmospheric flux estimation associated with advection terms cannot yet be measured with sufficient accuracy (Aubinet et al., 2010; Paw et al., 2000). On the other hand, when more than one method is available, e.g., different turbulence data post processing methods (Aubinet et al., 2000; Falge et al., 2001; Moffat et al., 2007), the choice of method can lead to different results and the resulting uncertainty can be estimated by applying all methods and comparing the results.

Another source of uncertainty is the spatial and temporal variability of the carbon fluxes. At heterogenic sites, flux representativeness needs careful investigation, but the tools available, the so-called flux footprint models, are themselves oversimplifications of the true flow regimes in complex terrain (Rannik et al., 2012). The small scale variability within ecosystems needs to be considered when comparing the representative flux-based NEP data to other ECB components, e.g. soil respiration (R_s), which is usually measured at a relatively small patch of the site. The sampling scheme should be optimized towards covering the local heterogeneity in order to be representative for a larger unit (Knohl et al., 2008). Similarly, the measurement frequency should resolve the typical temporal variability of the process measured, or, if this is not possible, the values need to be up-scaled by

modelling (e.g. Selsted et al., 2012). Again, the choice of the model and parameter estimation schemes can introduce systematic uncertainty, e.g. in the estimation of the annual R_s budget from discontinuous field campaigns (Richardson and Hollinger, 2005b).

The objective of this study is to provide a synthesis over all ECB related datasets collected so far at a Danish beech forest (DK-Sor) since 1996 when atmospheric CO_2 flux measurements were initiated. During this time several projects yielded additional ecological information for differing scientific purposes. In the second half of the investigation period (2006 to 2010) the data availability allows estimating the majority of the carbon fluxes and stock changes in this ecosystem. We test the hypothesis that the available data are consistent within the estimated uncertainty ranges and estimate ranges for so far unmeasured components. From this, we derive the most complete assessment possible for this site of the forests averaged carbon budget and its components. This enables us to a) investigate the fate of the carbon in the ecosystem b) relate the dynamic status of the ecosystem to other forests where such assessments have also been attempted, and c) provide information on the quality and consistency on the ECB datasets.

2 Material and methods

2.1 Site description

The Danish long-term CO_2 flux investigation site is located within a beech (*Fagus sylvatica* L.) forest, near the town of Sorø on Zealand, Denmark (55°29'13'N, 11°38'45'E). The soils are classified as alfisols or mollisols (depending on the base saturation) with a 10-40 cm deep organic layer. Tree density was 288 stems ha^{-1} in 2010 and seasonal peak leaf area index varied between 4 and 5 m^2 m^{-2} (Pilegaard et al., 2011). In 2010, the stand around the flux tower was 89 years old, the average tree height was 28 m and the average diameter at breast height was 42 cm. Mean annual temperature at the

site was 8.5 °C, and annual precipitation amounted to 564 mm. The flux tower is located in the centre of the forest. The forest fetch around the tower ranges between 300-700 m depending on the directions (Pilegaard et al., 2011). Further information about the site can be found in Pilegaard et al. (2001; 2011; 2003).

2.2 Flux data processing and uncertainty estimation

The net ecosystem exchange of CO_2 (NEE, a negative sign corresponds to a net sink of CO_2, see Table 1) between the biosphere and atmosphere was measured with a closed-path eddy covariance system. Five annual datasets (2006-2010) were used for this analysis. The NEE data processing and uncertainty estimation comprised (1) storage correction; (2) correction for low turbulent mixing (u_* filtering); (3) accounting for the site heterogeneity effects; (4) gapfilling and (5) flux partitioning.

2.2.1 Storage change correction

In previous publications the flux data from this site were corrected for storage change (S_c) in the air column underneath the sensor using the concentration measurements at the eddy covariance system (43 m). In this study, we derived new estimates of S_c with data obtained from a profile system. The S_c was calculated similar to Aubinet et al. (2001) in Eq. 1 and added to the measured flux.

$$S_c = \frac{P_a}{R \cdot T_a} \int_0^h \frac{\partial c(z)}{\partial t} dz \quad (1)$$

where P_a is the atmospheric pressure (P_a), R is the universal gas constant, T_a is the average air temperature in the column, c is the CO_2 concentration (mole fraction) at a specific height (z) along the vertical profile (7 depths) from the forest floor to the measurement height (h) and t is time. The annual sum of the storage change below canopy was almost identical with the two applied methods (ca. 3 and

4 g C m^{-2} yr^{-1}, for using single point or profile concentration measurements, respectively; this small methodical bias was thus neglected in the further analysis.

2.2.2 Exclusion of data at insufficient turbulent mixing

In general, the measured carbon fluxes can be systematically lower when the wind speed falls below a certain threshold (Aubinet et al., 2002). This is interpreted as an effect of unmeasured advective mass transport, or more correctly the divergence of advective mass transports. To avoid a systematic underestimation, the turbulent flux data were filtered for low turbulent mixing at stable stratification using two criteria. First, in accordance with previous publications at this site (Pilegaard et al., 2011; Wu et al., 2012), the nighttime fluxes were filtered when the friction velocity (u_*) was smaller than 0.1 m s^{-1} in all years. These filtered NEE datasets are denoted as $NEE_{0.1}$. Second, we applied the method according to Papale et al. (2006); the current standard data processing procedure in the European flux network. With this method, the u_* filtering was applied for both daytime and nighttime data. The u_* threshold varied between years and averaged at about 0.25 m s^{-1} and are here denoted as $NEE_{0.25}$.

2.2.3 Estimation of the effects of site inhomogeneity

A so far unresolved problem is the estimation of the uncertainty of NEE due to fetch limitation and site inhomogeneity. Micrometeorological flux measurements require large homogeneous areas (or so called fetch). In an ideal situation, the fluxes originated from different sectors of the site are expected to be the same under similar environmental conditions. However, such perfect homogeneous condition can hardly be met in intensively cultivated landscapes and many FLUXNET sites (Aubinet et al., 2002; Göckede et al., 2004; Oren et al., 2006). The natural site variability and forest management such as clear cut, re-planting and thinning can lead to structural and functional variability within the footprint of the flux measurement (Rannik et al., 2012). Depending on the wind directions and atmospheric

stability, the flux source area changes over time. Therefore, the annual sums of NEE may be biased by certain sectors of the sites.

Were therefore performed an empirical analysis to evaluate the effects of horizontal inhomogeneity on annual NEE estimates. It compares the NEE datasets (complete, daytime and nighttime NEE) from 8 different forest sectors (classified by wind directions) at similar environmental conditions (T_a, short wave radiation, R_g, and volumetric soil water content, θ) and ecosystem functional states (leafed and non-leafed periods). The analysis consisted of 4 steps. In the first step, the NEE data sets were classified into different conditions for comparison. The three NEE datasets, i.e. complete, daytime and nighttime NEE, respectively, were classified based on the full factorial combination of 10 equal distance T_a classes, 10 R_g classes (for nighttime 1 radiation class), 5 θ classes and 2 functional state classes. This yielded 1000, 1000 and 100 potential conditions for flux comparison at general, daytime and nighttime conditions, respectively. A specific condition for the flux comparison is denoted as Ω (e.g. non-leafed period when the T_a is with 2-5°C, R_g is within 34-96 W and θ is within 20-25%). The numbers of actual realisations of Ω, (K, J or L) are lower than the potential numbers (1000, 1000, 100) because not all of the potential combinations exist in the data. Additionally, this analysis is restricted to only those Ω where sufficient flux values existed from all of the 8 forest sectors. The classification related effects were also assessed by conducting the same following analysis with different class sizes and the uncertainty was calculated as the standard deviation in the final estimates.

In the second step, the mean NEE (for the complete, daytime or nighttime datasets) at each Ω was calculated for all forest sectors. Following this, a weighted average NEE for each wind direction class F_{wdi}, $F_{wdi,\,d}$ and $F_{wdi,\,n}$, which took into account the frequency (ϖ_Ω) of each Ω is calculated in Eq. 2-4:

$$F_{wdi} = \sum_{k=1}^{K} (\overline{f}_{\Omega_k, wd_i} \varpi_{\Omega_k}) \Big/ \sum_{k=1}^{K} \varpi_{\Omega_k} \quad (2)$$

$$F_{wdi,\,d} = \sum_{j=1}^{J} (\overline{fd}_{\Omega_j, wd_i} \varpi_{\Omega_j}) \Big/ \sum_{j=1}^{J} \varpi_{\Omega_j} \quad (3)$$

$$F_{wdi,\,n} = \sum_{l=1}^{L} (\overline{fn}_{\Omega_l, wd_i} \varpi_{\Omega_l}) \Big/ \sum_{l=1}^{L} \varpi_{\Omega_l} \quad (4)$$

where $\overline{f}_{\Omega_k, wd_i}$ $\overline{fd}_{\Omega_j, wd_i}$ and $\overline{fn}_{\Omega_l, wd_i}$ are the mean NEE (whole day, daytime and night time respectively) from the i[th] wind direction at each specific Ω; The symbols ϖ_{Ω_k} ϖ_{Ω_j} and ϖ_{Ω_l} denote the frequency of each Ω.

In the third step, the estimated F_{wdi} $F_{wdi,\,d}$ and $F_{wdi,\,n}$ were normalized in Eq. 5-7. The derived $F_{wd_i,\,norm}$, $F_{wd_i,\,d,\,norm}$ and $F_{wd_i,\,n,\,norm}$ represent the relative deviations of the NEE from a certain forest sector from the average.

$$F_{wdi,\,norm} = F_{wdi} \Big/ \overline{F_{wdi}} \quad (5)$$

$$F_{wdi,\,d,\,norm} = F_{wdi,\,d} \Big/ \overline{F_{wdi,\,d}} \quad (6)$$

$$F_{wdi,\,n,\,norm} = F_{wdi,\,n} \Big/ \overline{F_{wdi,\,n}} \quad (7)$$

These values should be equal to 1 if the site was homogeneous. The standard deviations (σ) of $F_{wd_i,\,norm}$, $F_{wd_i,\,d,\,norm}$ and $F_{wd_i,\,n,\,norm}$ (n=8), $\sigma_{F_{wd_i,\,norm}}$ $\sigma_{F_{wd_i,\,d,\,norm}}$ and $\sigma_{F_{wd_i,\,n,\,norm}}$ are calculated and interpreted to represent the site inhomogeneity-related flux uncertainty under general, daytime and nighttime conditions.

2.2.4 Gapfilling and flux partitioning

Gapfilling was conducted using two methods: (1) marginal distribution sampling (MDS; Reichstein et al., 2005) and (2) a hyperbolic light response regression model (HBLR; Lasslop et al., 2010). The NEE uncertainty induced by the data filtering and gapfilling is characterized by the standard deviation (σ) of the four annual NEE estimates that were calculated with different u_* thresholds and gapfilling methods (Eq. 8).

$$\delta_{\mathrm{NEE}u^*,\,GF} = \sigma(\mathrm{NEE}_{0.1,\mathrm{MDS}},\ \mathrm{NEE}_{0.25,\mathrm{MDS}},\ \mathrm{NEE}_{0.1,\mathrm{HBLR}},\ \mathrm{NEE}_{0.25,\mathrm{HBLR}}) \quad (8)$$

The net fluxes were partitioned into gross primary production (GPP, a positive sign corresponds to a net sink of CO_2) and ecosystem respiration (R_e, a positive sign corresponds to a release of CO_2 to the atmosphere) with two methods. (1) nighttime based (NB; Reichstein et al., 2005): respiration measured at night was extrapolated to daytime using a temperature regression model; (2) daytime based (DB; Lasslop et al., 2010): the HBLR model which takes into account the temperature sensitivity of respiration and the VPD related reduction of photosynthesis, was fitted to daytime NEE values. The uncertainty of the gross fluxes due to the choice of the flux partitioning method and u_* filtering thresholds is characterized by comparing all the four different GPP (Eq. 9) and R_e (Eq. 10) estimates.

$$\delta_{\mathrm{GPP}u^*,\,GF} = \sigma(\mathrm{GPP}_{0.1,\mathrm{DB}},\ \mathrm{GPP}_{0.25,\mathrm{DB}},\ \mathrm{GPP}_{0.1,\mathrm{NB}},\ \mathrm{GPP}_{0.25,\mathrm{NB}}) \quad (9)$$

$$\delta_{R_e u^*,\,GF} = \sigma(R_{e_{0.1,\,\mathrm{DB}}}, R_{e_{0.25,\,\mathrm{DB},}}\ R_{e_{0.1,\,\mathrm{NB}}}, R_{e_{0.25,\,\mathrm{NB}}}) \quad (10)$$

2.2.5 Overall flux data uncertainty

The overall uncertainties in NEE, GPP and R_e were characterized by combing the δ caused by u_* filtering, gapfilling and site heterogeneity. The absolute uncertainties of NEE ($\delta_{\mathrm{NEE}SH}$), R_e ($\delta_{R_e\,SH}$) and GPP ($\delta_{\mathrm{GPP}SH}$) caused by site heterogeneity were calculated by multiplying $\sigma_{Fwd_i,\,norm}$, $\sigma_{Fwd_i,\,n,\,norm}$ and $\sigma_{Fwd_i,\,d,\,norm}$ with the gapfilled annual NEE, R_e and GPP budgets, respectively. Subsequently, $\delta\mathrm{GPP}_{SH}$ and $\delta R_{e\,SH}$ were included in the overall flux uncertainties calculation as Eq. 11-13:

$$\delta^2_{\mathrm{NEE}} = \delta^2_{\mathrm{NEE}_{SH}} + \delta^2_{\mathrm{NEE}_{u*,\,GF}} \quad (11)$$

$$\delta^2_{\mathrm{GPP}} = \delta^2_{\mathrm{GPP}_{SH}} + \delta^2_{\mathrm{GPP}_{u*,\,GF}} \quad (12)$$

$$\delta^2_{R_e} = \delta^2_{R_{e\,SH}} + \delta^2_{R_{e\,u*,\,GF}} \quad (13)$$

2.3 Soil respiration

Soil respiration was measured using a portable gas exchange system combined with a soil CO_2 flux chamber (LI-6400; LICOR Bioscience, Lincoln, NE, USA). Permanent collars were inserted into the soil one year before the measurements. The R_s was measured every two weeks or monthly between the years 2002-2005 and 2008-2009. On most days, measurements were made hourly between 9:00 and 15:00 in 12 replicated locations (i.e. 84 measurements per day). Additionally, there was a one-day campaign when R_s was measured over 24 hours. Three empirical R_s models were parameterized to extrapolate the discontinuous R_s measurements to form a continuous time series and an annual R_s budget. First the datasets were fitted to Model I (Eq. 14), Model II (Eq. 15, Lloyd and Taylor, 1994) and Model III which considers also the soil water content (Eq. 16, Granier et al., 2000).

$$R_s = R_{10} Q_{10}^{(T_s - T_{10})/10} \quad (14)$$

where R_{10} is R_s at reference temperature T_{10}; Q_{10} is the temperature sensitivity; T_s is the soil temperature.

$$R_s = R_{283} \exp\left[-E_0\left(\frac{1}{T_s + 273.15 - T_0} - \frac{1}{T - T_0}\right)\right] \quad (15)$$

where R_{283} is the base respiration at soil temperature of 10˚C ; T_0 and E_0 are fitted parameters.

$$R_s = a_0 \theta \exp(b_0 T_s) \quad (16)$$

where θ is the volumetric soil water content and T_s is the soil temperature; a_0 and b_0 are fitted parameters.

We used Bayesian calibration, which simultaneously takes into account the uncertainties in the input data and model structures to estimate the probability distributions of the model parameters, thus quantifying the uncertainty in the model predictions (Van Oijen et al., 2005). For this the Markov Chain Monte Carlo (MCMC) Metropolis-Hastings random walk algorithm was used to search for the posterior distribution within the initially defined prior distributions of the parameter space. The likelihood function L is given in Eq. 17:

$$L = \prod_{i=1}^{n} \frac{1}{\sqrt{2\pi\sigma_i^2}} \exp\left[-\frac{1}{2}\left(\frac{o_i - s_i}{\sigma_i} \right)^2 \right] \quad (17)$$

where o_i is the ith observation; s_i is the ith simulated value; σ_i is the data uncertainty, represented as the standard deviation of the R_s measurements. The prior ranges of the parameters were set wide enough with uniform distribution; these distributions were sampled over the 50000 MCMC iterations performed for each model.

2.4 Litter production

Since 2003, aboveground litter (L_{AG}) was collected in 25 litter traps (80 cm diameter) located southwest of the flux tower (Pilegaard et al., 2003). Litter was collected from the traps every 2 months, oven dried (70 °C) and weighed. The collected litter included mainly the fallen leaves and fruits. Large woody debris (e.g. branches) was not collected. The measured C concentration in the litter samples was on average 0.51 g C per g dry mass. Total litter fall was calculated as the product of the average net weight and C concentrations, divided by the average sampling area of the litter traps (0.5 m^{-2}). The below ground litter inputs (L_{BG}) were not directly measured during the study period and assumed to be the same as fine root production, because the fine root longevity in mature beech forest was found

generally much lower than 1 year (Peek, 2007). This was calculated according to a DBH dependent regression model (Le Goff and Ottorini, 2001)..

2.5 Tree growth

Tree growth (G) for both the aboveground ground (G_{AG}) *and* belowground (G_{BG}) compartments was estimated based on tree ring data, height measurements, biomass expansion functions (BEF) and carbon contents of the specific plant compartments. In December 2009, 102 tree ring cores (2 cores per tree) were taken in a central plot proximal to the tower and a sub-plot covering the fetch to the prevailing wind direction (Flurin Babst and David Frank, Swiss Federal Institute of Technology, WSL, Switzerland). The summed tree ring widths were in accordance with DBH measurements in 2009, therefore the annual tree ring width was used as an approximation of DBH increments. Tree heights were measured in 2005 and 2008-2010 and a linear increment from 2005-2007 was assumed. The compartments of the standing biomass (stem, branches and coarse roots) for individual trees were calculated according to a BEF specific for beech trees in Denmark (Skovsgaard and Nord-Larsen, 2012). The standard error of the fitted parameter of the BEF was used to propagate the uncertainty range of the biomass stock and increment using 1000 Monte Carlo iterations. The carbon content of the biomass was measured in the European project Forest carbon and nitrogen trajectories (FORCAST) and set as 0.46, 0.47, and 0.48 g C per g dry mass for the stem, branches and coarse roots, respectively (personal communication, Giorgio Matteucci, CNR-ISAFOM, Italy). The stand was thinned in the beginning of the study period with a reduction of tree density by ca. 10 %. In the year of thinning, the tree growth was estimated as the sum of biomass increment and the mass of the harvested trees (H). The relation between of exported wood and biomass that was left on site was estimated using the BEF functions for brushwood and total tree biomass after Wutzler et al. (2008). It was assumed that timber was completely exported from the forest, while the remainder was converted to woody debris (W).

2.6 Calculation of other unmeasured ECB components

The independently estimated ECB components from this study, i.e. the EC-based estimates of NEP, GPP and R_e, chamber-based estimates of R_s, inventory-based estimates of $L_{AG,}$ L_{BG}, G_{AG}, G_{BG}, together with the estimated leaching of dissolved organic carbon (DOC_{leach}) using suction cups by Kindler et al. (2010) in 2006-2008 were used to derive other unmeasured ECB components using the mass balance equations. The small amount of dissolved biogenic inorganic carbon (Kindler et al., 2010) was added to the measure R_s and R_e. The calculation follows 5 steps as in Eq. 18-23. Firstly the net primary production (NPP) was calculated as the sum of biomass production in different plant components (Eq. 18).

$$\mathrm{NPP} = G_{AG} + G_{BG} + L_{AG} + L_{BG} \quad (18)$$

Second, R_a was calculated as the difference between GPP and NPP in Eq. 19:

$$R_a = \mathrm{GPP} - \mathrm{NPP} \quad (19)$$

Then, R_h was calculated as the difference between R_e and R_a in Eq. 20; the below ground autotrophic respiration $R_{a,\,BG}$ was calculated as the difference between R_s and R_h (Eq. 20); $R_{a,\,AG}$ was derived as Eq. 21; and the change in the SOC pools ΔSOC was calculated in Eq. 23.

$$R_h = R_e - R_a = \mathrm{NPP\text{-}NEP} \quad (20)$$

$$R_{a,\,BG} = R_s - R_h \quad (21)$$

$$R_{a,\,AG} = R_a - R_{a,\,BG} \quad (22)$$

$$\Delta\mathrm{SOC} = L_{AG} + L_{BG} - R_h - \mathrm{DOC}_{leach} \quad (23)$$

Additionally, the total below ground carbon allocation (A_{BG}) was calculated as the sum of $R_{a,\,BG}$, root growth and litter production (Eq 24). The net biome production (NBP) was calculated as the

differences between NEP (i.e. NEE times -1) and harvested wood (*H*) that is exported out of the ecosystem..

$$A_{BG} = L_{BG} + R_{a,\,BG} + G_{BG} \tag{24}$$

$$\mathrm{NBP} = \mathrm{NEP} - H \tag{25}$$

The uncertainties of the above derived ECB components were estimated by Gaussian error propagation.

3 Results

3.1 Net ecosystem CO_2 exchange

The NEE measurements covered approximately 94% of the study period (Table 2). After u_* filtering, the data coverage was reduced to 88% or 78%, using the two different u_* filtering methods (Table 2). To evaluate the effects of site inhomogeneity on the measured carbon fluxes, the u_* filtered NEE datasets were classified according to the different environmental conditions for flux comparison (section 2.2.3). The normalized NEE, $F_{wd_i,\,norm}$ was 12% higher and 11% lower than the average, when the wind came from 180-270˚ (main wind direction) and 45-90˚, respectively (Fig. 1). These differences are related to the forest composition in the specific forest sectors. The southwest forest sector (180-270˚) had the highest proportion of pure beech (Fig. 1) within a 500 m radius around the tower. In contrast, the percentage of beech in the 45-90˚ sector was the lowest (62%) while the rest was mostly cropland. The correlation between $F_{wd_i,\,norm}$ and the beech composition was significant (r = 0.62). The fraction of conifer species was highest in the east and southeast sectors, the normalized flux from these two sectors did not show systematic effects as they were either 8% higher or 11% lower than the average. When only the nighttime fluxes were used in the analysis, the pattern was similar but

the variation was higher ($\sigma_{F_{wd_i,n,norm}}$ = 11%). When only the daytime fluxes ($F_{wd_i,d,norm}$) were used, this relative variation was much lower ($\sigma_{F_{wd_i,n,norm}}$ = 4%).

The gapfilled NEE (Table 2) using the first method (NEE_{MDS}) for the two u_* filtered NEE datasets was similar, averaged at about -210 g C m^{-2} yr^{-1}. The difference between average $NEE_{MDS,u*1}$ and $NEE_{MDS,u*2}$ for 2006-2010 was only 6 g C m^{-2} yr^{-1}. The gapfilled NEE using the second method (NEE_{HBLR}) showed higher carbon uptakes. The averaged NEE_{HBLR} for the two u_* filtered datasets was -270 g C m^{-2} yr^{-1}. Because the effect of site inhomogeneity on the NEE was much higher at nighttime than at daytime, we decided to use the results from daytime based methods for the subsequent ECB synthesis. The uncertainty due to u_* filtering and gapfilling, $\delta_{NEE_{u*,GF}}$ (Eq. 8) was 34 g C m^{-2} yr^{-1}. Taken into account the potential uncertainty due to site heterogeneity, the overall NEE uncertainty δ_{NEE} was 41 g C m^{-2} yr^{-1} (Eq. 11). Accounting the leaching of biogenic DIC of 12 g C m^{-2} yr^{-1} (Kindler et al., 2010), the estimated NEE was -258 ± 41 g C m^{-2} yr^{-1}.

3.2 CO_2 flux components GPP and R_e

The estimated GPP and R_e using the nighttime methods were both generally 6% higher than daytime based estimates (Table 3). For the same reason of the site heterogeneity effects, daytime based estimates were used in the ECB synthesis. The estimated $\delta_{GPP_{u*,GF}}$ (Eq. 9) was 58 g C m^{-2} yr^{-1}. Taking into account the potential uncertainty due to site heterogeneity $\delta_{GPP,SH}$ of 75 g C m^{-2} yr^{-1}, the overall uncertainty in GPP, δ_{GPP} (Eq. 12) was 95 g C m^{-2} yr^{-1}. The uncertainty caused by u_* filtering and gapfilling for R_e, $\delta_{R_{e\,u*,GF}}$, was 92 g C m^{-2} yr^{-1}. Taken into account the site heterogeneity related uncertainty, $\delta_{R_{e\,SH}}$ (185 g C m^{-2} yr^{-1}), the overall uncertainty of R_e (Eq. 13) was more than twice than that for GPP, i.e. 197 g C m^{-2} yr^{-1}. Therefore, the average GPP and R_e was 1881 ± 95 g C m^{-2} yr^{-1} and 1624 ± 197 g C m^{-2} yr^{-1} for the five year period.

3.3 Soil respiration

The average daily R_s (Fig. 2) ranged between 0.3 and 4.4 g C m^{-2} d^{-1}. In general, the variability in R_s (Fig. 2) increased with the magnitude of the fluxes. This non uniform error variance was considered in the Bayesian calibration (Eq. 17). After 50000 iterations, the posterior parameters converged for each model (Table 4). Model I and II explained about 71% and 69% of the variation, respectively. Including soil moisture as an additional independent variable, Model III explained about 76% of the variation in R_s. Because the water content was not measured in 2007 and 2008, Model III could not be used for these two years and is only presented for comparison (Fig. 3). The uncertainties of the estimated annual R_s budgets were small compared to annual R_s budget estimates (Fig. 3). The estimated average annual R_s budget for 2006-2010 was 740 ± 30 g C m^{-2} yr^{-1} and when adjusted for the leaching of biogenic DIC, finally 752 ± 30 g C m^{-2} yr^{-1}.

3.4 Tree growth and litter production

The tree growth (including stem, branches and coarse roots) was calculated as the sum of the difference in the C stocks between years and the extracted biomass and woody debris (Table 5). The estimated tree growth showed that the forest has gained approximately 307 ± 57 g C m^{-2} yr^{-1} during this five year period. The growth rate was rather steady but peaked in 2007, when the summer precipitation and GPP was also the highest during the five years. A scheduled thinning was also conducted in 2007, which removed 533 g C m^{-2} wood from the forest and converted 204 g C m^{-2} tree biomass to woody debris. Due to a lack of exact data we assumed that the thinning was performed uniformly over the tree size distribution. It is likely that this lead to a small overestimation (< 13%) of the size of the removed trees and thus the growth estimate of the trees. The years 2006 and 2009 were mast years with on average 74 g C m^{-2} yr^{-1} higher aboveground litter production than in normal years. The mean above ground litter production was 218 ± 17 g C m^{-2} yr^{-1} for the period 2006-2010. The modelled below ground litter

production was similar to the above ground litter production and averaged 183 ± 27 g C m^{-2} yr^{-1} for the years 2006-2010.

3.5 Synthesis: carbon cycling in the investigated beech forest

The flow diagram in Figure 4 gives a comprehensive representation of the carbon cycling in the beech forest. It connects the carbon fluxes with either the system boundaries or the ecosystem internal pools. On the left hand side the CO_2 fluxes are given, on the right hand side the organic fluxes and stock changes. Most of the ECB components in the diagram have been measured in the field or been directly calculated from such measurements using models. A few of the entities have been derived as residuals from the mass balance equations (e.g. ΔSOC). This is the reason for perfect closure of the budget.

The GPP, the annual gross carbon influx into the ecosystem, is the largest flux of the carbon cycle. The arrows inside the tree pools (Fig. 4) show how the assimilated C was distributed in the ecosystem. More than half of the GPP, i.e., 62% was respired by the tree stand. The rest was, by definition, NPP, i.e., the sum of tree growth (44% of NPP) and litter production (56% of NPP). While the tree growth was clearly dominated by the aboveground wood production (85% of the tree growth) the litter production was of similar magnitude, with the aboveground litter production being ca. 20% higher than the belowground litter production. According to our estimation, about 35% of the average annual tree growth was removed by wood exports over the entire period and 13.4 % of the annual tree growth was transferred to woody debris. The input of organic C into the soil amounted to 442 g C m^{-2} yr^{-1} while the CO_2 loss by heterotrophic respiration was 451 g C m^{-2} yr^{-1}. Adding an additional loss of C as DOC leaching of 25 g C m^{-2} yr^{-1} (Kindler et al., 2011), the soil budget was closed at -33 g C m^{-2} yr^{-1}. The total CO_2 losses from the ecosystem amounted to 86 % of GPP, the remainder of 14 % was transformed to organic carbon in the ecosystem. The net biome productivity (Schulze et al., 2000), i.e. when

assuming that all the harvested wood is turned into CO_2 within the 5 year period, was 150 g C m^{-2} yr^{-1}. In summary, during the observed period the Sorø beech forest mainly produced wood, 1/3 of it exported by thinning and 2/3 staying at the site.

About 2/3 of the total ecosystem carbon content was in the tree stand (9886 ± 231 g C m^{-2} aboveground and 1846 ± 160 g C m^{-2} below), 1/3 was stored in the soil (9254 ± 2809 g C m^{-2}, 0-60 cm, sampling in 2004, Schrumpf et al. 2011). The very high variability in the soil is due to some areas of slightly lower relief that were subsequently wetter, where the SOC content was twice the amount often observed in the drier more elevated areas. The annual stock change in the vegetation was in the order of magnitude of the estimated error of the stock, while the change in SOC was several orders of magnitude lower (Table 6).

4 Discussion

4.1 The measured ECB components and their uncertainties

The ecosystem carbon budget at this site was evaluated for the first time by combining the ecosystem CO_2 fluxes and soil respiration measurements and inventory-based stock change estimates. The uncertainties of these estimates differ substantially due to the different applied methods and the scales of the different observations. In the following sections the uncertainties of the individual ECB component estimates are discussed.

The annual NEE, GPP and R_e budgets were derived using different gapfilling and flux partitioning methods (Table 2-3). The maximum difference in the four annual NEE estimates was 80 g C m^{-2} yr^{-1}, which is well within the reported gapfilling-related differences from -40 to 200 g C m^{-2} yr^{-1} by Falge et al. (2001) but higher than the estimated range of ±25 g C m^{-2} yr^{-1} by Moffat et al. (2007) after comparing 15 gapfilling methods. The differences in the four GPP and R_e estimates were less than 15%,

which is close to the variation found in the results of 23 different flux partitioning methods (Desai et al., 2008). Many published flux post processing methods are currently being used, which makes the selection of the "best" method difficult (Desai et al., 2008). This methodological uncertainty can be addressed by either using the ensemble mean of all different estimates or by selecting only those methods that are considered obviously superior. For instance, the nighttime and daytime based methods showed different results (Table 3). In order to analyse the reason for the differences, we investigated the effects of site inhomogeneity on the carbon fluxes under daytime and nighttime conditions (section 2.2.3). The results showed that, even after the u_* filtering, the nighttime NEE was still 2.5 times more affected by site inhomogeneity than the daytime NEE. For this reason, we decided only to use daytime based estimates (i.e. $NEE_{0.25,\ HBLR}$, $GPP_{0.25,\ DB}$, $R_{e0.25,\ DB}$) in the final ECB synthesis. However, the daytime based method is very sensitive to the gap size in the NEE datasets (Wu et al., 2012)and the nighttime based method keeps more real measurements. As a conservative uncertainty estimate we therefore used the standard deviation of the results from all four methods.

The calculation of the R_s budget has considered both the model and the data uncertainties. The parameters (e.g. base respiration) of the R_s model were estimated on an annual basis, thus the seasonal dynamics in the parameters was not captured. However, Janssens and Pilegaard (2003) showed that an annual parameterization is sufficient for estimating annual sums from discontinuous measurements that cover the seasonal variability. One important source of uncertainty in annual R_s estimations is whether the spatial variability of R_s is represented well enough by the field data. Knohl et al. (2008) showed that the choice of the experimental design strongly affected their annual R_s estimates. In their study, R_s was measured over a 300 m transect within the Hainich forest, an old growth beech forest in Central Germany. The annual R_s budget estimates in different nested plots varied between 730 and 1258 g C m^{-2} yr^{-1}. Our sampling scheme did not allow the estimation of large scale heterogeneity and thus these

effects are not included in the uncertainty estimate. If the soil heterogeneity at Sorø was comparable with Hainich, the uncertainty of R_s would be largely underestimated. In this respect our estimate characterises the minimum uncertainty. In addition, the unaccounted CO_2 storage change within the soil column during the field measurement can lead to an underestimation of the instantaneous soil respiration up to 15% (Maier et al., 2010). Furthermore, our R_s measurements did not include the respiration from the coarse woody debris. The estimated contribution of coarse woody debris respiration to R_s in different studies ranged between 1.7-8.3% (Curtis et al., 2002; Gough et al., 2007; Howard et al., 2004). The Sorø forest is regularly managed, and therefore, the contribution of coarse woody debris can be assumed to be at the lower margin of the above mentioned range. Summarising all these aspects, we can conclude that the both the magnitude and the uncertainties of our R_s estimates could possibly be underestimated.

The tree growth estimate in this study was much lower than an earlier estimate based on an inventory in a nearby forest which was conducted in the FORCAST project (personal communication, Giorgio Matteucci, CNR-ISAFOM, Italy). In this study, a much larger inventory dataset and biomass expansion function specific for beech in Denmark was used (Skovsgaard and Nord-Larsen, 2012). Thus our tree growth estimate was stronger with reduced uncertainty.

4.2 Carbon cycling in the investigated beech forest

A main objective of this study was to quantify the amount of carbon that cycle through the system and where in the system it is stored or mobilized. For this we combined all available data on ECB components in a system that is defined by several interrelated budget equations (see section 2). Such synthesis is particularly important to evaluate whether these independently measured datasets are consistent at ecosystem scale and to derive additional information on unmeasured components.

Practical outcomes of this analysis are recommendations on how these datasets can be used for model-data fusion studies.

A rigorous consistency evaluation of ECB datasets is very data demanding, because it requires multiple independent estimates of the same components. This is currently only possible at a few forest sites where atmospheric flux measurements have been amended by ecophysiological and inventory studies. In a pioneering work, Luyssart et al. (2009) reviewed 529 FLUXNET study sites and found only 16 sites that met their data requirements, i.e. that GPP, R_e, NPP, R_h, R_a and R_s were determined independently. The consistency was then evaluated by (1) whether the CO_2 balance could be closed within an acceptable predefined range of error and (2) whether the relationships between the major C fluxes and stock changes were considered as consistent with expert knowledge. Due to lack of independent R_a and R_h estimates at our site, we only used the second approach, i.e. comparing the relationships between fluxes with findings at other comparable sites. We focus here especially on the derived entities, i.e. the new information that was calculated from the measured entities as remainders of the mass conservation equations, and their uncertainties. With this approach we test, whether the independently measured inventory based data sets, the soil respiration measurements and the eddy covariance flux measurements result in 'reasonable' budgets of ecosystem components, i.e. the soil and the tree stand and the ecosystem as a whole. As a reference we use data from two other sites, the young, central European beech forest Hesse (Granier et al., 2008) and the old growth Central European beech forest Hainich (Knohl et al., 2003; Mund et al., 2010), where intensive inventory studies have been performed together with atmospheric flux studies. Additionally we used results of Luyssaert et al. (2007) who analysed the C flux data of the FLUXNET research network, including 24 temperate broadleaved deciduous forests.

A prerequisite for using the simple budget equations is that the CO_2 fluxes and the tree growth processes are balanced and that year-to-year fluctuations do not affect the balance in a dominant way. Tree internal buffer mechanisms, such as transport and storage of reserve carbohydrates in vessels and tissues, cause decoupling between carbon assimilation and tree growth. Only the structural growth is measured in the inventory approach. As an example, Granier et al. (2008) showed that the stem growth at Hesse stopped at some time in the vegetation period, while the net carbon assimilation still continued, filling those carbohydrate pools that would nourish the next year's initial leaf development. The interannual variability of tree growth is affected by fluctuations in the C input, i.e. GPP and by seasonally and inter-annually highly variable drivers like water availability, i.e. fine root mortality, or tree internal rhythms, e.g. fruiting. These cause deviations from more or less regular growth patterns (Mund et al., 2010) following a not yet well known tree internal, hierarchical system on how the carbon reserves are allocated (Campioli et al. submitted). Gough et al. (2008) showed in a mixed aspen dominated deciduous forest, at the University of Michigan Biological Station (UMBS), that five years averaging was long enough to compensate for decoupling effects and short term flux and growth fluctuations when building long-term sums. The thinning intervals at our site are 5 years as well (Møller, 1933). From these considerations we conclude that the chosen 5 years averaging period is long enough to consider the average effects of silvicultural management and exclude both decoupling effects between C assimilation and tree growth and year to year variability of the fluxes.

According to the atmospheric CO_2 flux measurements, the investigated beech forest was a moderate sink of carbon. The net C uptake of 258 g C m^{-2} yr^{-1} was lower than both in the younger (Hesse, Granier et al., 2008) and in the older temperate beech forest (Hainich, 2000 and 2001, Knohl et al., 2003), which took up 386 and 490 g C m^{-2} yr^{-1}, respectively. A lower net carbon uptake at Sorø could have been caused by the shorter growing season length at the higher latitude (Valentini et al., 2000) as

also speculated by Knohl et al. (2003). However, the component fluxes GPP and R_e at Sorø (1881 and 1624 g C m^{-2} yr^{-1}, respectively) were both much higher than that at Hesse (1397 and 1011 g C m^{-2} yr^{-1} in the period from 1996 to 2005, Granier et al., 2008) and at Hainich (1558 and 1068 in the years 2000 and 2001, Knohl et al., 2003) and also higher than the average from all comparable sites that were summarized by Luyssaert et al. (2007), i.e. 1375 ± 56 and 1048 ± 64 g C m^{-2} yr^{-1} for GPP and R_e, respectively. This comparison indicates a much more intensive CO_2 assimilation and carbon turnover at Sorø than at other comparable forest sites. A reason for such high GPP could be that Sorø is a mature forest with a high availability of nutrients which could stimulate both photosynthesis and the decomposition of organic matter; due to the uniform maritime climate at Sorø, the stand production might be less limited by drought stress during the growing season than at the more continental climates at Hanich and Hesse. Although the vegetation period measured in days is shorter, the longer day length in the higher latitude leads to more hours of light during the vegetation period that are available for use by photosynthesis. Due to the well known saturation effects in forest canopies (Ibrom et al., 2008; Pilegaard et al., 2001), low PAR intensities are used more effectively for photosynthesis than high PAR intensities.

The carbon use efficiency (CUE), i.e. NPP/GPP, relates CO_2 fluxes and organic carbon fluxes in the tree stand. At Sorø we found a CUE value of 37%, which lies within the range of several synthesis studies of 30-50% (Delucia et al., 2007; Litton et al., 2007; Luyssaert et al., 2007) but was lower than at Hesse (47% in 1995-2005, Granier et al., 2008) and at Hainich (50% in 2003-2007, Knohl et al., 2008). Delucia et al. (2007) showed that the CUE decreased with increasing forest age and according to their regression the CUE of Sorø would be expected to be around 45%. The low CUE value at Sorø indicates that either NPP is low or GPP is high, compared to other forest sites.

Looking at the respiration estimates, Piao et al. (2010) observed that the R_a to GPP ratio increased with age for the sites with mean annual temperatures between 8-12°C (8.5°C at Sorø). The calculated R_a at Sorø (1173±115 g C m^{-2} yr^{-1}) was 2.7 times as high as the R_h value (451±228 g C m^{-2} yr^{-1}). This ratio was similar at Hesse with R_a and R_h averaged at 730 and 281 g C m^{-2} yr^{-1}, respectively in 1996-2005 (Granier et al., 2008). At UMBS R_a/R_h was 1.8 (Gough et al., 2010) and on average from Luyssaerts et al. (2008) data set it was 1.7. Both the absolute value and the relationship to R_h indicate that the R_a estimate at Sorø was high compared to the other sites. Although the R_e value was much higher at Sorø, the magnitude of R_s (752 g C m^{-2} yr^{-1}) was only slightly higher than at Hesse, 619 g C m^{-2} yr^{-1} (Granier et al., 2000) but in the lower range of the highly variable values found at Hainich 898 (730-1258) g C m^{-2} yr^{-1}(Knohl et al., 2008). Compared to R_e and GPP that were derived from eddy covariance measurements, the values of R_s at Sorø, which was measured with a chamber system, were much closer to those of the two reference sites. Given the higher R_h at Sorø, the calculated $R_{a,BG}$ (340 g C m^{-2} yr^{-1}) accounted for only 29 % of the total R_a. This ratio was much smaller compared to 53% and 80% at Hesse and Hainich, respectively. The ratio $R_{a,BG}$ / R_s, 45% , at Sorø was at least similar to Hesse (47%) but much lower than at Hainich (74%). The high variability of these ratios doesn't allow a clear distinction of a typical pattern that can be used for plausibility evaluation.

The high $R_{a,AG}$ at Sorø (872 g C m^{-2} yr^{-1}) was unexpected because it was 2 times higher than the root respiration. This higher magnitude cannot be explained by the high biomass stock compared to the belowground compartment because (1) the leaf and root litter production was almost the same, thus the biological activity and respiration of these two compartments should rather be similar; (2) the respiration from the woody tissues is generally low compared to the more active leaf and root tissues.

There are two hypotheses that could explain the extremely high $R_{a,AG}$ estimates. First, the R_s could have been underestimated at our site, if the plots that were selected for the measurements were in an area

with lower soil respiration than in the footprint of the tower. According to Knohl et al. (2008) differences between larger areas in the forest can reach up to 500 g C m^{-2} yr^{-1}. If the true R_s was in fact higher, the estimates of belowground and aboveground R_a would be more similar, i.e., closer to our expectation. Second, if the R_e at our site was overestimated, both R_a and R_h would have subsequently been estimated to be lower. This would result in larger $R_{a,\,BG}$ and smaller $R_{a,\,AG}$ estimates. Above we pointed out that our GPP estimate is also likely to be too high. This supports the second hypothesis, because the GPP estimate depends directly on R_e. The two possible reasons for the high $R_{a,AG}$ estimates are not mutually exclusive and may occur simultaneously; this requires further investigation to disentangle.

The NPP estimate at Sorø was very similar to that of the other two forests, Hesse and Hainich (CV < 5%). However, the components of NPP differed much, reflecting the different ages of the trees, e.g., the tree growth was highest in the youngest stand and lowest in the oldest. Based on our approach, the overall balance of the soil carbon at Sorø was closed with a small residual term (-33 g C m^{-2} yr^{-1}). Small losses of C from forest soils have also been observed in three spruce forests (ΔSOC = 96-125 g C m^{-2} yr^{-1}) along a north-south climatic gradient in Sweden (Lindroth et al., 2008). In Hesse, the tree growth (418 g C m^{-2} yr^{-1}) was also found higher than the NEE (386 g C m^{-2} yr^{-1}, Granier et al., 2008), resulting in small loss of SOC of 32 g C m^{-2} yr^{-1}.

The estimated uncertainty of the soil carbon budget at Sorø (85 g C m^{-2} yr^{-1}) was lower than the uncertainty of intensive soil coring. With, e.g., 100 replicates, Schrumpf et al. (2011) determined a minimum detectable difference of 246 ± 64 g C m^{-2}, for the upper 10 cm of the soil. According to our estimate (-33 g C m^{-2} yr^{-1}) sequential soil coring will only detect a significant change in SOC after minimum 10 years. The uncertainty in such an inventory based estimate would, however, be much larger than that of our soil carbon budget estimate that was derived from the ecosystem carbon fluxes.

The main source of error in our estimate is the uncertainty in R_h. Direct estimations of R_h are possible with trenching and stable isotope analysis. This pioneering work has been undertaken during one day in June 2001 at Sorø and it was concluded that R_h amounted to 57% of soil respiration (Formanek and Ambus, 2004). The corresponding ratio from our 5 years estimate was 59%, given the scale differences this is a sufficiently close value and both estimates support each other. Further development of this technique will be most probably the only way to reduce the uncertainties in R_a, R_h and thus SOC stock changes.

The soil budget is constrained by the litter and woody debris input and the heterotrophic CO_2 losses. In the way we determined R_h it was constrained by the difference between the ecosystem CO_2 balance (NEE) and the NPP both determined with independent approaches. The plausible soil C budget together with the relatively high confidence in the NPP estimate suggests that the confidence in the NEE and R_h estimates is higher than in the GPP and R_e.

We therefore conclude that in the context of carbon cycling at the ecosystem scale, the measured carbon balance (NEE), the NPP and its components together with the estimate of carbon export and woody debris production through forest management and the soil respiration estimates fit well in a plausible ECB. The results from flux partitioning, i.e. the gross CO_2 flux estimates GPP and R_e, seem to be too high at the site. Although possible climatic and biological mechanisms might be discussed, the estimate of the aboveground autotrophic respiration is finally implausibly high and the most likely reason for this is over estimation of nighttime fluxes at the site. Apparently the use of daytime data for flux estimation did only reduce but not fully compensate for this site specific feature. The phenomenon points to a special situation related to the fetch of the forest that needs further investigation and possibly adjustment of the eddy covariance system setup. Unless clarified we recommend careful use of the GPP and R_e estimates from this site.

5 Conclusions

A synthesis of the ecosystem carbon budget (ECB) and its components was performed for the first time at Sorø. Four independently measured ECB component datasets (i.e. NEE, soil respiration, tree growth, litter production and dissolved organic and inorganic carbon leaching) were used to derive other unmeasured components of the ecosystem, i.e., tree and soil carbon budgets, providing an overview about the carbon cycling in this temperate deciduous forest. In general, the forest was a moderate sink for atmospheric CO_2. Approximately 62% of the gross assimilated carbon was respired by the plants as autotrophic respiration, while 21% was added to the soil as litter production, offsetting the total heterotrophic respiration. The remaining 17% were either stored in the plants (mainly as aboveground biomass increment) or extracted from the system as wood yield. The soil organic carbon stock remained generally unchanged during the study period, considering the much higher uncertainty associated with the small loss detected. In general, the ECB datasets were consistent after being cross-checked against each other; except some derived component fluxes such as the aboveground autotrophic respiration. The most likely reasons for this unexpectedly high value is the underestimation in R_s or and overestimation in R_e. Although not a rigorous consistency test, as none of the ECB components has been measured twice at this site, the combination of several independent data sets, including the estimates and their uncertainty, yielded valuable additional information. This helped us to describe the carbon cycling in unprecedented completeness at this site and evaluate the plausibility of the individual flux terms. As a result of our analysis, we recommend that the nighttime NEE, GPP and R_e estimates from this site are only used with the above reservations. Recalling that datasets from most flux monitoring sites are not sufficiently complete to apply a rigorous consistency analysis (Luyssaert, et al. 2009), we suggest that plausibility analyses similar to ours are performed putting together as

many as possible independently estimated components of ECB and their uncertainties in the ecosystem context using the mass balance equations.

Acknowledgement

Our work is funded by multiple sources: National Funding (Danish Environmental Research Programme, Danish Council for Strategic Research, DTU Climate Centre, Danish national project ECOCLIM), EU Funding (Euroflux, CarboEuroFlux, CarboEurope-IP, CORE, IMECC, Nitro-Europe, and CARBO-Extreme). We thank Flurin Babst and David Frank for providing the tree ring datasets within the project CARBO-Extreme. Poul Sørensen is thanked for the high methodological standard and care with which he conducted the soil respiration and litterfall and stand biometric measurements in the field. Without their efforts, this work would not have been feasible. Finally we thank the land-owner Sorø Akademi (Directors Jens Thomsen and Jens Kristian Poulsen and forest manager Anders Grube) for giving us access to the site and for providing site specific management data.

635 **Table 1:** List of abbreviations and symbols and their definitions, units and sign conventions

Abbreviation/ symbol	Definition	Unit	Sign convention
NEE	Net ecosystem exchange of CO_2	g C m^{-2} yr^{-1}	negative corresponds to a carbon sink
GPP	Gross primary production	g C m^{-2} yr^{-1}	positive corresponds to a carbon sink
R_e	Ecosystem respiration	g C m^{-2} yr^{-1}	positive corresponds to a carbon release
NEP	Net ecosystem production	g C m^{-2} yr^{-1}	negative value of NEE
NBP	Net biome production	g C m^{-2} yr^{-1}	
R_s	Soil respiration	g C m^{-2} yr^{-1}	
$R_{a,AG}$	Aboveground autotrophic respiration	g C m^{-2} yr^{-1}	
$R_{a,BG}$	Belowground autotrophic respiration	g C m^{-2} yr^{-1}	
R_h	Heterotrophic respiration	g C m^{-2} yr^{-1}	
L_{AG}	Aboveground litter production	g C m^{-2} yr^{-1}	
L_{BG}	Belowground litter production	g C m^{-2} yr^{-1}	
G	Tree growth	g C m^{-2} yr^{-1}	
W	Woody debris	g C m^{-2} yr^{-1}	
H	Harvest	g C m^{-2} yr^{-1}	
A_{BG}	Total below ground carbon allocation	g C m^{-2} yr^{-1}	
NPP	Net primary production	g C m^{-2} yr^{-1}	
DOC_{leach}	Leached dissolved organic carbon	g C m^{-2} yr^{-1}	
ΔSOC	Changes in the soil carbon pool	g C m^{-2} yr^{-1}	
T_a	Air temperature	˚C	
R_g	Global radiation	W m^{-2}	
θ	Soil water content	%	
u_*	Friction velocity	m s^{-1}	

Table 2: Data coverage after u_* filtering with two different threshold values and gap-filled annual net ecosystem CO_2 exchange (NEE) using two different methods, i.e. marginal distribution sampling (MDS) and a hyperbolic light response (HBLR) regression model.

Year	**Data coverage (%)**			**Gapfilled NEE (g C m^{-2} yr^{-1})**			
	Measured	After u_* filtering		MDS		HBLR	
		0.1	0.25	0.1	0.25	0.1	0.25
2006	95	89	76	-60	-80	-96	-121
2007	89	85	76	-232	-226	-305	-339
2008	98	92	83	-288	-267	-335	-358
2009	99	94	83	-292	-284	-298	-345
2010	87	82	74	-192	-180	-243	-272
Mean	94	88	78	-213	-207	-255	-287

640

Table 3: Ecosystem CO_2 flux components GPP and R_e (with two different methods) based on two different u_* filtered NEE datasets. The biologically related dissolved inorganic carbon into the ground water (12 g C m^{-2} yr^{-1}, Kindler et al. 2010) was added to estimate the total fluxes.

Year	**GPP (g C m^{-2} yr^{-1})**				**R_e (g C m^{-2} yr^{-1})**			
Partitioning method	nighttime based		daytime based		nighttime based		daytime based	
u_* thresholds (m s^{-1})	0.1	0.25	0.1	0.25	0.1	0.25	0.1	0.25
2006	1817	1876	1799	1774	1757	1796	1703	1653
2007	2065	2133	1973	1947	1832	1908	1668	1608
2008	1980	2058	1932	1919	1692	1791	1599	1564
2009	1947	2050	1958	1928	1654	1766	1660	1583
2010	1811	1899	1799	1784	1620	1719	1557	1520
Mean	1924	2003	1892	1870	1711	1796	1637	1586

645

Table 4: Prior ranges (max, min and mean) of the uniform distribution of three soil respiration model parameters, posterior parameter sets after Bayesian calibration and model performance parameters (using the mean posterior parameter sets) compared with observations.

Model /Parameter	**Prior**			**Posterior**		$\mathbf{R^2}$	**AIC**	**MAE**	**RMSE**
	max	***min***	***mean***	***mean***	***sd***				
Model I									
R10	10	0	5	4.1	0.3	71%	127	0.09	0.63
Q10	5	1	3	2	0.1				
Model II									
R283	25	1	13	10.1	1.1	69%	175	0.24	0.73
E0	-10	-50	-30	-27.4	2.5				
T0	260	280	270	275.8	1.1				
Model III									
a0	10	0	5	1.9	0.05	76%	115	0.15	0.77
b0	1	0.1	0.55	0.2	0.04				

650 **Table 5:** Carbon stocks in different tree compartments (g C m^{-2}), total biomass increment (G, g C m^{-2} yr^{-1}), above and below ground litter production (L_{AG} and L_{BG} in g C m^{-2} yr^{-1}) and net primary productivity (NPP in g C m^{-2} yr^{-1})

Year	**Tree carbon stock**				***G***	L_{AG}	L_{BG}	**NPP**
	stem	branches	coarse roots	total				
2006	8085±178	1744±157	1838±164	11667±288	272±41	275±28	192±26	739±56
2007	7832±164	1699±148	1784±153	11315±269	386±92	186±14	176±26	748±97
2008	8026±168	1742±152	1826±156	11594±275	279±46	187±8	179±27	645±54
2009	8236±172	1790±157	1874±160	11900±282	306±53	251±20	183±27	740±63
2010	8439±179	1833±161	1918±166	12190±292	290±52	193±15	187±27	670±60
Mean	8124±172	1762±155	1848±160	11733±281	307±57	218±17	183±27	708±65

Table 6: Estimates and their uncertainties (standard deviations) of the ECB components (g C m^{-2} yr^{-1}) in the investigated beech stand (averages for the years 2006 to 2010).

Independently estimated		**Partitioned or calculated**	
NEP	258 ± 41	GPP	1881 ± 95
G	307 ± 57	TER	1624 ± 197
W	41 ± 12	NPP	708 ± 65
L_{AG}	218 ± 17	R_a	1173 ± 115
L_{BG}	183± 27	R_h	451 ± 228
R_s	752 ± 30	ΔSOC	-33 ±85
DOC	25± 4	A_{BG}	519 ± 88
		NBP	150 ± 67

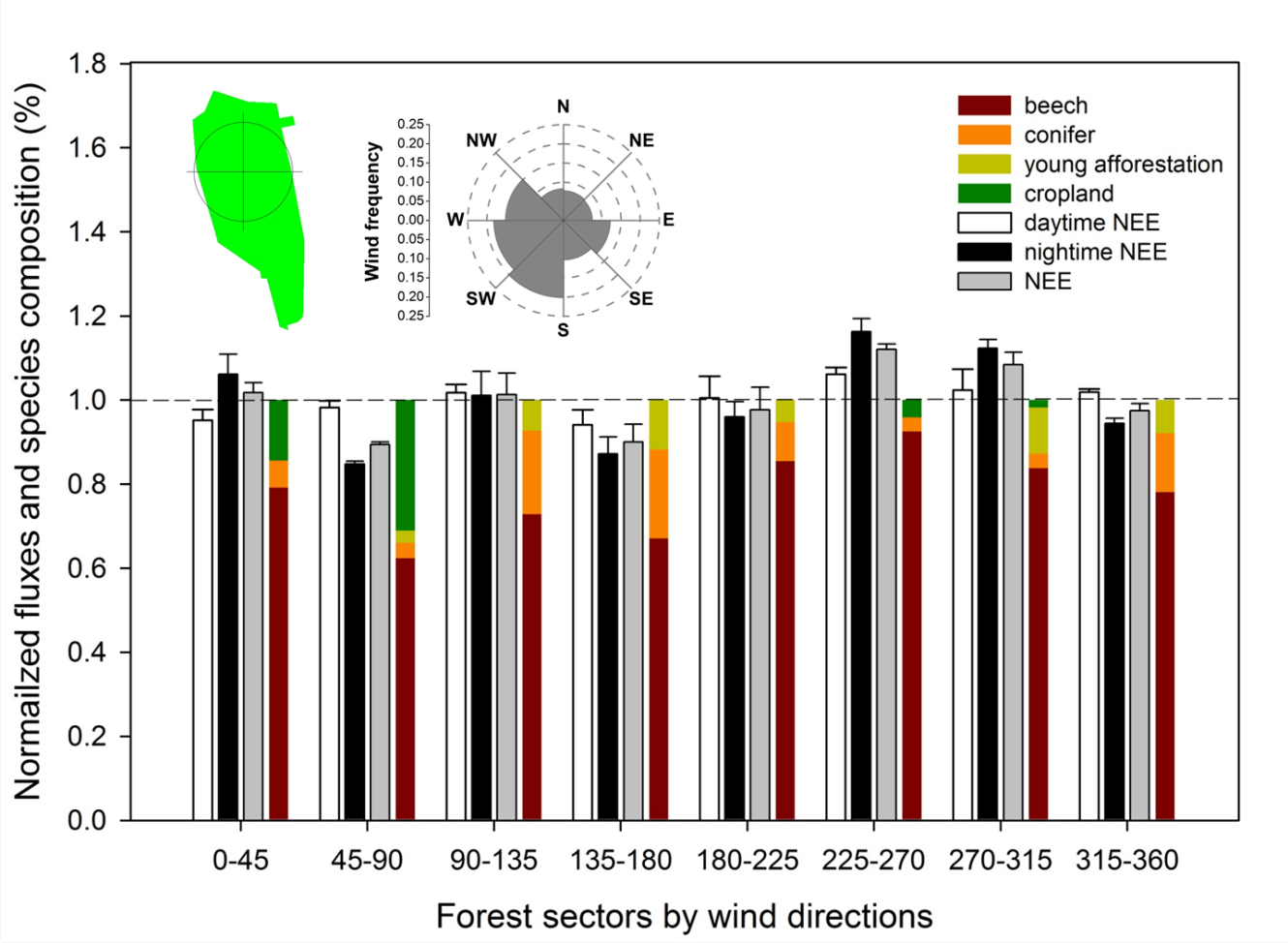

660 **Fig. 1:** Normalized average CO_2 fluxes and land use types within a 500 m radius from eight directions around the flux tower. The first inserted subplot in the top left is the forest map (green areas), within a 500 m radius circle around the flux tower. The second inserted subplot represents the frequency distribution of the wind directions.

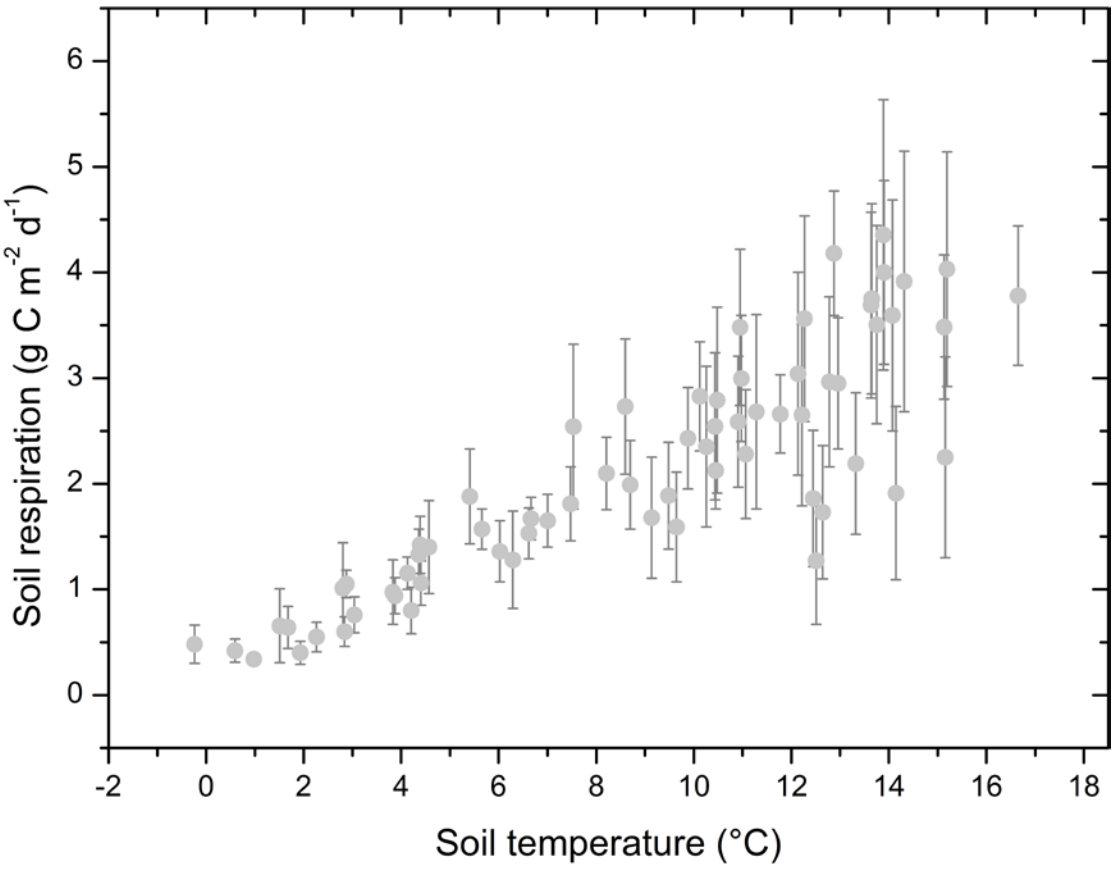

665

Fig. 2: Measured daily average soil respiration rate at different soil temperatures. The error bar represents the spatial variability in 12 replicated measurement locations and also the temporal variability (5-24 hours) within the specific measurement day.

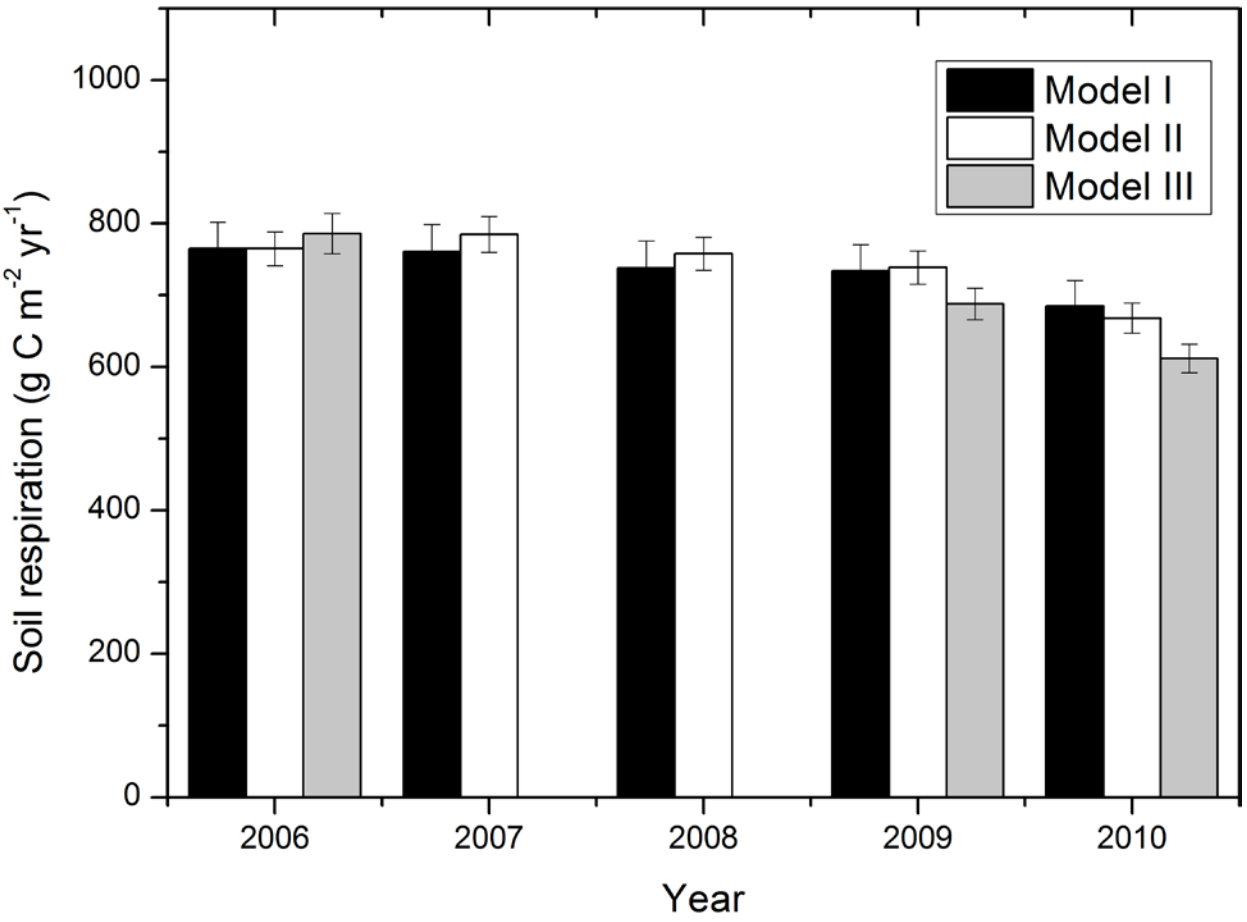

Fig. 3: Estimated annual soil respiration budgets using different models.

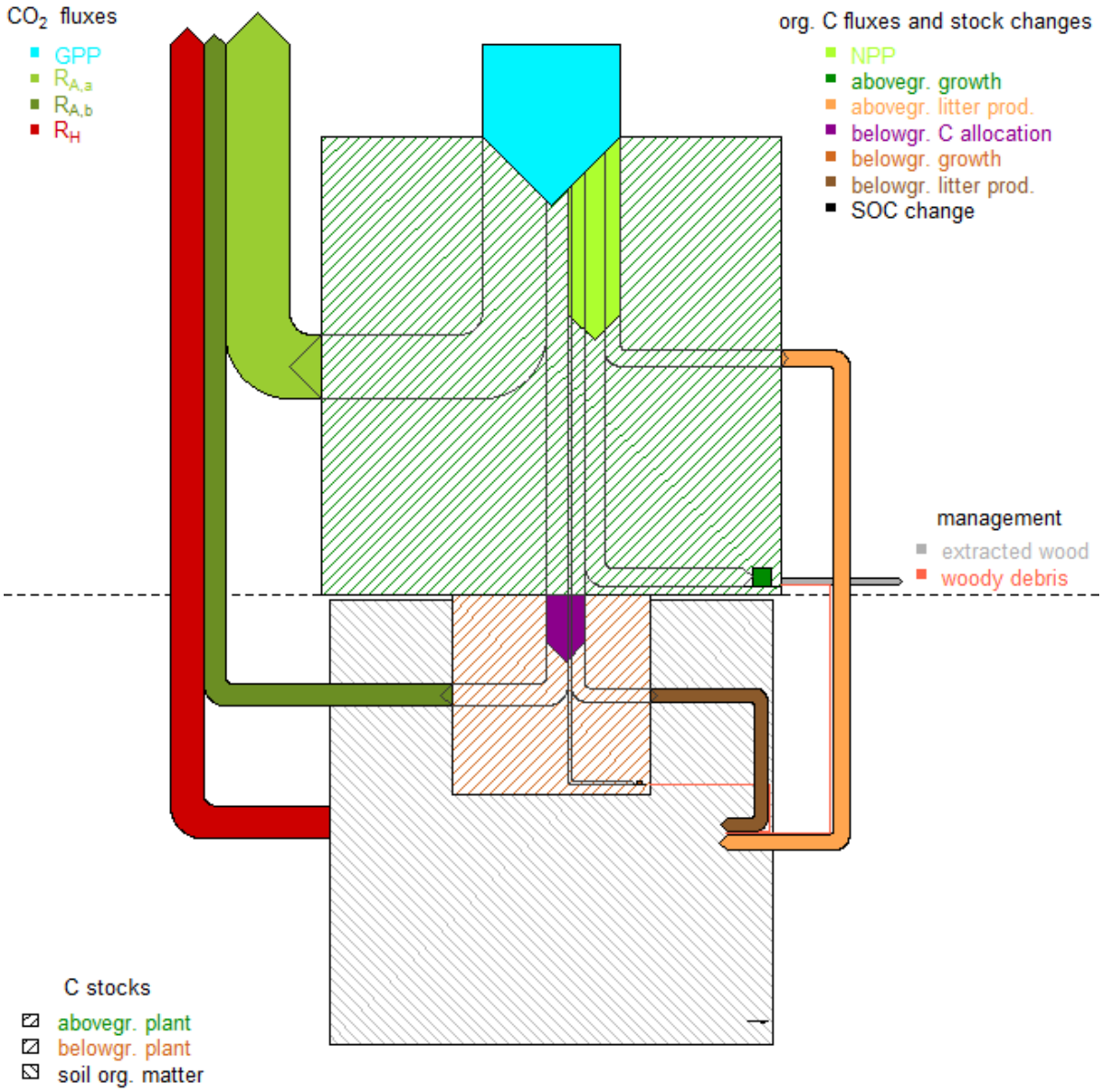

Fig. 4: Flow diagram of the carbon cycling in the beech forest at Sorø. Pools are displayed as quadratic rectangles filled with a line pattern; fluxes are represented by solid arrows and stock changes are bar charts. The widths of the flux arrows and stock change bars are scaled according to their absolute annual average values. The width of the GPP arrow represents 1882 g C m^{-2} yr^{-1}. The area of the rectangles of the pools is scaled to their sizes; the aboveground tree pool represents, e.g., 9885 g C m^{-2}. The 5 year average values and their uncertainties can be found in Tables 6. Fluxes of organic and

biologically related inorganic carbon (DOC, DIC) to the ground water, i.e. 25 and 12 g C $m^{-2}yr^{-1}$, for DOC and DIC respectively (Kindler et al., 2011), have been omitted in the graph but have been included in the stock change calculations (DOC) and ecosystem CO_2 losses (DIC).

6 References

Aubinet, M. et al., 2010. Direct advection measurements do not help to solve the night-time CO2 closure problem: Evidence from three different forests. Agricultural and Forest Meteorology, 150(5): 655-664.

Aubinet, M. et al., 2000. Estimates of the annual net carbon and water exchange of forests: the EUROFLUX methodology. Advances in Ecological Research, 30(30): 113-175.

Aubinet, M., Heinesch, B. and Longdoz, B., 2002. Estimation of the carbon sequestration by a heterogeneous forest: night flux corrections, heterogeneity of the site and interannual variability. Global Change Biology, 8(11): 1053-1071.

Baldocchi, D., 2003. Assessing the eddy covariance technique for evaluating carbon dioxide exchange rates of ecosystems: past, present and future. Global Change Biology, 9(4): 479-492.

Black, K. et al., 2007. Inventory and eddy covariance-based estimates of annual carbon sequestration in a Sitka spruce (Picea sitchensis (Bong.) Carr.) forest ecosystem. European Journal of Forest Research, 126(2): 167-178.

Carvalhais, N. et al., 2010. Identification of vegetation and soil carbon pools out of equilibrium in a process model via eddy covariance and biometric constraints. Global Change Biology, 16(10): 2813-2829.

Clark, D. et al., 2001. Measuring net primary production in forests: concepts and field methods. Ecological Applications, 11(2): 356-370.

Curtis, P.S. et al., 2002. Biometric and eddy-covariance based estimates of annual carbon storage in five eastern North American deciduous forests. Agricultural and Forest Meteorology, 113(1): 3-19.

Davidson, E., Savage, K., Verchot, L. and Navarro, R., 2002. Minimizing artifacts and biases in chamber-based measurements of soil respiration. Agricultural and Forest Meteorology, 113(1-4): 21-37.

Delucia, E., Drake, J.E., Thomas, R.B. and Gonzalez-Meler, M., 2007. Forest carbon use efficiency: is respiration a constant fraction of gross primary production? Global Change Biology, 13(6): 1157-1167.

Desai, A.R. et al., 2008. Cross-site evaluation of eddy covariance GPP and RE decomposition techniques. Agricultural and Forest Meteorology, 148(6): 821-838.

Falge, E. et al., 2001. Gap filling strategies for defensible annual sums of net ecosystem exchange. Agricultural and Forest Meteorology, 107(1): 43-69.

Field, C.B. and Kaduk, J., 2004. The carbon balance of an old-growth forest: building across approaches. Ecosystems, 7(5): 525-533.

Formanek, P. and Ambus, P., 2004. Assessing the use of δ13C natural abundance in separation of root and microbial respiration in a Danish beech (Fagus sylvatica L.) forest. Rapid Communications in Mass Spectrometry, 18(8): 897-902.

Göckede, M., Rebmann, C. and Foken, T., 2004. A combination of quality assessment tools for eddy covariance measurements with footprint modelling for the characterisation of complex sites. Agricultural and Forest Meteorology, 127(3): 175-188.

Gough, C., Vogel, C., Schmid, H., Su, H.B. and Curtis, P., 2008. Multi-year convergence of biometric and meteorological estimates of forest carbon storage. Agricultural and Forest Meteorology, 148(2): 158-170.

Gough, C.M. et al., 2007. Coarse woody debris and the carbon balance of a north temperate forest. Forest Ecology and Management, 244(1–3): 60-67.
Granier, A., Bréda, N., Longdoz, B., Gross, P. and Ngao, J., 2008. Ten years of fluxes and stand growth in a young beech forest at Hesse, North-eastern France. Annals of Forest Science, 65(7): 704-704.
Granier, A. et al., 2000. The carbon balance of a young beech forest. Functional Ecology, 14(3): 312-325.
Harmon, M.E. et al., 2004. Production, respiration, and overall carbon balance in an old-growth Pseudotsuga-Tsuga forest ecosystem. Ecosystems, 7(5): 498-512.
Heimann, M. and Reichstein, M., 2008. Terrestrial ecosystem carbon dynamics and climate feedbacks. Nature, 451(7176): 289-292.
Houghton, R., 2003. Why are estimates of the terrestrial carbon balance so different? Global Change Biology, 9(4): 500-509.
Howard, E.A., Gower, S.T., Foley, J.A. and Kucharik, C.J., 2004. Effects of logging on carbon dynamics of a jack pine forest in Saskatchewan, Canada. Global Change Biology, 10(8): 1267-1284.
Ibrom, A. et al., 2006. A comparative analysis of simulated and observed photosynthetic CO2 uptake in two coniferous forest canopies. Tree Physiology, 26(7): 845-864.
Ibrom, A. et al., 2008. Variation in photosynthetic light-use efficiency in a mountainous tropical rain forest in Indonesia. Tree Physiology, 28(4): 499-508.
Janssens, I.A. and Pilegaard, K., 2003. Large seasonal changes in Q10 of soil respiration in a beech forest. Global Change Biology, 9(6): 911-918.
Keith, H. et al., 2009. Multiple measurements constrain estimates of net carbon exchange by a Eucalyptus forest. Agricultural and Forest Meteorology, 149(3-4): 535-558.
Kindler, R. et al., 2010. Dissolved carbon leaching from soil is a crucial component of the net ecosystem carbon balance. Global Change Biology: no-no.
Knohl, A., Schulze, E.D., Kolle, O. and Buchmann, N., 2003. Large carbon uptake by an unmanaged 250-year-old deciduous forest in Central Germany. Agricultural and Forest Meteorology, 118(3-4): 151-167.
Knohl, A., Søe, A.R.B., Kutsch, W.L., Göckede, M. and Buchmann, N., 2008. Representative estimates of soil and ecosystem respiration in an old beech forest. Plant and Soil, 302(1): 189-202.
Lasslop, G., Reichstein, M., Kattge, J. and Papale, D., 2008. Influences of observation errors in eddy flux data on inverse model parameter estimation. Biogeosciences, 5(5): 1311-1324.
Lasslop, G. et al., 2010. Separation of net ecosystem exchange into assimilation and respiration using a light response curve approach: critical issues and global evaluation. Global Change Biology, 16(1): 187-208.
Le Goff, N. and Ottorini, J.M., 2001. Root biomass and biomass increment in a beech (Fagus sylvatica L.) stand in North-East France. Annals of Forest Science, 58(1): 1-13.
Lindroth, A., Klemedtsson, L., Grelle, A., Weslien, P. and Langvall, O., 2008. Measurement of net ecosystem exchange, productivity and respiration in three spruce forests in Sweden shows unexpectedly large soil carbon losses. Biogeochemistry, 89(1): 43-60.
Litton, C., Raich, J. and Ryan, M., 2007. Carbon allocation in forest ecosystems. Global Change Biology, 13(10): 2089-2109.
Lloyd, J. and Taylor, J., 1994. On the temperature dependence of soil respiration. Functional Ecology: 315-323.

Luo, Y. et al., 2009. Parameter identifiability, constraint, and equifinality in data assimilation with ecosystem models. Ecological Applications, 19(3): 571-574.
Luyssaert, S. et al., 2007. CO2 balance of boreal, temperate, and tropical forests derived from a global database. Global Change Biology, 13(12): 2509-2537.
Luyssaert, S. et al., 2009. Toward a consistency cross-check of eddy covariance flux–based and biometric estimates of ecosystem carbon balance. Global Biogeochemical Cycles, 23(3).
Maier, M., Schack-Kirchner, H., Hildebrand, E. and Holst, J., 2010. Pore-space CO2 dynamics in a deep, well-aerated soil. European Journal of Soil Science, 61(6): 877-887.
Miller, S.D. et al., 2004. Biometric and micrometeorological measurements of tropical forest carbon balance. Ecological Applications, 14(sp4): 114-126.
Moffat, A.M. et al., 2007. Comprehensive comparison of gap-filling techniques for eddy covariance net carbon fluxes. Agricultural and Forest Meteorology, 147(3-4): 209-232.
Møller, C.M., 1933. Bonitetstabeller og bonitetsvise tilvækstoversigter for bog, eg og rødgran i Danmark. Dansk Skovforenings 18: 457-623.
Mund, M. et al., 2010. The influence of climate and fructification on the inter-annual variability of stem growth and net primary productivity in an old-growth, mixed beech forest. Tree Physiology, 30(6): 689-704.
Ocheltree, T. and Loescher, H., 2007. Design of the AmeriFlux portable eddy covariance system and uncertainty analysis of carbon measurements. Journal of Atmospheric and Oceanic Technology, 24(8): 1389-1406.
Oren, R. et al., 2006. Estimating the uncertainty in annual net ecosystem carbon exchange: spatial variation in turbulent fluxes and sampling errors in eddy-covariance measurements. Global Change Biology, 12(5): 883-896.
Papale, D. et al., 2006. Towards a standardized processing of Net Ecosystem Exchange measured with eddy covariance technique: algorithms and uncertainty estimation. Biogeosciences, 3(4): 571-583.
Paw, K.T., Baldocchi, D.D., Meyers, T.P. and Wilson, K.B., 2000. Correction of eddy-covariance measurements incorporating both advective effects and density fluxes. Boundary-layer meteorology, 97(3): 487-511.
Peek, M.S., 2007. Explaining variation in fine root life span. Progress in Botany: 382-398.
Piao, S. et al., 2010. Forest annual carbon cost: a global-scale analysis of autotrophic respiration. Ecology, 91(3): 652-661.
Pilegaard, K., Hummelsh j, P., Jensen, N. and Chen, Z., 2001. Two years of continuous CO2 eddy-flux measurements over a Danish beech forest. Agricultural and Forest Meteorology, 107(1): 29-41.
Pilegaard, K., Ibrom, A., Courtney, M.S., Hummelsh j, P. and Jensen, N.O., 2011. Increasing net CO2 uptake by a Danish beech forest during the period from 1996 to 2009. Agricultural and Forest Meteorology, 151(7): 934-946.
Pilegaard, K. et al., 2003. Field measurements of atmosphere-biosphere interactions in a Danish beech forest. Boreal Environment Research, 8(4): 315-333.
Rannik, Ü. et al., 2012. Footprint Analysis. Eddy Covariance: 211-261.
Raupach, M. et al., 2005. Model–data synthesis in terrestrial carbon observation: methods, data requirements and data uncertainty specifications. Global Change Biology, 11(3): 378-397.
Reichstein, M. et al., 2005. On the separation of net ecosystem exchange into assimilation and ecosystem respiration: review and improved algorithm. Global Change Biology, 11(9): 1424-1439.

Richardson, A. and Hollinger, D., 2005a. Statistical modeling of ecosystem respiration using eddy covariance data: maximum likelihood parameter estimation, and Monte Carlo simulation of model and parameter uncertainty, applied to three simple models. Agricultural and Forest Meteorology, 131(3-4): 191-208.

Richardson, A.D. et al., 2012. Uncertainty Quantification. Eddy Covariance: 173-209.

Richardson, A.D. and Hollinger, D.Y., 2005b. Statistical modeling of ecosystem respiration using eddy covariance data: maximum likelihood parameter estimation, and Monte Carlo simulation of model and parameter uncertainty, applied to three simple models. Agricultural and Forest Meteorology, 131(3-4): 191-208.

Santaren, D., Peylin, P., Viovy, N. and Ciais, P., 2007. Optimizing a process-based ecosystem model with eddy-covariance flux measurements: A pine forest in southern France. Global Biogeochemical Cycles, 21(2).

Schimel, D.S., 1995. Terrestrial ecosystems and the carbon cycle. Global Change Biology, 1(1): 77-91.

Schrumpf, M., Schulze, E., Kaiser, K. and Schumacher, J., 2011. How accurately can soil organic carbon stocks and stock changes be quantified by soil inventories? Biogeosciences Discussions, 8: 723-769.

Schulze, E.D., Wirth, C. and Heimann, M., 2000. Managing forests after Kyoto. Science, 289(5487): 2058-2059.

Selsted, M.B. et al., 2012. Soil respiration is stimulated by elevated CO2 and reduced by summer drought: three years of measurements in a multifactor ecosystem manipulation experiment in a temperate heathland (CLIMAITE). Global Change Biology, 18(4): 1216-1230.

Skovsgaard, J.P. and Nord-Larsen, T., 2012. Biomass, basic density and biomass expansion factor functions for European beech (Fagus sylvatica L.) in Denmark. European Journal of Forest Research, 2: 1-19.

Valentini, R. et al., 2000. Respiration as the main determinant of carbon balance in European forests. Nature, 404(6780): 861-865.

Van Oijen, M., Rougier, J. and Smith, R., 2005. Bayesian calibration of process-based forest models: bridging the gap between models and data. Tree Physiology, 25(7): 915-927.

Wang, Y.P., Trudinger, C.M. and Enting, I.G., 2009. A review of applications of model–data fusion to studies of terrestrial carbon fluxes at different scales. Agricultural and Forest Meteorology, 149(11): 1829-1842.

Williams, M. et al., 2009. Improving land surface models with FLUXNET data. Biogeosciences, 6(7): 1341-1359.

Wu, J. et al., 2012. Effects of climate variability and functional changes on the interannual variation of the carbon balance in a temperate deciduous forest. Biogeosciences, 9(1): 13-28.

Wutzler, T., Wirth, C. and Schumacher, J., 2008. Generic biomass functions for Common beech (Fagus sylvatica) in Central Europe: predictions and components of uncertainty. Canadian Journal of Forest Research, 38(6): 1661-1675.

Paper III

Modelling the decadal trend of ecosystem carbon fluxes demonstrates the important role of biotic changes in a temperate deciduous forest

J. Wu[1], P.E. Jansson[2], L. van der Linden[1,3], K. Pilegaard[1], C. Beier[1], A. Ibrom[1]

1. Technical University of Denmark, Department of Chemical and Biochemical Engineering, Center for Ecology and Environmental Sustainability, 4000, Roskilde, Denmark
2. Royal Institute of Technology (KTH), Department of Land and Water Resources Engineering, 10044 Stockholm, Sweden
3. Australian Water Quality Centre, 5000, Adelaide, Australia

Correspondence to: J. WU (jiwu@kt.dtu.dk)

Abstract

Temperate forests are globally important carbon stocks and sinks. Trends in net ecosystem exchange (NEE) and carbon uptake period (CUP) have recently been observed in a beech forest and this trend cannot be entirely attributed to variability in climate. This study sought to clarify the mechanisms responsible for the observed trend, using an ecosystem model (CoupModel) and model data fusion (MDF) with multiple constraints and model experiments. The model was able to simulate the observed data well (R^2 = 0.8, mean error = 0.1 g C m^{-2} d^{-1}) but did not reproduce the observed trends in NEE when global parameter estimates were used. Annual parameter estimates were able to reproduce the decadal scale trends; the yearly fitted posterior parameters (e.g. the light use efficiency) indicated a role for ecosystem functional change. A role for nitrogen demand during mast years is also supported by the inter-annual variability in the estimated parameters. The inter-annual variability of biological parameters was fundamental to

simulating inter-annual trends in carbon fluxes in the investigated beech forest at Sorø. This demonstrates the importance of biotic changes. Nitrogen cycling and dynamics were identified as possible stand internal factors and need further investigation.

Key words: Net ecosystem exchange, CoupModel, Functional change, Model data fusion, Multiple constraints approach

1. Introduction

Terrestrial ecosystems are dynamic components of the global carbon (C) cycle, acting as a net C sink of 1.0 to 2.6 Pg C yr^{-1} globally (Metz, 2007). Forests are important C stocks, covering 31% of the Earth's land surface (FAO, 2010) and storing approximately 861 Pg C (Pan et al., 2011), more than the total atmospheric C stock of 805 Pg (Houghton, 2007). The estimated net C uptake by the world's forests (excluding the emission of 3 Pg C yr^{-1} due to tropical deforestation) is on average 4 Pg C yr^{-1} in 1990-2007 (Pan et al., 2011), equivalent to almost half of the anthropogenic C emissions in 2009 (Friedlingstein et al., 2010). Temperate forests contribute roughly 20% and 14% to the global forest area and forest C stock, respectively (Pan et al., 2011). Despite this relatively low proportion, the C sink in temperate forests has increased by 17% during the past two decades, contrary to boreal and tropical forests, which were either unchanged or decreased by 23%, respectively. In Europe, temperate forests span large areas of the western and central parts (FAO, 2010). Historically, the natural composition of forests in Europe was mainly deciduous, until human management resulted in an increase in the proportion of conifers, predominantly for economic reasons (Spiecker, 2003). Today the fraction of coniferous species in the European temperate forests far exceeds their natural range. This has stimulated concerns about their ecological functioning and new management plans to reverse the compositional change of European forests to contain more deciduous tree species (Spiecker, 2003). Given the high C sink potential and increasing importance of temperate deciduous forests in the future, questions such as how they will respond to the changing climate and whether they can continue to serve as a strong sink of atmospheric CO_2 is of interest to scientists, policy makers and the public in general.

Process-based models are important tools to simulate the ecosystem responses and states under future climatic conditions. Eco-physiological processes can be described either mechanistically, e.g. the CO_2 diffusion through the stomata and leaf surface (Collatz et al., 1991) or semi-empirically, e.g. the light response of photosynthesis (Jarvis, 1976) and environmental controls on plant phenology (Hänninen, 1995; Richardson et al., 2012). Many different process-based ecosystem models have been developed and validated against measured C fluxes in different ecosystems. Generally, the models perform reasonably well at the site level to predict the seasonal or short-term interannual variability of ecosystem C fluxes (e.g. Williams et al., 2005; Wu et al., 2011). However, they have been found to be less able to reproduce the long-term dynamics (Keenan et al., 2012b). Keenan et al. (2012a) assessed the ability of 16 ecosystem models to simulate 11 long-term flux datasets and found that none of the models could consistently reproduce the observed interannual variability in the C fluxes. Similarly, several cross-site model inter-comparison studies demonstrated strong divergences in model predictions (Kramer et al., 2002; Morales et al., 2005; Siqueira et al., 2006). Another recent modeling study in a boreal pine forest showed however exceptional good model performance for the long-term ecosystem C dynamics as the boreal ecosystem processes were found strongly controlled by the interannual variation in the soil and air temperature (Wu et al., 2012b).

The optimization of process models and the investigation of future ecosystem C cycling can be integrated in so-called model data fusion (MDF) studies (Wang et al., 2009). The uncertainty in the model projections can be reduced if the observed ecological datasets are assimilated by the model to constrain the parameter ranges, determine parameter sensitivity and indentify potential model structural deficits. MDF studies are especially beneficial when conducted at sites which have been intensively studied for long periods. For instance, the models can be applied at sites

which have experienced summer heat waves (Reichstein et al., 2007) or abnormal spring snow pack melting (Hu et al., 2010) to evaluate whether they could capture the extreme or lagged ecosystem responses. Also, for some sites that have a systematic phenomenon, e.g. a trend of increasing carbon uptake (Keenan et al., 2012b; Pilegaard et al., 2011), it is also particularly interesting to investigate whether models could identify the possible causes for the ecosystem responses, e.g. whether the trend is caused by climatic forcing or by internal ecosystem functional change.

In a temperate deciduous forest near Sorø, Zealand Denmark, net ecosystem exchange of CO_2 (NEE) was continuously measured over the past 13 years (1997–2009), showing a decadal trend of increasing C uptake of 23 g C m^{-2} yr^{-2} (Pilegaard et al., 2011). The extended C uptake period and enhanced canopy photosynthetic capacity were identified as the main drivers of the trend (Pilegaard et al., 2011). Using a semi-empirical model, Wu et al. (2012a) confirmed that the long-term ecosystem C dynamics at this site cannot be solely explained by the direct effect of climate variability whereas the functional changes during the 13-year period were the most important drivers. Based on these previous findings, it is of interest to evaluate whether process-based models could dynamically simulate the changes in the ecosystem functioning (e.g. phenology and canopy development) and the long-term variability in the carbon uptake at this site. In this study, a process-based model was optimized and applied to simulate the ecosystem C dynamics, using a multiple constraint approach. We examine the model performance at diurnal, seasonal and inter-annual time scales and identify the drivers for the short-term variability and long-term trend of increasing carbon uptake.

2. Materials and Methods

2.1 *Site*

The data used in this study were measured in a beech (*Fagus sylvatica* L.) forest in the Danish long-term CO_2 flux investigation site, Sorø (55°29'13'N, 11°38'45'E). In 2011, the stand around the flux tower was 90 years old, the average tree height was 28 m and the average diameter at breast height was 42 cm. Annual mean temperature and precipitation sum (1997-2009) at the site were 8.5 °C and 564 mm, respectively. The soils are classified as alfisols or mollisols (depending on the base saturation) with a 10-40 cm deep organic layer. Further information about the site can be found in Pilegaard et al. (2001; 2011; 2003).

2.2 *Data*

Hourly gap-filled meteorological data from August 1996 to December 2009 (Pilegaard et al., 2011) were used as drivers of the model. Quality controlled (corrected for below-canopy storage and low turbulence mixing) carbon, latent and sensible heat fluxes (Pilegaard et al., 2011) from the years 1997 to 2009 were used for model calibration. Data of the aboveground and belowground biomass stocks were estimated based on tree ring data, height measurements and biomass expansion functions (Skovsgaard and Nord-Larsen, 2012). Peak leaf area index (LAI) was measured during summer from 2004-2009; together with the continuously measured PAR transmission, the LAI time series were reconstructed using an empirical light extinction function that was fitted to the peak LAI measurements. Soil temperatures were measured in the top 5 and 10 cm while soil water content was measured at 15 cm. The C uptake periods (CUP) were calculated from both the measured and simulated NEE time series after Pilegaard et al (2011).

2.3 *Model description*

The CoupModel is a one-dimensional process-based ecosystem model that can be used to simulate the coupled biological and physical processes in soil-plant-atmosphere systems (Jansson, 2012; Jansson and Karlberg, 2004; Jansson et al., 2008). Hourly meteorological measurements of air temperature, global radiation, relative humidity, wind speed and precipitation were used as boundary conditions. The model represents vertical layers of the soil profile and heat and water fluxes are calculated based on the soil physical parameters and climate inputs. The simulated soil temperature and moisture, together with the climate drivers regulate the biotic ecosystem processes such as phenology, photosynthesis, plant respiration and decomposition of litter and soil organic matter. In addition, the biotic ecosystem dynamics feed back to the simulated physical environment. For instance, the simulated plant structure will affect the aerodynamic conductance at the atmosphere and leaf surface; likewise, changes in LAI alter the energy and water balance at the soil surface. A detailed description of CoupModel can be found in Jansson and Moon (2001), Jansson and Karlberg (2004) and Wu et al. (2011). The model equations and parameters relevant for this paper are given in Appendix 1.

2.4 *Model setup and calibration*

The model was initialized (spin up) as of August 1996 and calibrated for the period 1997-2009. The initial C pools in vegetation and soil were given as parameters based on the measured and estimated data. The soil physical parameters were either measured, e.g. parameters for the water retention curve or estimated based on soil texture data, e.g. the soil thermal properties. Some other biological parameters such as the specific leaf area and plant height were also measured on site. The data necessary for the model initialization are available in BADM (Biological-ancillary-disturbance-management) format at the European Flux Database (http://gaia.agraria.unitus.it/).

Two modelling experiments were performed. In the first, the model was calibrated against the whole 13 year (1997-2009) data, where 29 parameters that were expected to be sensitive to the carbon and water dynamics (Table 1) were selected for calibration according to experiences of model application and a sensitivity study by Svensson et al. (2008b). The prior distributions of the model parameters (Table 1) were set to reasonably wide ranges with uniform distribution based on literature and previous model applications (e.g. Svensson et al., 2008a; Wu et al., 2011). A total number of 30000 model runs were performed in the first modelling experiment. The acceptance of behavioural models (i.e. models simulation with same structure but different parameter values) was based on specific user-defined criteria (Beven and Freer, 2001; Liu et al., 2009). Two different constraints were considered: 1) only the hourly NEE data (denoted as Ω_{NEE}) and 2) the hourly daytime and night-time NEE, latent (λE) and sensible heat (H) fluxes and other biological data (denoted as $\Omega_{Multiple}$) were used to select the behavioural models to determine the posterior parameter distributions. The detailed acceptance criteria are given in Table 2. In this case residuals between simulated and measured variables represents changes in the behaviour of the real world systems.

In order to test the hypothesis that functional changes in the ecosystem (e.g. photosynthetic capacity, litter decomposition) have occurred over the observation period and affected the annual C uptake capacity of the forest, a second modelling experiment (3000 model runs) was designed based on the optimized posterior parameter sets in the first modelling experiment. In this modelling experiment, the number of sampled parameters was reduced to seven of those that control photosynthesis and respiration and they were allowed to vary between years (Table 1). In this case the inter-annual variability of ecosystem functioning is captured and represented by the

parameter estimates generated for each year. Trends in and residuals from the first experiments are removed and instead represented by changes in calibrated parameters.

3. Results

4.1 *Improved model simulation using the multiple constraint approach*

The posterior distribution of most parameters was different from their prior uniform distributions after the calibration (Fig. 1). With the first constraint, Ω_{NEE}, only a few parameters (e.g. ε_1, l_{Lc1} and ψ_c) were constrained; the posterior ranges of most other parameters were still similar to their prior. This low degree of parameter identification was improved when the multiple constraint approach was imposed ($\Omega_{Multiple}$). The posterior ranges of 9 key parameters controlling photosynthesis (e.g. ε_1, p_{ol}), respiration (e.g. k_l and k_h), phenology (e.g. t_{el}), allocation (e.g. f_l and f_r) and transpiration (e.g. T_{trig} and g_{vpd}) were clearly narrowed down as the day-time NEE, night-time NEE, LAI, biomass stocks, and λE were jointly used to constrain the model ($\Omega_{Multiple}$, Table 2). In addition, all the remaining 20 calibrated parameters were also more precisely determined, as the posterior distributions was changed from their prior uniform distributions to normal or log normal type distributions.

With both of the two different constraints, Ω_{NEE} and $\Omega_{Multiple}$, the ensemble mean of the modelled outputs represented the measurements well, with almost equally good R^2 and mean error (ME). The variability of the hourly NEE during the 13-year period was captured by the model (R^2: 0.72 and 0.75), partly as a product of the well simulated the LAI dynamics (R^2: 0.86 and 0.88). The soil heat processes were better simulated than the soil water transport and storage. The model explained approximately 92% and 60% of the variability in the measured soil temperature and soil water content, respectively. In contrast, the uncertainty (i.e. the range of the R^2 and ME for the accepted runs) of all the model outputs was significantly lower with $\Omega_{Multiple}$ compared to

Ω_{NEE} (Table 2). The model simulation using the modes of the posterior parameters of $\Omega_{Multiple}$ (see Fig. 1) performed equally well as the ensemble mean of the accepted runs (Table 2). However, the simulation using the mode of the posterior parameters of Ω_{NEE} performed worse than the corresponding ensemble means (Table 2).

4.2 *Model performance at diurnal and seasonal time scale*

The correlation between the daily modelled and measured NEE was higher than that at hourly time scale with R^2 = 0.8 (Fig. 2). The model residuals showed an overestimation of carbon uptake at high radiation (Fig. 2), which was also seen at the monthly diurnal course for the model-data mismatch (Fig. 3) where the simulated C uptake was higher than the measurements at mid-day during the growing season. In general, the diurnal cycle was well simulated throughout the year except in April when the simulated daytime NEE was apparently lower than the measurements. After May when the canopy was fully developed, the starting and ending of photosynthesis were correctly represented by the model (Fig. 2). The magnitude of night-time NEE was also well simulated during both the winter and the growing season.

Apart from the diurnal pattern, the flux and LAI seasonality was also reasonably well simulated. In all years, the peak LAI during summer was within the simulated uncertainty range. However, the ensemble mean of the simulated LAI was higher in 2004-2005 and lower in 2009 than the observations. The interannual variability in the leaf flush dates was correctly identified, except in 2006 and 2007 when the model predictions were earlier and later than the observations, respectively (Fig. 3). The leaf fall during autumn was less well represented in the model than the leaf flush. The simulated leaf fall was earlier than the measurements in 2002, 2003, 2004 and 2009, while it was later in 2000. In addition to the well simulated phenology, the estimated carbon uptake periods (CUP) based on the modelled NEE (Fig. 5a) also showed a similar trend

as the measurements (Pilegaard et al., 2011), with an extension of the CUP of 1.7 d yr^{-1} during the 13 year period.

4.3 *Model performance at interannual time scale*

With the globally fitted parameter sets in the first modelling experiment (i.e. calibrated against the whole 13-year datasets), the decadal trend of increasing carbon uptake of the forest was not reproduced by the model (Fig. 5b). The carbon uptake was overestimated in 1997-2000 and underestimated in 2005-2009. In the second step of the model calibration, the interannual variability in the carbon uptake was successfully simulated with yearly fitted model parameters (Fig. 5b). For the 7 yearly fitted parameters, only light use efficiency showed an increasing trend in 1997-2009 (Fig. 5c). The other 6 parameters were less well constrained and the mode of the posterior parameter distributions did not show a trend during the 13 year period (Table 3).

4. Discussion

By constraining the process-based model with long-term measurements of NEE datasets, the ensemble mean of the model outputs produced reasonably good estimates for both the NEE and other validation datasets. However, the accepted ensemble of behavioural models showed a high degree of equifinality, i.e. a number of different models could produce equally good results when compared to calibrated variables (Beven and Freer, 2001), resulting in high uncertainties in the estimates of other validated variables. This indicated that some behavioural models with certain parameterizations were accepted for the wrong reasons. For instance, the model could well represent the NEE (R^2: 0.71-0.73) when the LAI dynamics was incorrectly represented (lowest R^2=0.46). The problem of equifinality was also shown in the unconstrained posterior parameters (Fig. 1) which was similar to many other MDF studies, where it was shown that the information content of the high frequency NEE datasets was not sufficient enough to constrain the parameters

related to the different ecosystem component C flux, e.g. the autotrophic and heterotrophic respirations from different C pools (Keenan et al., 2012b; Richardson et al., 2012; Sacks et al., 2007; Wang et al., 2009).

On the other hand, the success of MDF studies also depends on how efficient the information in the assimilated datasets was used. For example, the uncertainty in the model outputs was reduced when the NEE datasets were averaged in times (e.g. monthly and annually) and added to the model calibration (Keenan et al., 2012b). Sacks et al. (2007) showed that optimizing the model on a twice daily (instead of hourly or daily) time step significantly improved the model's ability to accurately predict the component C fluxes. Mahecha et al. (2010) proposed a method to quantify the model-data disagreements at various time-frequency domains; the decomposed high or low frequency signals could also potentially be used to optimize the model parameters. In this study, when NEE was separated into daytime and night-time values before use in the model calibration (in $\Omega_{\mathrm{Multiple}}$), the parameters controlling the litter and humus decomposition rate were better constrained.

In general, the parameter uncertainties were significantly reduced when additional constraints were incorporated. Including the LAI, biomass stock and λE in the calibration strongly constrained 9 key model parameters and successfully reduced posterior uncertainty in all of the remaining 20 parameters. The way the parameters were constrained could be attributed to the specific information content of the assimilated data which were related certain ecosystem processes. For instance, the respiration parameters (r_{ml}, r_{mr}, k_{l} and k_{h}) were better constrained when the nighttime NEE was separately included in the calibration. However, because the autotrophic and heterotrophic respirations were not distinguished in the data, these parameters were still inter-correlated. Nevertheless, the additionally constrained posterior parameters are

more meaningful as showed by the more realistic distribution of these parameters. The inclusion of LAI into the calibration specifically constrained 4 parameters controlling the phenology (t_{el}, t_{L2}), litter fall rate during the growing season (l_{LC1}), and allocation (f_l). Using the multiple constrain approach, some constrained parameters shifted their distributions. For instance, the light use efficiency, ε_1 shifted its distribution to a higher magnitude when the daytime NEE was separated used in the calibration. In a ideal situation, using the multiple constraints approach is expected to facilitate the process-based model optimization, and it is interesting to investigate e.g. the which additional datasets are most beneficial for the model calibration. However, adding more constraints does not necessarily always lead to a better model optimization because the data quality, e.g. the consistency of the ecosystem C budget datasets (Luyssaert et al., 2009) is of crucial importance for the MDF. In our case, the soil respiration measured with the auto-chamber was found systematically underestimated based on a synthesis of the ecosystem C budget at this site (unpublished), thus was not used for the model calibration.

With the multiple constraints approach, the diurnal and seasonal dynamics of the ecosystem C fluxes can be well represented by the model. The diurnal cycle of NEE was correctly simulated in all different seasons, except in the winter-spring transition periods, as the small amount of the emerging coniferous photosynthesis was not accounted for in the model. In May-August, the measured NEE at mid-day was lower than the modelled value, probably because linear light use efficiency models in general tend to overestimate the photosynthesis when the radiation is already saturated (Ibrom et al., 2008). On the other hand, as the model was calibrated against the daytime NEE, the underestimation during the winter periods (i.e. the unaccounted coniferous photosynthesis) could be compensated by an overestimation of the daytime NEE during the growing season. The uncertainty of the measured NEE was shown to be higher during night, thus

the criteria for acceptance for the night-time NEE was also less strictly set. Nevertheless, the magnitude of night-time NEE was correctly simulated.

As for the diurnal pattern, the seasonality of the ecosystem dynamics was also well simulated. The leaf flush dates were reasonably well estimated with the temperature sum function (Eq. A8). An interesting model data mismatch was in 2007 when the spring temperature was the warmest during the 13-year period (see Fig. 1 in Wu et al., 2012a), the predicted leaf flush date was apparently earlier than the observation (Fig. 3). One possible explanation for the "delayed" leaf flush could be the effect of late frosts (Linkosalo et al., 2000). However, after a screening of the temperature datasets, no such late frost events were recorded from March-May 2007. Therefore, it is likely that the phenology sub-model is over sensitive in periods with extreme temperature records. This was also the case for the spring 2006 (coolest during the 13-year), when the model predicted a late leaf flush. The prediction of phenology has proven challenging. Richardson et al. (2012) analyzed the performance of 14 different models and showed that almost all the models consistently predicted a too early leaf flush. In our case, the model did not show systematic bias but a poor performance in periods with extreme temperature records (i.e. warmest and coolest within decades). As the average and variability of global temperature is expected to increase, it is unlikely that the phenology model used will correctly project the seasonality of future ecosystem responses. The simulated interannual variation in the peak LAI was lower than that observed. For instance, in 2008 and 2009, the measured LAI was higher and lower than the 13-year average, while the simulated LAI didn't show considerable differences, showing that the fixed allocation scheme in the model can be still improved.

Although the process-based model performed reasonably well at diurnal and seasonal time scales, it failed to accurately reproduce the interannual variability in the ecosystem C uptake (Fig. 5).

The small short-term model errors in some years accumulated and resulted in a large bias in the simulated annual C balances at the interannual time scale; similar results have been found in many other modelling studies (e.g., Siqueira et al., 2006; Keenan et al., 2012). This indicated that long-term C dynamics cannot be solely explained by the climate variables included in this study, as demonstrated in our previous study using semi-empirical modelling (Wu et al. 2012).

The failure to predict the long-term C dynamics can be caused by the inaccurate representation of the biotic ecosystem responses (Richardson et al., 2007; Wu et al., 2012). One hypothesis for this model-data mismatch is that the applied model structures (within CoupModel) used a fixed nitrogen response to photosynthesis, and thus did not dynamically simulate the effects of, e.g., changing canopy nitrogen contents. In the second model experiment, the 7 parameters controlling photosynthesis, phenology and respiration, were allowed to vary inter-annually and considered proximate for the ecosystem functional change. The estimated light use efficiency varied between years and showed a systematic trend during the 13-year period, corresponding to the hypothesis presented by Pilegaard et al. (2011). On the other hand, this model-data mismatch can also be caused by the missing model divers. For instance the CO_2 fertilization effects during the 13 year period were not accounted in the model as the present version of CoupModel used a light use efficiency dependent photosynthesis module. On a global scale the atmospheric CO_2 concentration has increased by 25ppm during study period (Friedlingstein et al., 2010). This could only partly have contributed to the increased light use efficiency in 1997-2009. Therefore, it is most likely the ecosystem internal nitrogen cycling has affected light use efficiency. An interesting finding was that the strong negative light use efficiency fluctuations were strongly associated with the occurrence of mast years. This indicates that the reallocation of nitrogen to the nuts might deplete stored nutrients and lowered the N content of the leaves To prove this

hypothesis, direct measurements on the nut production and its role in the N-turnover of the ecosystem are needed. Direct evidence of resource depletion in the masting trees is rare. Sala et al. (2012) examined the timing and magnitude of stored nutrient depletion after a heavy mast events in a conifer forest and confirmed that mast events deplete stored tree internal nutrients (including nitrogen and phosphorus) and reduced the leaf photosynthetic rates. Therefore, changes in the biophysical parameters such as the canopy photosynthetic capacity, leaf chlorophyll content and canopy nitrogen distribution need to be monitored, using both field observations or remote sensing (Houborg and Boegh, 2008). The processes governing nitrogen dynamics and their interaction with photosynthesis needs to be incorporated into process-based models.

5. Conclusions

Process-based models are needed for the projection of future ecosystem response to climate change. We used a 13-year dataset from Sorø to test whether the model could simulate the short-term and long-term ecosystem C dynamics. After the model calibration, the diurnal and seasonal patterns of carbon were successfully simulated, while the degree of equifinality was significantly reduced using the multiple constraints approach. The interannual variability in the ecosystem C uptake could not be correctly simulated unless the biological parameters were allowed to vary temporally. Our results confirmed that the long-term trend of increasing C uptake at Sorø were strongly driven by the biotic changes in the ecosystem status. Processes such as the nitrogen cycling in the ecosystem needs to be further investigated and incorporated into the process-based models.

Acknowledgement

This work is supported by the EU FP7 project CARBO-extreme, the DTU Climate Centre and the Danish national project ECOCLIM (Danish Council for Strategic Research).

Table 1: Calibration model parameters and their prior ranges (with uniform distribution) ; the parameters marked with * were also fitted annually in the second model experiment.

355

Parameter	Unit	Symbol	Eq. / Note	Prior *Min*	*Max*
Plant biotic processes					
RadEfficiency(1) *	g Dw MJ^{-1}	ε_1	Eq. (A1)	1	8
RadEfficiency(2)	g Dw MJ^{-1}	ε_2	Eq. (A1)	1	8
T Lmin	°C	p_{mn}	Eq. (A2)	–5	5
T Lopt1	°C	p_{o1}	Eq. (A2)	10	20
Allocation leaf	–	f_l	Eq. (A5)	0.2	0.6
Allocation root	–	f_r	Eq. (A5)	0.2	0.6
Maitaince Res. leaf *	day^{-1}	$r_{m,l}$	Eq. (A6)	5.00E-04	0.005
Maitaince Res. root *	day^{-1}	$r_{m,r}$	Eq. (A6)	5.00E-04	0.005
Emerge Tsum(1) *	°C	t_{el}	Eq. (A8)	100	200
LeafTsum2(1) *	°C	t_{L2}	Eq. (A9)	100	200
LeafRate1(1)	day^{-1}	l_{Lc1}	Eq. (A9)	1.00E-04	0.01
LeafRate2(1)	day^{-1}	l_{Lc2}	Eq. (A9)	0.05	0.5
Plant abiotic processes					
CritThresholdDry	cm water	ψ_c	Eq. (A16)	100	1.00E+04
TempCoefA	–	t_{WA}	Eq. (A17)	0.2	1.5
TempCoefC	–	T_{trig}	Eq. (A17)	0	6
Conduct Ris(1)	J m^{-2} day^{-1}	g_{ris}	Eq. (A18)	1.00E+06	1.00E+07
Conduct VPD(1)	Pa	g_{vpd}	Eq. (A18)	50	300
Conduct Max(1)	m s^{-1}	g_{max}	Eq. (A18)	0.01	0.03
Soil carbon processes					
RateCoefLitter1 *	day^{-1}	k_l	Eq. (A21)	0.02	0.05
RateCoefHumus*	day^{-1}	k_h	Eq. (A22)	1.0E–05	5.0E–04
TempMin	°C	t_{min}	Eq. (A23)	–10	0
TempMax	°C	t_{max}	Eq. (A23)	20	30
SaturationActivity	–	$p_{qSatact}$	Eq. (A24)	0	0.5
ThetaLowerRange	%	p_{qLow}	Eq. (A24)	3	20
ThetaUpperRange	%	p_{qUp}	Eq. (A24)	3	20
Soil physical processes					
Air Entry(0-0.05 m)	cm water	ψ_a	Eq. (A26)	1	20
Air Entry(0.05-0.15 m)	cm water	ψ_a	Eq. (A26)	1	20
DrainLevel	m	z_p	Eq. (A27)	–2	–1
DrainSpacing	m	d_p	Eq. (A27)	0	100

Table 2: Two different acceptance criteria (Ω_{NEE} and $\Omega_{Multiple}$) applied in the model calibration; Model performances (minimum R^2 and maximal deviation from zero as mean error, ME) for the different variables used in model calibration and validation. The model predictions include the ensemble mean of the accepted model runs (*EnM*) and single run using the modes of the posterior parameter distributions (Fig. 1). The value within brackets for the *EnM* was the range (maximum-minimum) of for the accepted runs. The NEE, λE, H, soil temperature (T_s) and soil water content (Θ) are hourly datasets while the LAI and aboveground (B_{AG}) and belowground (B_{BG}) biomass C stock were daily and yearly respectively.

Variables	**n**	**Acceptance Criteria**				**Model Performance**							
						R^2				ME			
		Ω_{NEE}		$\Omega_{Multiple}$		Ω_{NEE}		$\Omega_{Multiple}$		Ω_{NEE}		$\Omega_{Multiple}$	
		R^2	ME	R^2	ME	EnM	ModeP	EnM	ModeP	EnM	ModeP	EnM	ModeP
NEE	82315	0.70	0.20			0.72 (0.07)	0.70	0.75 (0.03)	0.75	-0.01 (0.4)	-0.33	-0.1 (0.53)	-0.03
NEE_d	47453			0.70	0.40	0.68 (0.07)	0.69	0.71 (0.01)	0.72	0.59 (5.06)	-0.43	0 (0.56)	0.24
NEE_n	32100			0.60	1.00	0.59 (0.09)	0.61	0.62 (0.02)	0.62	-0.79 (6.28)	-0.89	-0.21 (1.73)	-0.38
λE	81889			0.60		0.67 (0.34)	0.73	0.68 (0.14)	0.68	16.81 (32.86)	22.37	17.09 (17.6)	16.81
H	81339			0.50		0.57 (0.37)	0.55	0.58 (0.07)	0.57	19.74 (33.32)	15.05	20.25 (17.26)	20.98
T_{s1}	107728					0.88 (0.24)	0.86	0.90 (0.05)	0.90	0.89 (2.13)	0.95	0.82 (0.86)	0.78
T_{s2}	107020					0.91 (0.12)	0.88	0.92 (0.04)	0.93	0.83 (1.96)	0.89	0.77 (0.77)	0.74
Θ	85590					0.54 (0.43)	0.55	0.60 (0.16)	0.60	5.75 (25.29)	4.32	5.64 (11.08)	6.80
LAI	4018			0.80	1.00	0.86 (0.4)	0.88	0.88 (0.05)	0.89	-0.16 (4.18)	-0.13	-0.04 (1.37)	-0.02
B_{AG}	13			0.60	1000	0.74 (0.81)	0.74	0.75 (0.03)	0.75	-395.34 (2795.77)	173.92	-34.09 (1803.57)	94.02
B_{BG}	13			0.60	500	0.66 (0.7)	0.74	0.77 (0.31)	0.78	-267.25 (764.37)	-157.67	-171.58 (32.13)	-124.83

Table 3: Linear regression fit statistics for the analysis of the trend in the annually fitted parameters in 1997-2009.

Parameter	**unit**	**symbol**	**slope**	R^2	***p* value**
RadEfficiency(1)	g C MJ^{-1}	ε_1	0.13	0.72	0.0001
Emerge Tsum(1)	°C	t_{el}	0.71	0.31	0.051
LeafTsum2(1)	°C	t_{L2}	0.21	0.15	0.20
RateCoefLitter1	d^{-1}	k_l	0	0.16	0.18
RateCoefHumus	d^{-1}	k_h	0	0.01	0.72
MCoefRoot(1)	d^{-1}	$r_{m,r}$	0	0	1.00
MCoefLeaf(1)	d^{-1}	$r_{m,l}$	0	0.06	0.41

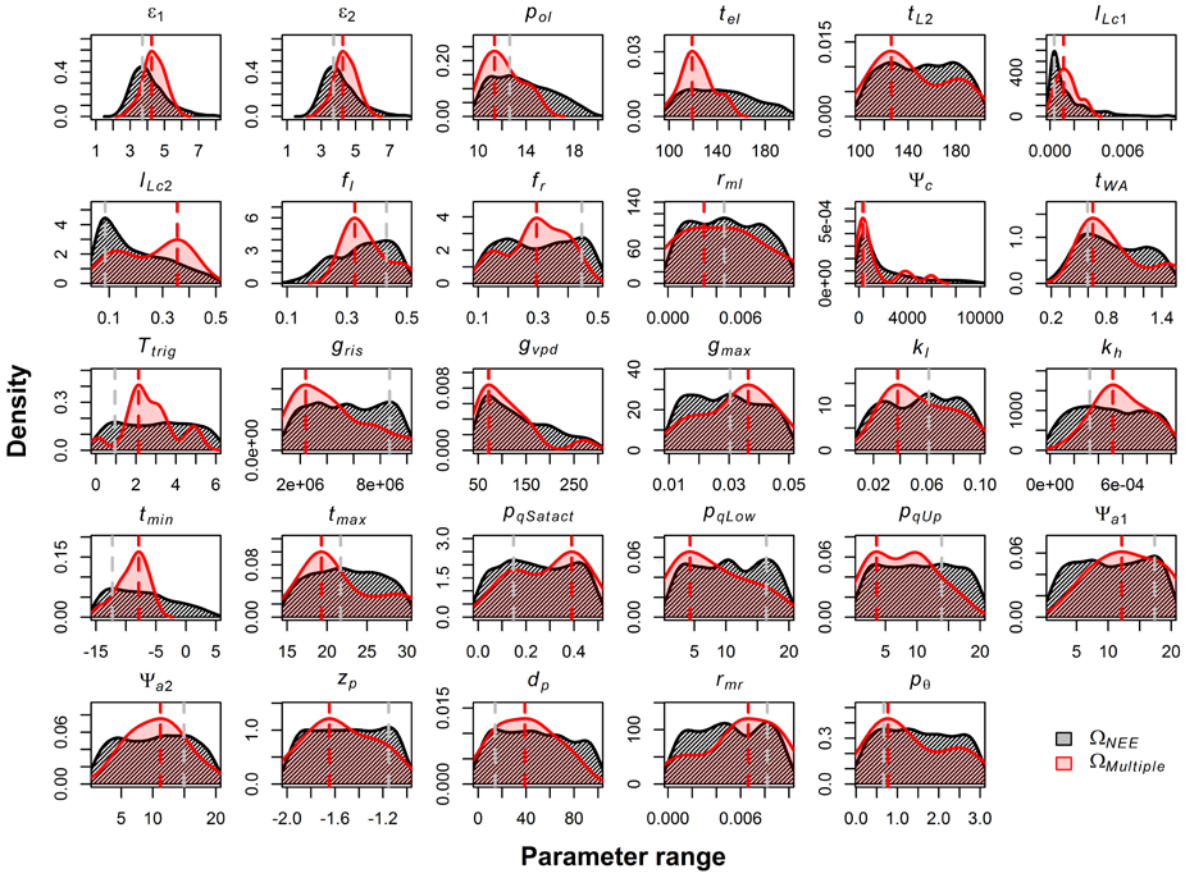

Figure 1: Posterior parameter distributions (density plots) after the model was globally fitted to the 13-year datasets using two different constraints, Ω_{NEE} and $\Omega_{Multiple}$ (see text for details). The prior parameter distributions are set as uniform and the parameter descriptions are given in Table 1. The dashed vertical lines are the modes of the posterior parameter distributions. Acceptance criteria of the behavioural models are given in Table 2.

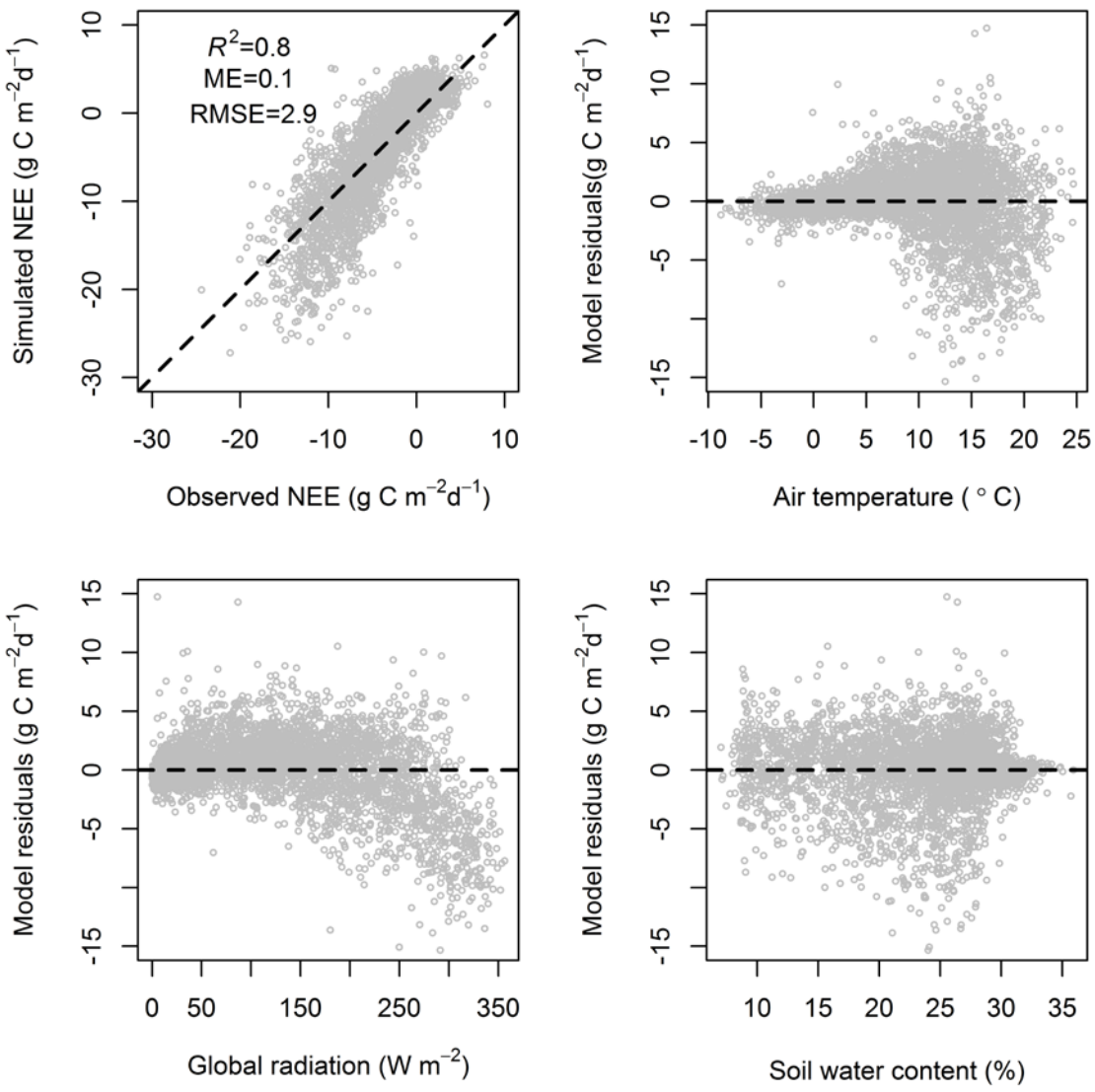

Figure 2: Observed and simulated (ensemble mean of accepted models) NEE (daily value) from 1997-2009; Model residuals (simulated-observed) plot against climatic variables.

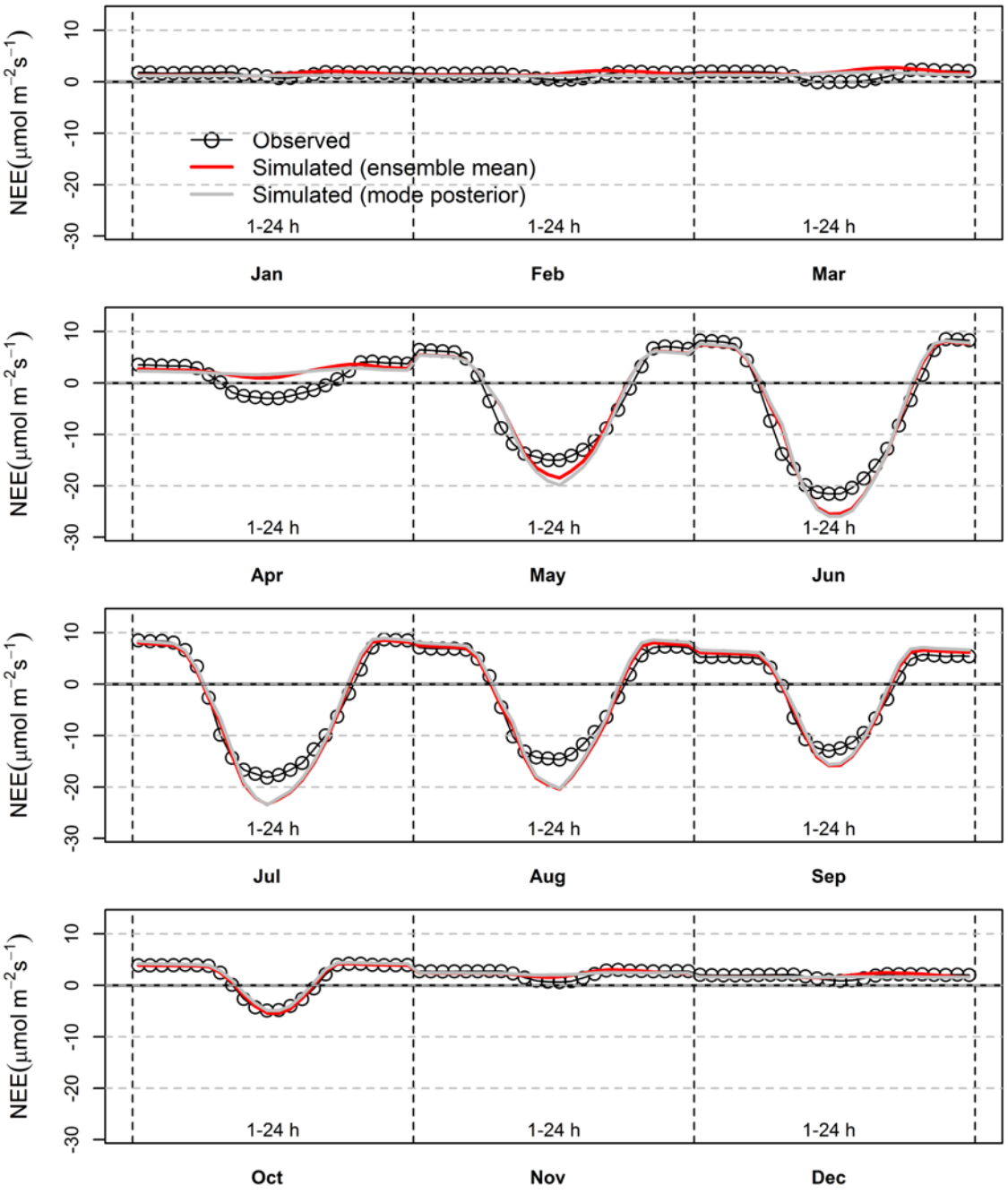

Figure 3: 13 year averages, of observed and simulated mean monthly diurnal courses of NEE (ensemble means and single run using the modes of the posterior parameter distributions).

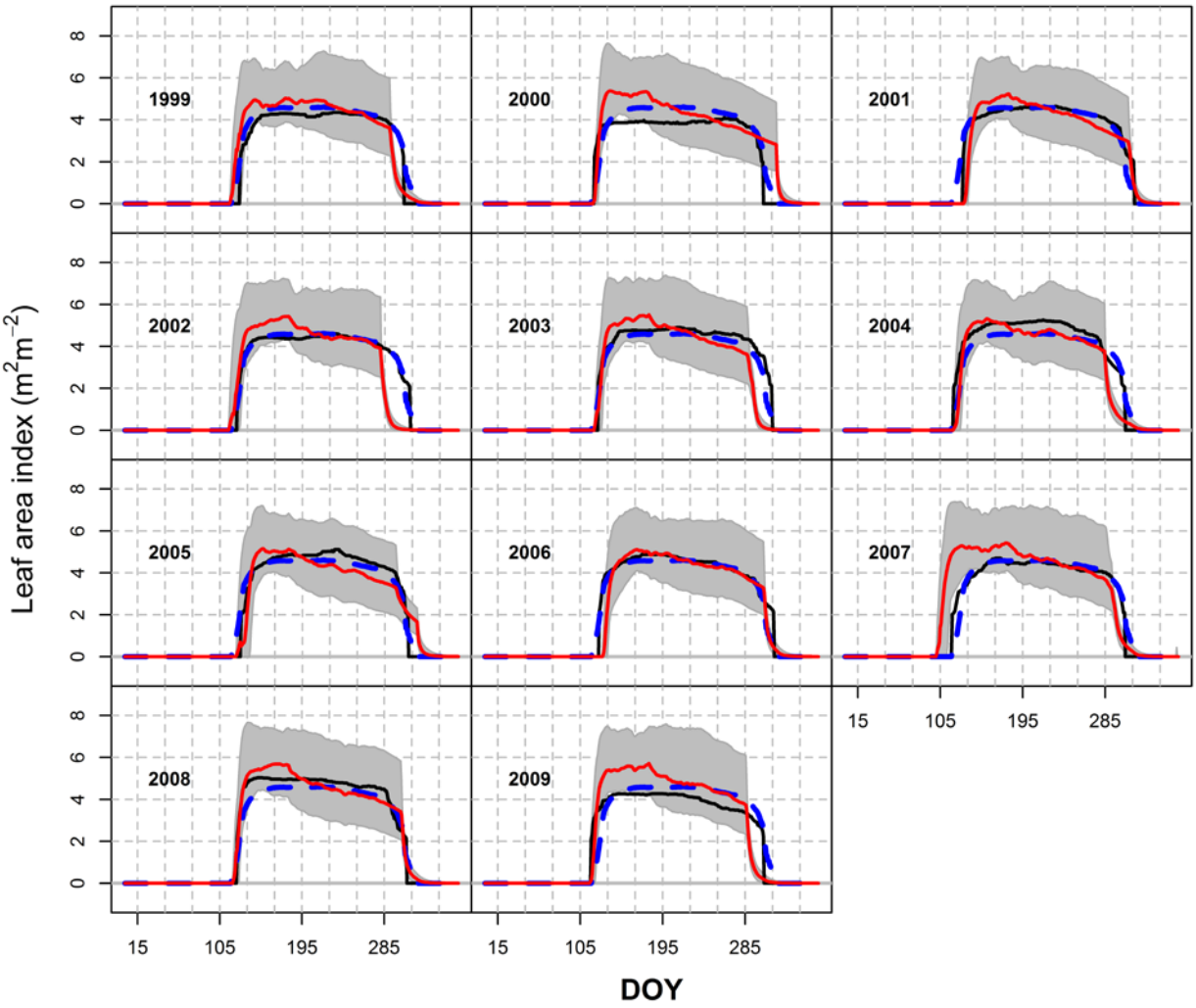

Figure 4: Observed (black) and simulated ensemble mean (red line and grey area for the maximum and minimum) LAI development in 1999-2009. The blue dashed lines are the averaged seasonal LAI dynamics for 1999-2009.

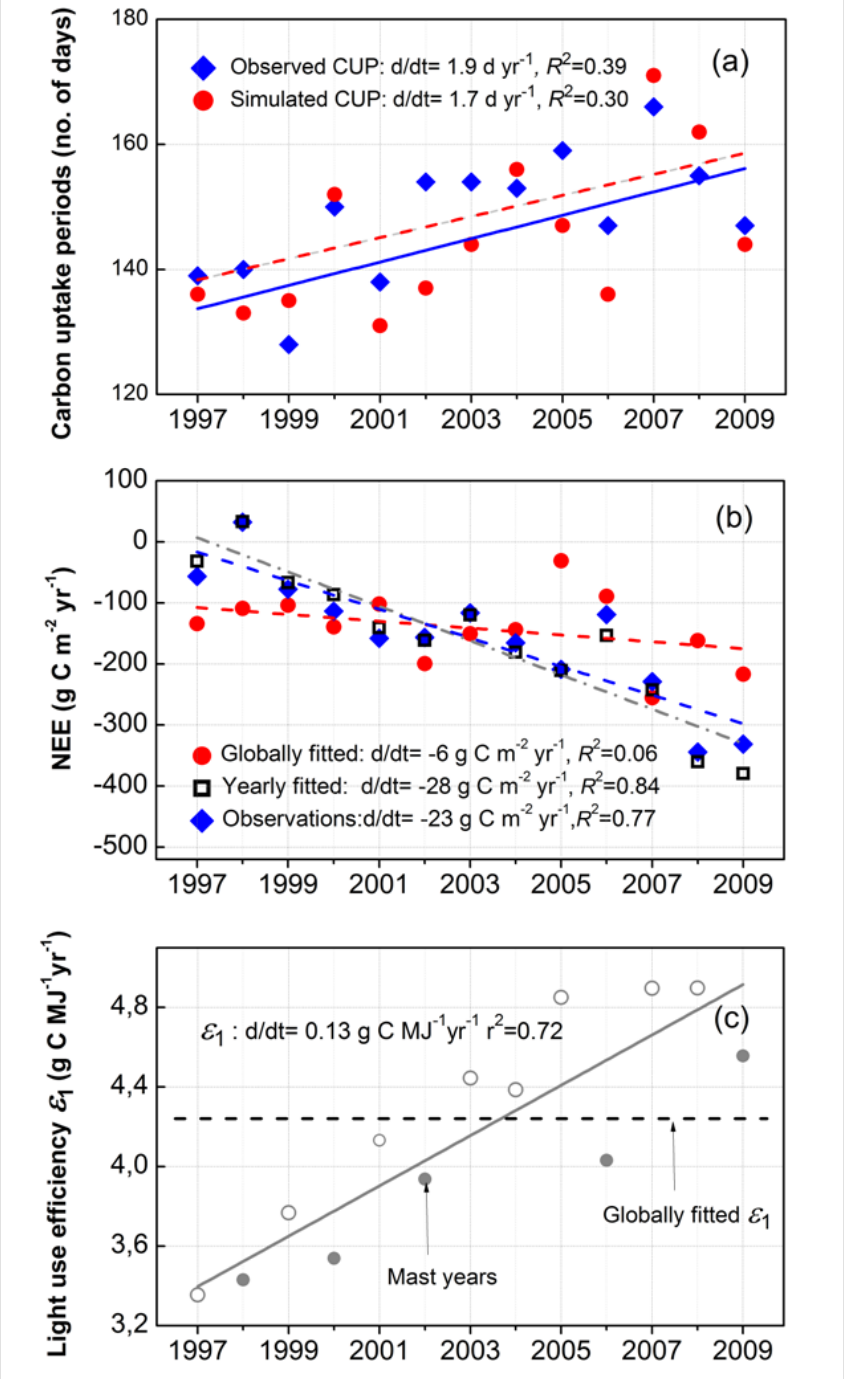

Fig. 5:(a) Observed and simulated carbon uptake period (CUP) in 1997-2009. **(b)** Observed and simulated (using globally and yearly fitted parameter sets) annual NEE in 1997-2009, the trend lines were linear regressions of the observation and model outputs with yearly fitted parameters. **(c)** Interannual variation in the yearly fitted light use efficiency, ε_1 the solid grey dots represent mast years and the horizontal dashed line was the globally fitted ε_1.

Appendix 1: CoupModel Equations.

Equations	No.	Description
Plant biotic processes		
$C_{Atm\to a} = \varepsilon_L f(T_l) f(CN_l) f(E_{ta}/E_{tp}) R_{s,pl}$ where ε_L is the radiation use efficiency and $R_{s,pl}$is the global radiation absorbed by the plant canopy.	(A1)	Rate of photosynthesis (g C m^{-2} day^{-1})
$f(T_l) = \begin{cases} 0 & T_l < p_{mn} \\ (T_l - p_{mn})/(p_{o1} - p_{mn}) & p_{mn} \le T_l \le p_{o1} \\ 1 & p_{o1} < T_l < p_{o2} \\ 1-(T_l - p_{o2})/(p_{mx} - p_{o2}) & p_{o2} \le T_l \le p_{mx} \\ 0 & T_l > p_{mx} \end{cases}$ where p_{mn}, p_{o1}, p_{o2} and p_{mx} are parameters.	(A2)	Response function for leaf temperature (–)
$f(CN_l) = p_{fixedN}$ where p_{fixedN} is a parameter.	(A3)	Response function for fixed leaf C:N ratio (–)
$f(E_{ta}/E_{tp}) = E_{ta}/E_{tp}$	(A4)	Response function for transpiration (–)
$C_{a\to Leaf} = f_l C_{Atm\to a}$ where f_l is the fixed allocation parameter to leaf, the carbon allocated to roots and stem can be calculated by exchanging f_l to$f_r$and f_s.	(A5)	Carbon allocation to leaf root and stem (g C m^{-2} day^{-1})
$C_{respleaf} = k_{mrespleaf} \cdot f(T) \cdot C_{leaf} + k_{gresp} \cdot C_{a\to Leaf}$ where $k_{mrespleaf}$ is the maintenance respiration coefficient for leaves, k_{gresp} is the growth respiration coefficient, and *f(T)* is the temperature response function. The equation calculates respiration from stem, roots by exchanging $k_{mrespleaf}$ to $k_{mrespstem}$, $k_{mresproo}$and using the corresponding stocks.	(A6)	Plant growth and maintenance respiration from leaves (g C m^{-2} day^{-1})
$f(T) = \begin{cases} 1 & T > t_{max} \\ \left(\frac{T - t_{\min}}{t_{\max} - t_{\min}}\right)^2 & t_{min} \le T \le t_{max} \\ 0 & T < t_{min} \end{cases}$ where t_{max}andt_{min} are parameters and T is the air temperature.	(A7)	Response function for air temperature (Ratkowsky function) (–)
$\mathrm{DOY}_{lf} = \mathrm{DOY}_i$ if $\sum_{\mathrm{DOY}_{start}}^{\mathrm{DOY}_i} T = T_{em,sum}$ where $\mathrm{DOY}_{lf}$is the day of year when leaf flushes; $\mathrm{DOY}_{start}$is the date when the air temperature is higher than 5°C for 3 consecutive days; T is the air temperature and $T_{em,sum}$ is the temperature threshold.	(A8)	Leaf flush date (-)
$f(l_{Lc}) = l_{Lc1} + (l_{Lc2} - l_{Lc1}) \min\left(1, \frac{\max(0, T_{dorm,sum} - t_{L1})}{\max(1, t_{L2} - t_{L1})}\right)$ where l_{Lc1} is a average rate parameter for leaf litterfall throughout the year and l_{Lc2} is the litterfall rate during autumn when the dorming temperature sum reaches a threshold value. $T_{dorm,sum}$ is calculated at the end of the growing season when the air temperature is below 5°C as the accumulated difference between T_a and 5°C. t_{L1} *and* t_{L2} are model parameters controlling the temperature threshold.	(A9)	Leaf litter fall rate (day^{-1})
$A_l = \frac{B_l}{p_{l,sp}}$ where $p_{l,sp}$is a parameter and B_l is the total mass of leaf.	(A10)	Leaf area index (m^2 m^{-2})
Plant abiotic processes		
$R_{s,pl} = (1 - e^{-k_{rn}\frac{A_l}{f_{cc}}}) \cdot f_{cc}\left(1 - a_{pl}\right) R_{is}$ where k_{rn} is the light use extinction coefficient given as a single parameter	(A11)	Plant interception of global radiation (MJ m^{-2} day^{-1})

common for all plants, f_{cc} is the surface canopy cover, and $a_{pl}$is the plant albedo.		
$f_{cc} = p_{c\max}(1-e^{-p_{ck}A_l})$ where p_{cmax} is a parameter that determines the maximum surface cover and p_{ck} is a parameter the governs the speed at which the maximum surface cover is reached. A_l is the leaf area index of the plant.	(A12)	Surface canopy cover (m^2 m^{-2})
$S_{i\max} = i_{LAI}A_l + i_{base}$ where i_{LAI} and i_{base} are parameters.	(A13)	Interception storage (mm)
$E_{ta}^{*} = E_{tp}^{*}\int_{z_r}^{0} f(\psi(z))\, f(T(z))\, r(z)$ where $r(z)$ is the relative root density distribution, z is root depth and $f(\psi(z))$ and $f(T(z))$ are response functions for soil water potential and soil temperature.	(A14)	Actual transpiration before compensatory uptake (mm day^{-1})
$E_{ta} = E_{ta}^{*} + f_{umov}\cdot(E_{tp}^{*} - E_{ta}^{*})$ where f_{umov} is the degree of compensation, E_{ta}^{*} is the uptake without any account of compensatory uptake, and E_{tp}^{*} is the potential transpiration with eventual reduction due to interception evaporation.	(A15)	Actual transpiration (mm day^{-1})
$f(\psi(z)) = \min\left(\left(\frac{\psi_c}{\psi(z)}\right)^{p_1E_{tp}+p_2}, f_\theta\right)$ where p_1, p_2 and $\psi_c$are parameters, and an additional response function, f_θ, corresponds to the normal need of oxygen supply to fine roots.	(A16)	Response function for soil water potential (–)
$f(T(z)) = \begin{cases} 1-e^{-t_{WA}\max(0,T(z)-T_{trig})^{t_{WB}}} & I_{day} \le p_{daycut} \\ 1 & I_{day} > p_{daycut} \end{cases}$ where $t_{WA,}$ p_{daycut} and t_{WB} are parameters. T_{trig} is the trigger temperature.	(A17)	Response function for soil temperature (–)
$L_\upsilon E_{tp} = \frac{\Delta R_n + \rho_a c_p \frac{(e_s-e_a)}{r_a}}{\Delta + \gamma\left(1+\frac{r_s}{r_a}\right)}$ where R_n is net radiation available for transpiration, e_s is the vapour pressure at saturation, e_a is the actual vapour pressure, ρ_a is air density, c_p is the specific heat of air at constant pressure, $L_v$is the latent heat of vaporisation, Δ is the slope of saturated vapour pressure versus temperature curve, γ is the psychrometer 'constant', r_s is 'effective' surface resistance and r_a is the aerodynamic resistance.	(A18)	Potential transpiration (mm day^{-1})
$r_s = \frac{1}{\max(A_l g_l, 0.001)}$ where g_l is the leaf conductance.	(A19)	Stomatal resistance (s m^{-1})
$g_l = \frac{R_{is}}{R_{is}+g_{ris}}\frac{g_{\max}}{1+\frac{(e_s-e_a)}{g_{vpd}}}$ where g_{ris}, g_{max} and g_{vpd} are parameter values.	(A20)	Stomatal conductance per leaf area (m s^{-1})
Soil carbon and nitrogen processes		
$C_{DecompL} = k_l f(T) f(\theta) C_{Litter}$ where k_l is a parameter.	(A21)	Decomposition of litter (g C m^{-2} day^{-1})
$C_{DecompH} = k_h f(T) f(\theta) C_{Humus}$ where $k_h$is a parameter.	(A22)	Decomposition of humus (g C m^{-2} day^{-1})

$$f(T)=\begin{cases}1 & T>t_{max}\\ \left(\dfrac{T-t_{\min}}{t_{\max}-t_{\min}}\right)^2 & t_{min}\le T\le t_{max}\\ 0 & T<t_{min}\end{cases}$$ (A23) Response function for soil temperature (Ratkowsky function) (–)

where t_{max}andt_{min} are parameters and simultaneously optimized in Eq. A7.

$$f(\theta)=\min\begin{cases}p_{\theta satact} & \theta=\theta_s\\ \left(\dfrac{\theta_s-\theta}{p_{\theta Upp}}\right)^{p_{\theta p}}\left(1-p_{\theta satact}\right)+p_{\theta satact}, & \theta_{wilt}\le\theta\le\theta_s\\ \left(\dfrac{\theta-\theta_{wilt}}{p_{\theta Low}}\right)^{p_{\theta p}} & \\ 0 & \theta<\theta_{wilt}\end{cases}$$ (A24) Response function for soil moisture (–)

where $p_{\theta Upp}$, $p_{\theta Low}$, $p_{\theta Satact}$, and $p_{\theta p}$ are parameters and the variables, θ_s, θ_{wilt}, and θ, are the soil moisture content at saturation, the soil moisture content at the wilting point, and the actual soil moisture content, respectively.

Soil physical processes

$$q_h(0)=k_{ho}\frac{(T_s-T_1)}{\Delta z/2}+C_w\left(T_a-\Delta T_{Pa}\right)q_{\text{in}}+L_v q_{vo}$$ (A25) Soil surface heat flow (J m^{-2} day^{-1})

where k_{ho} is the conductivity of the organic material at the surface, T_s is the surface temperature, T_1 is the temperature in the uppermost soil layer, ΔT_{Pa} is a parameter that represents the temperature difference between the air and the precipitation, q_{in}, is the water infiltration rate, q_{vo} is the water vapour flow, and L_v is the latent heat. The temperature difference, $T_a - \Delta T_{Pa}$, can optionally be exchanged to surface temperature, T_s.

$$S_e=\left(\frac{\psi}{\psi_a}\right)^{-\lambda}$$ (A26) The effective saturation (–)

where $\psi_a$is the air–entry tension, ψ is the pressure head or actual water tension, and λ is the pore size distribution index.

$$q_{wp}=\int_{z_p}^{z_{sat}} k_s\frac{\left(z_{sat}-z_p\right)}{d_u d_p}d_z$$ (A27) Groundwater outflow (mm day^{-1})

where k_{sat} is the saturated conductivity, d_u is the unit length of the horizontal element, z_p is the lower depth of the drainage pipe, $z_{sat}$is the simulated depth of the watertable, and d_p is a characteristic distance between drainage pipes.

6. References

Beven, K. and Freer, J., 2001. Equifinality, data assimilation, and uncertainty estimation in mechanistic modelling of complex environmental systems using the GLUE methodology. Journal of Hydrology, 249(1): 11-29.

Collatz, G., Ball, J., Grivet, C. and Berry, J., 1991. Physiological and environmental regulation of stomatal conductance, photosynthesis and transpiration: a model that includes a laminar boundary layer. Agricultural and Forest Meteorology, 54(2-4): 107-136.

FAO, 2010. Global forest resources assessment forestry paper. Food and Agriculture Organization of the United Nations, Rome.

Friedlingstein, P. et al., 2010. Update on CO2 emissions. Nature Geoscience, 3(12): 811-812.

Hänninen, H., 1995. Effects of climatic change on trees from cool and temperate regions: an ecophysiological approach to modelling of bud burst phenology. Canadian Journal of Botany/Revue Canadienne de Botanique, 73(2): 183-201.

Houborg, R. and Boegh, E., 2008. Mapping leaf chlorophyll and leaf area index using inverse and forward canopy reflectance modeling and SPOT reflectance data. Remote sensing of environment, 112(1): 186-202.

Houghton, R., 2007. Balancing the global carbon budget. Annu. Rev. Earth Planet. Sci., 35: 313-347.

Hu, J., Moore, D., Burns, S. and Monson, R., 2010. Longer growing seasons lead to less carbon sequestration by a subalpine forest. Global Change Biology, 16(2): 771-783.

Ibrom, A. et al., 2008. Variation in photosynthetic light-use efficiency in a mountainous tropical rain forest in Indonesia. Tree Physiology, 28(4): 499-508.

Jansson, P., 2012. CoupModel: Model Use, Calibration, and Validation. Transactions of the ASABE, 55(4): 1337-1346.

Jansson, P. and Karlberg, L., 2004. COUP manual–Coupled heat and mass transfer model for soil-plantatmosphere systems. Technical manual for the CoupModel: 1–453.

Jansson, P., Svensson, M., Kleja, D. and Gustafsson, D., 2008. Simulated climate change impacts on fluxes of carbon in Norway spruce ecosystems along a climatic transect in Sweden. Biogeochemistry, 89(1): 81-94.

Jansson, P.E. and Moon, D.S., 2001. A coupled model of water, heat and mass transfer using object orientation to improve flexibility and functionality. Environmental Modelling & Software, 16(1): 37-46.

Jarvis, P., 1976. The interpretation of the variations in leaf water potential and stomatal conductance found in canopies in the field. Philosophical Transactions of the Royal Society of London. Series B, Biological Sciences, 273(927): 593-610.

Keenan, T.F. et al., 2012a. Terrestrial biosphere model performance for inter-annual variability of land-atmosphere CO2 exchange. Global Change Biology, 18(6): 1971-1987.

Keenan, T.F., Davidson, E., Moffat, A.M., Munger, W. and Richardson, A.D., 2012b. Using model-data fusion to interpret past trends, and quantify uncertainties in future projections, of terrestrial ecosystem carbon cycling. Global Change Biology, 18(8): 2555-2569.

Kramer, K. et al., 2002. Evaluation of six process based forest growth models using eddy covariance measurements of CO2 and H2O fluxes at six forest sites in Europe. Global Change Biology, 8(3): 213-230.

Linkosalo, T., Carter, T.R., Häkkinen, R. and Hari, P., 2000. Predicting spring phenology and frost damage risk of Betula spp. under climatic warming: a comparison of two models. Tree Physiology, 20(17): 1175-1182.

Liu, Y., Freer, J., Beven, K. and Matgen, P., 2009. Towards a limits of acceptability approach to the calibration of hydrological models: Extending observation error. Journal of Hydrology, 367(1-2): 93-103.

Luyssaert, S. et al., 2009. Toward a consistency cross-check of eddy covariance flux–based and biometric estimates of ecosystem carbon balance. Global Biogeochemical Cycles, 23(3).

Mahecha, M. et al., 2010. Comparing observations and process-based simulations of biosphere-atmosphere exchanges on multiple timescales. Journal of Geophysical Research, 115(G2): G02003.

Metz, B., 2007. Climate change 2007: mitigation of climate change: contribution of Working Group III to the Fourth Assessment Report of the IIntergovernmental Panel on Climate Change. Cambridge University Press.

Morales, P. et al., 2005. Comparing and evaluating process-based ecosystem model predictions of carbon and water fluxes in major European forest biomes. Global Change Biology, 11(12): 2211-2233.

Pan, Y. et al., 2011. A large and persistent carbon sink in the world's forests. Science, 333(6045): 988-993.

Pilegaard, K., Hummelsh j, P., Jensen, N. and Chen, Z., 2001. Two years of continuous CO2 eddy-flux measurements over a Danish beech forest. Agricultural and Forest Meteorology, 107(1): 29-41.

Pilegaard, K., Ibrom, A., Courtney, M.S., Hummelsh j, P. and Jensen, N.O., 2011. Increasing net CO2 uptake by a Danish beech forest during the period from 1996 to 2009. Agricultural and Forest Meteorology, 151(7): 934-946.

Pilegaard, K. et al., 2003. Field measurements of atmosphere-biosphere interactions in a Danish beech forest. Boreal Environment Research, 8(4): 315-333.

Reichstein, M. et al., 2007. Reduction of ecosystem productivity and respiration during the European summer 2003 climate anomaly: a joint flux tower, remote sensing and modelling analysis. Global Change Biology, 13(3): 634-651.

Richardson, A.D. et al., 2012. Terrestrial biosphere models need better representation of vegetation phenology: results from the North American Carbon Program Site Synthesis. Global Change Biology.

Sacks, W.J., Schimel, D.S. and Monson, R.K., 2007. Coupling between carbon cycling and climate in a high-elevation, subalpine forest: a model-data fusion analysis. Oecologia, 151(1): 54-68.

Sala, A., Hopping, K., McIntire, E.J.B., Delzon, S. and Crone, E.E., 2012. Masting in whitebark pine (Pinus albicaulis) depletes stored nutrients. New Phytologist, 196(1): 189-199.

Siqueira, M. et al., 2006. Multiscale model intercomparisons of CO2 and H2O exchange rates in a maturing southeastern US pine forest. Global Change Biology, 12(7): 1189-1207.

Skovsgaard, J.P. and Nord-Larsen, T., 2012. Biomass, basic density and biomass expansion factor functions for European beech (Fagus sylvatica L.) in Denmark. European Journal of Forest Research, 2: 1-19.

Spiecker, H., 2003. Silvicultural management in maintaining biodiversity and resistance of forests in Europe--temperate zone. Journal of Environmental Management, 67(1): 55-65.

Svensson, M., Jansson, P. and Berggren Kleja, D., 2008a. Modelling soil C sequestration in spruce forest ecosystems along a Swedish transect based on current conditions. Biogeochemistry, 89(1): 95-119.

Svensson, M. et al., 2008b. Bayesian calibration of a model describing carbon, water and heat fluxes for a Swedish boreal forest stand. Ecological Modelling, 213(3-4): 331-344.

Wang, Y.P., Trudinger, C.M. and Enting, I.G., 2009. A review of applications of model–data fusion to studies of terrestrial carbon fluxes at different scales. Agricultural and Forest Meteorology, 149(11): 1829-1842.

Williams, M., Schwarz, P., Law, B., Irvine, J. and Kurpius, M., 2005. An improved analysis of forest carbon dynamics using data assimilation. Global Change Biology, 11(1): 89-105.

Wu, J. et al., 2012a. Effects of climate variability and functional changes on the interannual variation of the carbon balance in a temperate deciduous forest. Biogeosciences, 9(1): 13-28.

Wu, S.H., Jansson, P.E. and Kolari, P., 2011. Modeling seasonal course of carbon fluxes and evapotranspiration in response to low temperature and moisture in a boreal Scots pine ecosystem. Ecological Modelling.

Wu, S.H., Jansson, P.E. and Kolari, P., 2012b. The role of air and soil temperature in the seasonality of photosynthesis and transpiration in a boreal Scots pine ecosystem. Agricultural and Forest Meteorology, 156: 85-103.

The research within ECO aims to evaluate the impacts of various energy technologies on the environment and climate, the potentials to promote environmental adaptation to changed climatic conditions and the possibilities to mitigate positive and promote negative feedbacks to the atmosphere through land use and land management.

DTU-KT

Center for ecosystem and environmental sustainability (ECO)

Department of Chemical and Biochemical Engineering

Technical University of Denmark

Kongens Lyngby,

DK-2800, Copenhagen

Denmark

Phone +45 4677 4100

Fax +45 4677 4100

http://www.kt.dtu.dk/